INTESTINAL BARRIER FUNCTION ALTERS BONE DENSITY

By

Sandra Ann Raehtz

A DISSERTATION

Submitted to
Michigan State University
in partial fulfillment of the requirements
for the degree of

Genetics --- Doctor of Philosophy

2016

ABSTRACT

INTESTINAL BARRIER FUNCTION ALTERS BONE DENSITY

By

Sandra Ann Raehtz

1 in 2 women over 50 will experience a fracture due to osteoporosis. Current therapeutics work to prevent further bone loss, however, new therapies which can build bone or prevent bone loss are necessary to identify. The gut-bone axis is a promising target for the prevention of bone loss. Recent studies have shown that the probiotic *Lactobacillus reuteri* prevents bone loss during estrogen deficiency (OVX), type 1 diabetes (T1D) as well as increases bone density in healthy male mice. This finding lead us to examine what changes occur in the intestine following estrogen deficiency. We found that ovariectomy (OVX) leads to decreased intestinal permeability which is prevented by estrogen supplementation. Additionally, OVX was found to decrease epithelial cell turnover as well as mucus production. To determine how treating the intestinal epithelial barrier can affect bone loss, we utilized a high molecular weight polymer, MDY, which is neither metabolized or absorbed to decrease intestinal inflammation and increase mucus in the intestine. MDY treatment in OVX mice prevented estrogen deficiency induced bone loss, highlighting the role of the intestinal barrier in bone density. In addition to characterizing how OVX alters intestine function, T1D was found to alter intestinal motility and permeability, both of which were correlated to bone loss. Treatment of diabetic mice with MDY prevented intestinal inflammation and increased bone density with respect to diabetic controls. Together our studies indicate an

important role for the intestinal barrier in the health of bone. Understanding the role of the gut-bone axis can lead to the prevention of bone loss as well as the development of new bone building therapies.

ACKNOWLEDGMENTS

This work would not have been possible if I did not have such a passionate, enthusiastic and encouraging mentor, Dr. McCabe. I was lucky to not only learn how to pursue research questions, but also to have fun while doing it and to never stop exploring. In addition to Dr. McCabe, the support of my husband has been outstanding and absolutely essential in the pursuit of this degree. I have been so lucky to have been surrounded by such wonderfully supportive and loving people. Thank you so much.

TABLE OF CONTENTS

LIST OF TABLES

LIST OF FIGURES

KEY TO ABBREVIATIONS

OVX – Ovariectomy

T1D – Type 1 Diabetes

BMU – Basic Multicellular Unit

M-CSF – Macrophage Colony Stimulating Factor

RANKL – Receptor for Nuclear Factor Kappa Beta Ligand

TRAP – Tartrate-Resistant Acid Phosphatase

OC - Osteocalcin

OPG – Osteoprotegrin

TGFβ – Transforming Growth Factor β

IGF – Insulin Growth Factor

BMP – Bone Morphogenic Protein

BMD – Bone Mineral Density

ER α – Estrogen Receptor α

ER β – Estrogen Receptor β

NFkB – Nuclear Factor Kappa Beta Ligand

TNF – Tumor Necrosis Factor

IL – Interleukin

LRP – Lipoprotein Receptor-Related

DKK – Dickkoff

STZ – Streptozotocin

NOD – Non-Obese Diabetic

PTH – Parathyroid

SERM – Selective Estrogen Receptor Modulator

GALT – Gut-Associated Lymphoid Tissue

MUC2 – Mucin 2

GI – Gastrointestinal

IBD – Inflammatory Bowel Disease

FITC – Fluoroscein Isothiocyanate

RITC – Rhodamine Isothiocyanate

CPP – Colonic Paracellular Permeability

TER – Transepithelial Resistance

BVF – Bone Volume fraction

E – Estrogen

EtOH – Ethanol

PAS – Perodic Acid Schiff

CHAPTER 1

1. LITERATURE REVIEW

1.1. BONE

The skeletal system is responsible for the structure and locomotion of the human body in addition to playing an important role in the protection of organs, acting as a calcium reservoir and housing bone marrow. The skeleton is made up of both trabecular (spongy) (20%) and cortical (compact) (80%) bone with trabecular bone being more metabolically active and cortical bone serving more of a structural and protective role (Figure 1) (1). Bone remodeling is a continuous process with the entire skeleton renewing itself approximately every 10 years with 5-10% of bone remodeled each year in the adult skeleton (2). Bone remodeling consists of a balance between the building of new bone by osteoblasts and the resorption of bone by osteoclasts. A defect in either of these processes can lead to the buildup of too much bone leading to brittleness or a breakdown in bone quantity and quality.

1.1.1. Bone Development and Anatomy

Bones are made up of both dense (cortical) and spongy/cancellous (trabecular) bone (Figure 1) (2). The outer surface of the bone is lined by the periosteum while the endosteum lines the inner surface. Embryonic development of bones consists of both endochondrial bone formation (vertebra and long bones such as the femur) and intramembranous bone formation (flat bones such as the calvaria/skull) (2). During endochondrial bone formation mesenchymal-derived chondrocytes form a matrix of

cartilage which is followed by vascularization then matrix deposition and mineralization by osteoblasts (2). Continued endochondrial ossification, which occurs at the growth plate or metaphysis, leads to bone lengthening which ends during young adulthood and leads to the mineralization of the growth plate in humans. Mice, however, never completely mineralize the metaphysis and bone growth continues into adulthood, albeit at a much slower rate (2). Intramembranous bone formation occurs when osteoblasts do not follow a cartilage matrix and directly deposit and mineralize bone matrix (2).

The space inside of the bone structure houses the bone marrow which is comprised of cells from both the hematopoietic and mesenchymal lineages. The bone marrow cells are in close proximity with the bone surface and are thought to signal and contribute to the regulation of bone remodeling. As the marrow is the site for hematopoiesis, or blood production, bone also contains blood, lymphatic vessels, leukocytes and nerves (3).

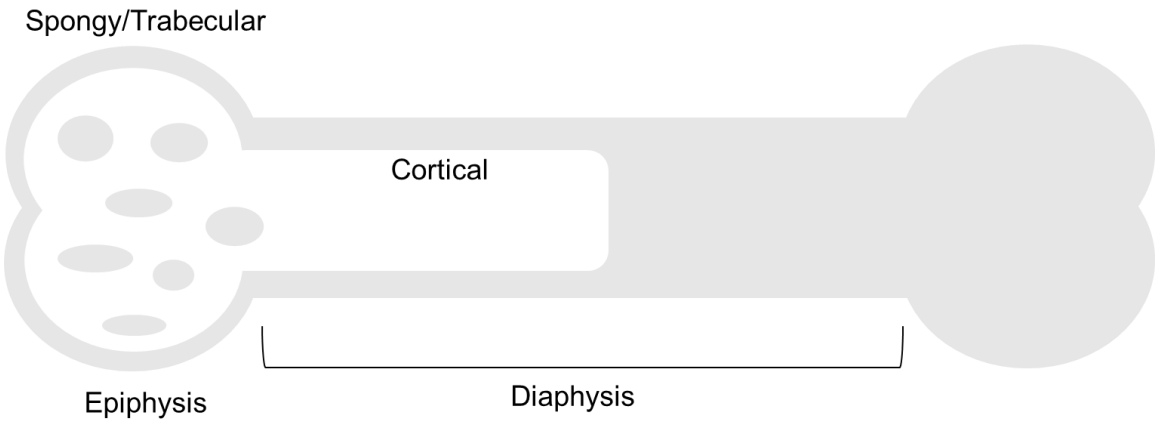

Figure 1. Bone Anatomy

Cartoon of bone depicting the spongy or trabecular bone at the epiphysis and cortical bone along the diaphysis.

1.1.2. Bone Remodeling

Bone remodeling is a constant process which relies on the communication of many cell types. Remodeling occurs at various, distinct sites of the skeleton and is triggered by mechanical loading, calcium levels and various paracrine and endocrine signals (4). The main cells required for bone remodeling make up the basic multicellular unit (BMU) and consist of osteoblasts, osteoclasts and osteocytes (Figure 2) (4). Remodeling begins when osteocytes sense areas of bone damage and recruit osteoblasts to signal to hematopoietic osteoclast precursors to proliferate and migrate to the site of bone requiring remodeling. Osteoblasts secrete factors such as macrophage colony stimulating factor (M-CSF) and receptor for nuclear factor kappa beta ligand (RANKL) to stimulate osteoclast precursor proliferation and fusion to form multinucleated osteoclasts which bind to the surface of the bone via integrin proteins (3). Once the osteoclasts bind to the bone, they form a resorption pit where they create an acidic environment and release lysosomal enzymes such as tartrate-resistant acid phosphatase (TRAP) and cathepsin K, to dissolve the matrix below. Active osteoclasts secrete TRAP5b into the serum which can be quantified and used to measure whole body bone resorption status. In addition to activating osteoclasts, osteoblasts also secrete osteoprotegrin (OPG), a soluble decoy for RANKL, which can inhibit osteoclast differentiation and activation and subsequent resorption (Figure 2) (3).

After bone is resorbed, osteoclasts are cleared from the bone remodeling site and osteoblasts are signaled to begin forming new bone matrix. Osteoclasts recruit osteoblasts by releasing growth factors from the bone matrix, such as transforming growth factor beta (TGFβ), insulin-like growth factor (IGF) and bone morphogenic proteins

(BMPs) which increase the migration of osteoblasts to the remodeling site as well as bone formation activity (5). In addition to releasing factors from the bone, osteoclasts secrete several factors which can regulate osteoblasts. These factors include Wnt10b, BMP6 and sphingosine-1-phosphate and they work to enhance osteoblast activity (6). As new mineral is laid down, some osteoblasts become embedded within the new bone and differentiate into osteocytes. Osteocytes occupy lacunae, circular structures within the bone, and play an important role in responding to mechanical stimuli and signaling to the other cells in the BMU to begin the remodeling process (Figure 2) (3). Osteocyte apoptosis has been shown to stimulate osteoclast activity by increasing the production of RANKL (7) and can decrease osteoblast activity by the release of the protein sclerostin. Sclerostin inhibits WNT signaling and correspondingly bone formation and mineralization and can also increase osteoblast apoptosis (8). Osteoblasts may also become bone lining cells which line the surface of the bone. Bone lining cells have been suggested to form a canopy around the bone remodeling area, localizing the BMU to the area of active remodeling (Figure 2) (6).

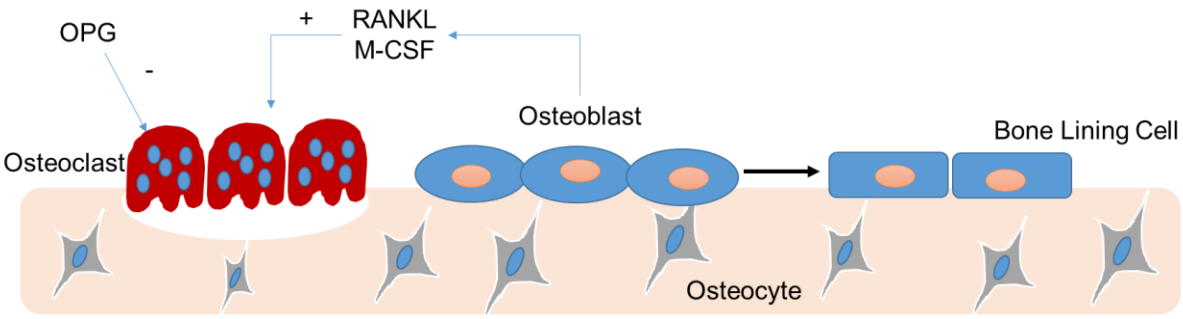

Figure 2. Bone Remodeling

The basic multicellular unit for bone remodeling consists of 3 main cells: osteoclasts, osteoblasts, and osteocytes. Osteoclasts are activated by the combination of RANK and M-CSF (secreted by osteoblasts) and then form a resorption pit where they release enzymes (TRAP and cathepsin K) to break down bone (not pictured). The bone releases factors to signal osteoblast differentiation and activity and osteoblast begin to lay down new mineral (called osteoid). As osteoblasts become trapped within the bone matrix they become osteocytes. Osteoblasts can also become bone lining cells.

1.2. OSTEOPOROSIS

Osteoporosis is characterized by decreased bone strength and altered bone architecture which leads to an increased risk of fracture. Decreased bone quality is due to the combinatory effects of decreased bone mineral density, defects in the microarchitecture of trabeculae including increased trabecular spacing and decreased trabecular thickness and an inability to effectively balance bone remodeling (3). Clinically, osteoporosis is defined as having a bone mineral density (BMD) less than 2.5 standard deviations lower than the average population BMD for that location. This number is referred to as the T-score (3). Osteoporotic fractures cost more than $20 billion in the United States annually and can leave patients hospitalized with decreased mobility and increases the risk of secondary complications such as infections like pneumonia (9,10).

Primary or idiopathic osteoporosis is a result of menopause (typically occurring after the 5^{th} decade of life) and is found in the absence of any disease or pathological condition. In contrast, secondary osteoporosis occurs as a consequence of disease pathology or drug side effects. These conditions include: corticosteroid treatment, nutrient deficiencies due to intestinal disease, chronic disease, cancer, various autoimmune diseases, endocrinopathies, and several medications (11). The focus of this dissertation will be on both primary osteoporosis due to estrogen deficiency and secondary osteoporosis caused by the autoimmune disease type 1 diabetes mellitus.

1.2.1. Estrogen Deficiency Induced Osteoporosis

Of women over the age of 50, 1 in 2 are expected to experience an osteoporotic fracture (National Osteoporosis foundation). This is the result of menopause or the cessation of estrogen production by the ovaries (12). The loss of estrogen leads to a marked increase in bone resorption and a reciprocal increase in bone formation, however, the two processes are no longer coupled resulting in bone remodeling favoring a resorptive environment and net bone loss (13).

Estrogen plays an important role in inducing osteoclast apoptosis. Osteoclast-specific deletion of ERα results in decreased trabecular bone mass which was due to an increase in osteoclast lifespan as a result of decreased apoptosis (14,15). Estrogen also suppresses RANKL-induced osteoclast differentiation (16–19). Estrogen deficiency leads to an increase in NFκB activity which can go on to activate osteoclast activity. In addition to these direct effects of estrogen on osteoclasts, estrogen can indirectly decrease RANKL production by osteoblasts, T and B lymphocytes and increases the production of OPG by osteoblasts (20,21). Estrogen also decreases the production of cytokines which can increase bone resorption via osteoclasts; these include IL-1, IL-6, TNFα, M-CSF as well as prostaglandins (22–27). It has also been proposed that following the loss of estrogen, there is a rapid increase in T cell population which leads to an increase in the production of TNFα levels, subsequently enhancing osteoclastogenesis (28,29).

In addition to its effects on osteoclasts, estrogen has been shown to both inhibit osteoblast apoptosis and increase osteoblast lifespan (30). Estrogen deficiency leads to increased production of reactive oxygen species which can decrease both osteoblast and osteocyte lifespan as well as increase osteoclast number and activity (31). Deletion of

ERα from osteoblast cell lineage does not lead to a marked bone phenotype as compared to a deletion of ERα from osteoclasts (14,15). Taken together, estrogen acts to prolong osteoblast activity and lifespan and decrease osteoclast activity. Thus, states of estrogen deficiency such as menopause favor osteoclastogenesis and lead to increased bone resorption.

1.2.2. Type 1 Diabetes Induced Osteoporosis

Type 1 diabetes (T1D) is an autoimmune disease characterized by the loss of insulin production by the pancreatic beta cells (32). T1D generally occurs in adolescents or young adults and must be controlled by regular blood glucose monitoring and insulin delivery. Better education, early diagnosis and glycemic control has led to the increase in the lifespan of T1D patients. However, long term diabetic conditions are still associated with several secondary consequences including retinopathy, microvasculature abnormalities, nephropathy, and bone loss (33).

A retrospective cohort study in the United Kingdom studying osteoporosis in type 1 diabetic patients determined that there is a lifelong risk of fracture in T1D patients which begins at childhood (or onset of the disease) and persists through old age (34). Fracture risk is correlated with the duration of diabetes (35,36) and there is an association between fracture risk and the presence of microvascular complications (35–40). However, there is no association between fracture risk and glycemic control (35–40). Understanding how T1D leads to bone loss is crucial for the prevention and treatment of osteoporosis in this patient population.

Diabetes induced osteoporosis has been shown to be largely due to the decrease in osteoblast lineage selection from mesenchymal stem cells as well as decreased osteoblast maturation and activity. Osteoblasts and adipocytes originate from the same mesenchymal stem cell lineage (41). Osteoblastogenesis occurs with activation of the WNT signaling pathway (42). WNT signaling consists of both the canonical (WNT/beta-catenin) and noncanonical pathways (43). Canonical signaling begins when WNT ligands bind the Frizzled receptors and the low-density lipoprotein receptor-related (LRP) 5 or LRP-6 co-receptors (43). The signal leads to beta-catenin degradation and activity. Sclerostin and Dickkoff (DKK-1) (produced by osteocytes) inhibit the WNT signaling pathway by interacting with the LRP co-receptors (44–46). The WNT signaling pathway controls mesenchymal stem cell differentiation by repressing both chondrocyte and adipocyte differentiation (47,48). Promotion of WNT signaling leads to increased osteoblast differentiation and proliferation via the action of osteogenic transcription factors such as Runx2 and osterix (48). T1D leads to a decrease in WNT signaling and thus a decrease in osteoblastogenesis (49). Decreased WNT signaling leads to an increase in adipogenesis as the PPARγ signaling pathway is no longer suppressed.

In addition to the decrease in WNT signaling, insulin has an anabolic effect on osteoblasts and hypoinsulinemia can lead to decreased bone formation (50). Insulin increases Runx2, a transcription factor necessary for the differentiation of osteoblasts, by suppressing Twist2 the inhibitor of Runx2 (51). Models of T1D show decreased levels of Runx2 expression and decreased numbers of mature osteoblasts (52).

While the role of osteoblasts in T1D is well understood, osteoclasts have been shown to have differing roles in different studies. In animal studies, osteoclasts have been

found to increase, decrease or stay the same, depending on the study. Clinical studies support no change in T1D osteoclast activity as determined by levels of serum markers of resorption such as deoxypyridinoline, c-terminal telopeptide of type 1 collagen (CTX) (53–56). As noted earlier, T1D leads to a decrease in osteoblastogenesis which can also lead to a decrease in osteoclast number as osteoblasts are needed for the activation and maturation of osteoclasts.

1.2.3. Animal Models of Type 1 Diabetes

In order to better understand and study T1D-induced bone loss, there are several animal models currently in use. Most animal models of T1D are either pharmacologic or spontaneous (57). Pharmacological agents used to model T1D include streptozotocin (STZ), alloxan, dithizone, vacor and 8-hydroxyquinolone (57). Most commonly used is STZ. STZ is a glucose mimetic that diffuses into insulin secreting pancreatic β cells via the GLUT2 glucose transporter (58). STZ leads to β-cell apoptosis and subsequent hypoinsulinemia (58). In mice, the typical STZ dosing regimen used to induce T1D does not cause an increase in osteoclast parameters (59). However, increasing the dose causes an increase in osteoclast activity (59,60). Spontaneous models of T1D include the non-obese diabetic (NOD) and $Ins2^{+/-Akita}$ mouse. NOD mice typically develop diabetes between 12 and 30 weeks of age with only 60% of male mice actually developing a diabetic phenotype (57,61). NOD mice show an increase in expression of genes favoring adipogenesis (PPARg2 ad AP2) as well as an overall increase in adipocyte number (60,62,63). In line with this, osteocalcin (a marker of osteoblast maturation) was

decreased and correlated with low bone density in both NOD and STZ diabetic animals (60,62,63).

The Ins2$^{+/-Akita}$ mouse becomes spontaneously diabetic around 4-5 weeks of age due to a mutation in one allele of the insulin-2 gene. This mutation leads to intracellular accumulation of mutated protein in the pancreas which promotes endoplasmic reticulum stress which ends in β-cell death (64). Ins2$^{+/-Akita}$ mice experience a more dramatic bone loss than STZ diabetic mice, displaying a decrease in osteoblast markers (osteocalcin) and an increase in adipogenesis (65).

1.2.4. Current Osteoporosis Therapies

Current treatments for osteoporosis include bisphosphonates, calcitonin, intermittent PTH, Denosumab (anti-RANKL) and selective estrogen receptor modulators (SERMs). While there seems to be a wide range of therapies for osteoporosis, their use has started to reveal unwanted side effects. Long term use of bisphosphonates has been shown to increase risk of osteonecrosis of the jaw and increased risk of irregular fractures (66). Denosumab inhibits the differentiation and activation of osteoclasts, however it's inhibition of bone resorption resolves within 1 year after stopping treatment (Geusens 2014). Raloxifene (a SERM) may increase the risk of venous thromboembolic disease and stroke. Daily injections of PTH promotes osteoblast differentiation and inhibits osteoblast and osteocyte apoptosis (67). PTH may also inhibit the production of sclerostin, which inhibits bone formation by inhibiting WNT and bone morphogenic protein (BMP) signaling (68). However, teriparatide, recombinant human parathyroid hormone, is

costly, requires cumbersome daily subcutaneous injection and can only be used for a short time (2 years) as it begins to stimulate bone resorption (Geusens 2014). Hormone replacement therapy is successful in the prevention and treatment of osteoporosis, however it has been shown to increase risk of certain cancers (69). While several new therapies are being examined (new formulations of bisphosphonates, sclerostin inhibitors, integrin antagonists, cathepsin K inhibitors) there is real need for therapies which have reduced side effects.

1.3. BONE-GUT LINKAGE

In recent years, studies have identified a link between the gastrointestinal tract and bone health. There are several mechanisms in which the gut plays a role in regulating bone health. These include, but aren't limited to, calcium and vitamin D absorption, serotonin signaling, incretin production, and the microbiome. In addition, our lab previously identified that intestinal inflammation induced by colitis leads to bone inflammation and subsequent bone loss (70,71). Our lab has also identified a link between the intestinal microbiota and bone health. When treated by gavage with the probiotic *lactobacillus reuteri*, both healthy male mice and ovariectomized female mice show an increase in bone density as compared with controls (72,73). Furthermore, we identified a critical role for inflammation since intact female mice that undergo a minimal surgery (dorsal incision) have increases in inflammatory cytokines in the intestine and are then able to respond to treatment with probiotics with a decrease in inflammation and increase in bone volume compared to control, untreated mice (74).

1.3.1. Intestine – General

The intestine is part of the gastrointestinal tract which occurs between the stomach and the anus. The intestinal tract is composed of both the small and large intestine and has several layers of tissue which aid in its function. Starting in the intestinal lumen is the lining of epithelial cells, followed by the lamina propria, the submucosa which contains blood vessels, lymph vessels and nerves (the submucosal enteric nerve plexus), the

muscular layer containing both an inner circular and outer longitudinal layer (with the myenteric nerve plexus between the two layers), and the outer serosal layer.

The intestine is comprised of the small intestine which is responsible for the majority of nutrient absorption and contains many folds and villi, and the large intestine which is responsible for removing water from the stool and is composed of crypts but not villi. The small intestine is comprised of three main areas: the duodenum, jejunum and ileum. The stomach empties first into the duodenum which receives bile and pancreatic enzymes to further digest food (75). The next region of the small intestine is the jejunum. The jejunum is lined with enterocytes which are important for the absorption of nutrients from the food broken down in the duodenum. The ileum follows and is important in the absorption of B12 and bile acids as well as containing Peyer's patches which house immune cells important for the surveillance of the intestine (75). The large intestine consists of the cecum, colon and rectum. The main function of the large intestine is to absorb water.

The intestinal tract plays an important role in the immune system as it is often the first site of exposure to pathogens and toxins. Both the large and small intestine contain gut-associated lymphoid tissue or GALT to protect the body from infection and disease. In addition to lymph tissue, the intestine houses a large population of bacteria (the largest numbers in the colon) called the microbiome which aids in intestinal health by breaking down molecules that cannot be metabolized by the gut as well as preventing the overgrowth of harmful or pathogenic bacteria (75).

1.3.2. Intestinal Epithelial Barrier

The intestine is the gateway from the outside world into the human body; therefore, it requires several defense mechanisms in order to maintain health. The intestinal microbiota serves as the first line of defense against pathogenic organisms as well as contributing to the breakdown of nutrients and secretion of anti-inflammatory molecules (76). The barrier also consists of two mucus layers: the stirred (outer) mucus layer and the unstirred (inner) mucus layer. Both layers are composed of mucins and antimicrobial peptides, however, the outer layer is more dilute and allows the presence of microbes. Mucus layer thickness depends on the location in the intestine with the distal colon having the thickest layer (77). Goblet cells within the epithelium layer are the main source of mucins and antimicrobial peptides. Mucin2 (MUC2) is the predominant mucin found in the large intestine. Mice deficient in MUC2 will spontaneously develop colitis, indicating the importance of the mucus layer in barrier function (Figure 3) (78).

The intestinal epithelial barrier is responsible for the passage of water and nutrients via the paracellular pathway. In addition to this, the intestinal epithelium must provide a protective barrier against pathogens and toxins. Paracellular transit is regulated by tight junctions, which are made up of integral membrane proteins (claudins and occludins), junctional complex proteins (zona occludens), and the cellular cytoskeleton (microtubules, actin). The claudins are a large family of transmembrane proteins which work to either form pores or strengthen the barrier (79,80). In addition to tight junctions, which are on the apical end of epithelial cells, adherens junctions are more basolateral and are made up of cadherin proteins (81). Compromised barrier function has been linked

with active inflammation although whether it is the cause or the consequence has not yet been identified (82–84).

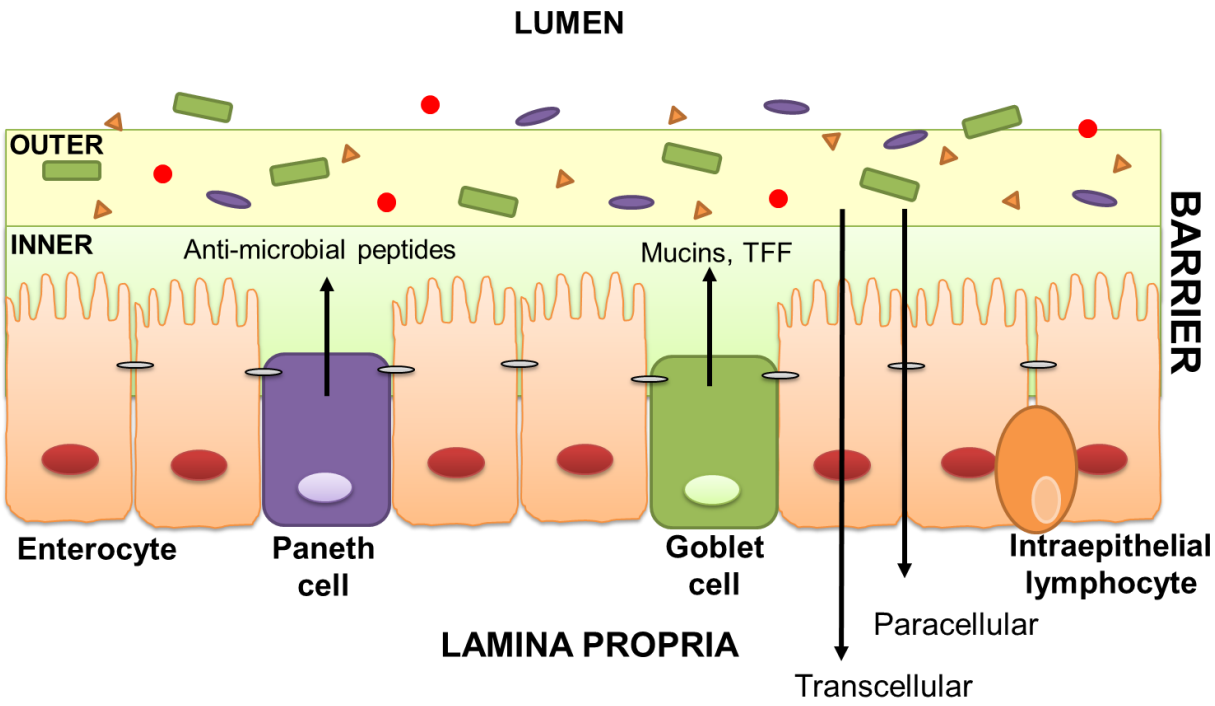

Figure 3. Intestinal Barrier

The intestinal barrier is made up of commensal bacteria (microbiota), two mucus layers (the inner, thinner layer is not shown), goblet cells which produce mucus, epithelial cells connected via tight junctions (adherens junctions and desmosomes not shown), as well as immune cells in both the epithelial layer (Paneth cells) and the lamina propria.

1.3.3. Estrogen and Intestinal Barrier Function

Estrogen is a steroid hormone primarily produced in the ovary of females and the testes of males; however, it can also be converted from androgens in both sexes during both physiological and pathophysiological states. Extragonadal sites of estrogen production include adipose tissue, skin, osteoblasts, osteoclasts, aorta, and the brain. After menopause, adipose tissue is the main source of estrogen. There are several forms of estrogen, 17β estradiol being the most prevalent circulating estrogen. Only a small amount in the plasma is free and active, most is bound to sex hormone binding globulin or albumin. The two primary receptors for estrogen are estrogen receptor α (ERα) and estrogen receptor β (ERβ), both of which are nuclear receptors. ERα is typically associated with secondary sex characteristics and regulation of the menstrual cycle in females and sperm maturation in males (85). ERβ has less of a role in the classical estrogen target tissues and has been found to be more dominant in the brain, cardiovascular system and the colon (86,87).

The role of estrogen in the intestine is not well understood. Several papers have described an increased incidence of inflammatory bowel disease (IBD) in women who have a history of oral contraceptive use (88–90) which resolves after stopping therapy (91). In addition to this, there is an increased risk for developing IBD in postmenopausal women who have a history of or are currently using hormone therapy (89,90). In ovariectomized mice, estrogen treatment predisposes to the development of ulcerative colitis as well as increased tumor development (92). While these studies show that estrogen decreases barrier function to induce IBD, there have been several studies which report that estrogen treatment decreases colonic paracellular permeability and reduces

IBD symptom severity (93–95). A better understanding of the physiologic role of estrogen throughout the intestine is needed in order to understand how it affects intestinal pathologies.

1.3.4. Diabetes and Intestinal Barrier Function

The GI system has the largest immune population in the body and creates an interface between the external environment and the host and has been linked with numerous autoimmune diseases (96). It has been proposed that there is an interplay between changes in the intestinal microbiota, intestinal permeability and mucosal immunity in the intestine which leads to the pathogenesis of type 1 diabetes (T1D) (97). In rodent models of T1D, intestinal permeability or the “leakiness” of the gut has been studied by measuring the amount of disaccharides and monosaccharides in the urine following their oral administration. The spontaneously diabetic biobreeding (BB) rat model of T1D shows an increased amount of permeability in the stomach, small intestine and the colon (98). The increased permeability in both the stomach and small intestine appeared prior to the development of overt diabetic symptoms (98). During the pre-diabetes stage, BB rats that were diabetes prone had increased intestinal permeability, altered tight junction proteins (specifically claudin 7), increased gut infiltration by neutrophils and decreased numbers of gut natural killer cells in comparison to BB rats which were diabetes resistant (99,100).

Examination of intestinal permeability in human patients with T1D has been limited and has shown diverse outcomes. An initial study examining the permeability of the

monosaccharide mannitol in T1D patients showed an increase in intestinal permeability (101,102). However, a subsequent study using pediatric T1D patients showed no difference in the permeability to lactulose or mannitol except in patients with a high-risk allele for celiac disease (24 from Li). Taken together, the role of gut permeability in T1D is not well understood and further research is needed to understand how hypoinsulinemia affects barrier function.

1.4. SUMMARY

The intestine is the barrier between the outside world and the body. Disruptions in intestinal health such as inflammation, decreased barrier integrity, absorption abnormalities and increased cell death can lead to whole body consequences, including decreased bone density. Understanding how intestinal pathology can interact with bone health can lead to the development of new therapeutics to enhance both intestine and bone health.

CHAPTER 2

2. ESTROGEN DEFICIENCY DECREASES INTESTINAL PERMEABILITY

2.1. ABSTRACT

Estrogen deficiency which occurs after menopause or ovariectomy, is associated with decreased bone density and increased fracture risk. As recent studies have elucidated a role for intestinal health in the maintenance of bone density, we wanted to examine the effect of estrogen deficiency on intestinal health. Decreased bone density in inflammatory bowel diseases is attributed to increased intestinal inflammation which leads to an increase in permeability across the epithelial barrier. As estrogen is a known anti-inflammatory agent, we sought to determine if there were changes in intestinal permeability which could result in bone loss. Surprisingly, we found that ovariectomy (OVX) leads to a decrease in whole intestinal permeability as measured *in vivo*. On closer examination of changes in permeability using Ussing chambers, we found that the colon was the only section which lead to significant differences in permeability *ex vivo*. Furthermore, this decrease in colonic paracellular flux was positively correlated with bone volume. Estrogen supplementation either *in vivo* or *ex vivo* in Ussing chambers in OVX (and male) mice revealed an increase in colonic flux which was comparable to control, intact mice. Using the HT-29 MTX E12 colon cell line we found that treatment with estrogen increased flux across the cell monolayer, consistent with our *in vivo* results. When cells were treated with the estrogen and the estrogen receptor (ER) antagonists PHTPP (ERβ antagonist) or G15 (GPR30 antagonist), there was a decrease in paracellular permeability. In contrast to this, treatment with estrogen and ICI (ERα and ERβ antagonist, GPR30 agonist) or MPP (ERα antagonist) lead to no change in

permeability, indicating a role for both ERβ and GPR30 in the alteration of monolayer permeability. Finally, we observed that OVX leads to a decrease in epithelial cell turnover in the intestine and that this was correlated with the decrease in intestinal permeability. Together, our results indicate a role for the intestine in bone health following estrogen deficiency and may lead to new targets for bone loss prevention.

2.2. INTRODUCTION

Menopause is the most common cause of bone loss in women. Osteoporosis-related fractures occur in 1 in every 2 women over the age of 50 and represent a significant health concern in post-menopausal women (103). Along with its associated increase in fracture risk, bone loss may have negative effects on metabolism (104,105). Despite all the anti-resorptive treatments on the market, the number of osteoporotic patients is on the rise in the U.S. and worldwide.

Recent studies have identified a role for intestinal health in the maintenance of bone density (71,72,106–109). While the gastrointestinal tract is responsible for the digestion and absorption of nutrients, it can affect bone density through a variety of mechanisms including modulation of the microbiome, inflammation and secreting bone regulating hormones (72,107,108,110–112). In addition, the gastrointestinal associated lymphoid tissue (GALT) contains the largest populations of immune cells which maintain overall health and mount an attack when the intestinal barrier is damaged or penetrated (113). The GALT is required since the intestine is home to a large and diverse population of bacteria that influence intestinal and overall health (113–117). The intestinal microbiome, along with pre- and probiotics have been shown to increase bone density in healthy animals as well as maintain bone density in the presence of adverse bone pathology (72–74,118,119). Studies with germ free mice have shown an increase in femoral bone density (both trabecular and cortical) when compared to conventionally raised mice indicating the role of the microbiome in bone remodeling (120). Consistent with this finding, depletion of the microbiome through the use of antibiotics in juvenile mice results in an increase in bone density (121). The finding that the gut microbiome can

alter bone density lead to studies investigating the role of both pre- and probiotics in bone health. Prebiotics are non-digestible (by humans) fermentable nutrients which promote the growth of beneficial microorganisms (122). Many studies have identified that supplementation with prebiotics has a beneficial role in mineral metabolism, specifically calcium absorption in both rodents and humans (123,124). Under healthy conditions prebiotics (fructo-oligosaccharides (FOS) and inulin) increase bone parameters (125,126). In ovariectomized, estrogen deficient mice and rats prebiotic treatment was able to prevent femoral bone loss (127,128). In addition to the effects of prebiotics on bone health, probiotics, or live microorganisms which have a beneficial effect on the host, have also been shown to increase bone health. The probiotic *Lactobacillus reuteri* has anti-TNFα properties and was able to increase bone density in healthy male (but not female) mice in addition to preventing bone loss in both female ovariectomized mice and type 1 diabetic male mice. Taken together, these data indicate the health of the microbiome and intestine in maintaining bone density.

While the microbiome plays an important part in bone health, intestinal diseases such as inflammatory bowel disease (IBD) and celiac disease can also impact bone, albeit in a negative way (70,71,129,130) Mouse models of colitis lead to significant bone loss in male mice, but surprisingly, not female mice indicating the role of not only the intestine, but also estrogen in affecting bone health (71). One of the key mechanisms attributed to the pathogenesis of bone via IBD is a leaky intestinal barrier (130–132). As estrogen has anti-inflammatory properties and prevents bone loss in models of IBD, we wanted to identify how estrogen deficiency alters intestinal barrier function, specifically intestinal permeability and determine if these changes are associated with subsequent loss in bone.

In the present study we focused our investigation on how changes in intestinal permeability relate to estrogen deficiency induced osteoporosis. Interestingly, we reveal that ovariectomized balb/c mice have decreased overall intestinal permeability and that the colon is the primary site responsible for this. Furthermore, we show that exogenous estrogen supplementation both *in vivo* and *ex vivo* restores barrier function to that similar to sham control animals. *In vitro* analysis using HT-29 MTX E12 colon cells treated with estrogen and estrogen receptor (ER) antagonists revealed a role for both ERβ and the recently discovered g-protein coupled estrogen receptor, GPR30, in barrier function. Finally, we show that decreased cell turnover in estrogen deficient mice is correlated to the decrease in intestinal permeability seen during estrogen deficiency.

2.3. MATERIALS AND METHODS

2.3.1. Mice

Female and male 10 week old Balb/c mice were purchased from Jackson Laboratories and allowed to acclimate to the animal facility for one week. Female mice were either ovariectomized or sham-operated at 11 weeks of age. At the time of surgery, a 0.25mg 17 β-estradiol 60-day slow release pellet (Innovative Research of America, Sarasota, FL) was subcutaneously implanted behind the shoulder. Mice were given Teklad 2019 chow (Madison, WI) and water ad libitum and were maintained on a 12-hour light/dark cycle. Food and water intake were monitored during the course of the experiment and did not differ between groups. Both female and male mice were sacrificed at 15 weeks of age, 4-weeks post-surgery. All animal procedures were approved by the Michigan State University Institutional Animal Care and Use Committee and NIH (as before).

2.3.2. Microcomputed Tomography

At the time of euthanasia, femurs were fixed in formalin and transferred to 70% ethanol after 24 hours. A GE Explore Locus microcomputed tomography system was used to scan the femurs. Beam strength was set at 80 peak KV and 450 µA with an angle increment of 0.5. 720 views were taken with a voxel resolution of 20 µm. A phantom bone was used with each scan in addition to bones from each experimental group, to maintain consistency throughout scans. A fixed threshold of 865 was used to separate bone from bone marrow. The length of the femur was measured and 1% of the total length, starting

at the distal metaphysis and extending toward the diaphysis was measured for trabecular bone. Bone parameters were computed using GE healthcare MicroView software. Cortical measurements were performed using a 2 x 2 x 2 mm cube centered midway down the bone and using a threshold of 1400 to separate bone from marrow.

2.3.3. Permeability Studies

To determine the permeability of the intestinal tract *in vivo,* mice were gavaged 4 hours prior to harvest with 300 mg/kg of 4 kD fluorescein isothiocyanate (FITC)-dextran. At the time of harvest, blood was collected via cardiac puncture, allowed to sit at room temperature for 5 minutes and spun down at 10,000 RCF for 10 minutes. The resulting serum was collected. Levels of FITC-dextran that had passed into the blood stream from the intestine was measured on Tecan Infinite M1000 plate reader at an excitation wavelength of 485nm and an emission wavelength of 530nm. The times of gavage and blood collection as well as the rate of FITC flux into the serum were calculated and normalized to the sham control for each day of the experiment.

Ussing chambers (Physiologic Instruments) were used to measure paracellular permeability *ex vivo*. Whole-thickness, 1.5 cm intestinal sections, (midway down the duodenum, jejunum, ileum and distal colon; whole thickness including the mucosa, submucosa, muscular layer and serosa) were flushed with PBS, cut along the mesenteric border, mounted on 0.3 cm^2 aperture inserts and placed between two chambers. Each chamber was filled with 5 mL Krebs bicarbonate buffer (Sigma). The buffer was maintained at 37°C and continuously oxygenated with 95% O_2 and 5% CO_2. After a 20-minute equilibration period, 2.2 mg/mL FITC was added to the mucosal chamber.

Rhodamine isothiocyanate dextran (RITC, 10 kD size, 0.55 mg/mL concentration) was also added to the mucosal chamber as a control for tissue integrity. Samples from both chambers were taken in triplicate at 0 and 60 minutes into the study and fluorescence was measured at 485/530nm for FITC and 595/615nm for RITC on a Tecan Infinite M1000 plate reader.

Differences in paracellular permeability and measurement of tissue viability were performed by measuring the transepithelial electrical resistance (TER). This was calculated by dividing successive measurements of the potential difference across the tissue by the transepithelial current (which was obtained by measuring the current necessary to clamp the offset potential to zero and normalized to the surface area of the insert).

To evaluate the effect of estradiol on colonic permeability *ex vivo* in male, sham and ovariectomized mice, 17-beta estradiol (E8875, Sigma) was dissolved in ethanol and placed in the mucosal and serosal chambers at a concentration of 50nM, after the initial 20-minute equilibration period. An ethanol control diluted to the same degree as the estradiol and was used as a vehicle control. Both FITC and RITC were added at the same time as the estradiol and flux measurements taken as indicated above.

2.3.4. Cell Culture Experiments

Human intestinal cells HT-29 MTX-E12 cells (E12) (133), selected for their ability to differentiate into goblet cells, produce mucus and form polarized epithelial layers were used for all studies. E12 cells were grown on porous membranes (0.4 μ) with a 12 mm diameter (Snapwell^{TM} insert, Corning, USA). 8 x 10^4 cells in 200uL of αMEM media were

seeded on the apical side of the membrane and 4mL of αMEM media was added to the basolateral compartment. E12 cells were cultured until confluent at 37°C 5% CO_2, with media changed every other day (α MEM media with 10% FBS and 1% (v/v) penicillin-streptomycin). After reaching confluency, a semi-wet interface was used to produce a polarized epithelial layer and encourage mucous production. This was achieved by culturing cells with 100uL of αMEM media in the apical compartment, 1mL in the basolateral compartment and placing cell culture plates on a nutator in the incubator for mechanical stimulation.

To determine the role of estrogen receptors in intestinal permeability, cells were cultured as stated above with the addition of either 10nM of vehicle (ethanol), 17-β estradiol (E, Sigma), ICI, PHTPP, MPP, G15, ICI+G15, ICI+E, PHTPP+E, MPP+E, G15+E and ICI+G15+E (unless otherwise noted, reagents were purchased from Caymen) in the media of both the apical and basolateral compartments. Cells were treated for 10 days under semi-wet interface conditions. For all permeability studies, Snapwell inserts were removed from their frame and placed into the Ussing chambers for measurement of FITC and RITC dextran flux as noted above for tissue sections.

2.3.5. Intestine RNA Analysis

Immediately following sacrifice, intestine segments were flushed with PBS, snap frozen in liquid nitrogen and stored at -80C. Samples were crushed under liquid nitrogen conditions with a Bessmen Tissue Pulverizer (Spectrum Laboratories, Rancho Dominguez, CA) and RNA was isolated using TriReagent (Molecular Research Center,

Cincinnati, OH). The integrity of the RNA was assessed by formaldehyde-agarose gel electrophoresis. cDNA was synthesized by reverse transcription using Superscript II Reverse Transcriptase Kit and oligoDT (12-18) primers (Invitrogen, Carlsbad, CA) and amplified by real-time PCR with iQ SYBR Green Supermix (BioRad, Hercules, CA), and gene specific primers (synthesized by Integrated DNA Technologies, Coralville, IA). RNA levels of the housekeeping gene hypoxanthine guanine phosphoribosyltransferase (HPRT) do not fluctuate between conditions and was used as an internal control. Primers for real-time PCR can be found in table 1. Real-time PCR was carried out for 40 cycles using the iCycler (Bio-Rad) and data were evaluated using iCycler software. Each cycle consisted of 95C for 15 sec, 60C for 30 sec and 72C for 30 sec. cDNA free samples did not produce amplicons.

2.3.6. Immunohistochemistry

Sections of intestine were fixed in formalin, transferred to 70% ethanol after 24 hours, processed, embedded in paraffin and sectioned on a rotary microtome at 4 - 5μm's. Sections were placed on charged slides and dried at 56°C overnight. Slides were subsequently depariffinized, placed in Tris buffered saline (TBS) pH 7.4 (Scytek Labs – Logan, UT) for pH adjustment. Following TBS, slides were placed in a steamer for epitope retrieval in Citrate Plus pH 6.0 (Scytek) followed by 10-minute room temperature incubation and rinses in several changes of distilled water. Following pretreatment, standard micro-polymer staining steps were performed at room temperature on the Biocare intelliPATH automated staining instrument. All staining steps were followed by

rinses in TBS Autowash Buffer + surfactant (Biocare – Concord, CA). After blocking for non-specific protein with Background Punisher (Biocare) for 5 minutes, sections were incubated with Monoclonal Rabbit anti Ki-67 (SP6) at 1:150 (Cell Marque – Rocklin, CA) in Normal Antibody Diluent (NAD) (Scytek) for 60 minutes. Slides were subsequently incubated with HRP – Polymer (Biocare) 60 minutes. Slides were counterstained in Gill 2 Hematoxylin (Cancer Diagnostics –Durham, NC) for 5 seconds, followed by dehydration, clearing and mounting with synthetic mounting media.

2.3.7. Statistics

Unless otherwise noted, all data is presented as the mean +/- the standard error. Student's t-test, one-way ANOVA and two-way ANOVA were calculated using GraphPad Prism Software. Data was considered significant when $p<0.05$.

2.4. RESULTS

2.4.1. Estrogen Deficiency Leads to Decreased Intestinal Permeability Which is Correlated to Bone Loss

To investigate the relationship between estrogen deficiency, intestinal permeability and bone density, 11 week old balb/c female mice were sham operated or ovariectomized (OVX) and after 4 weeks intestinal permeability and femur bone volume were measured. As expected, microcomputed tomography analysis demonstrated that OVX mice lost a significant amount (31%, p=0.0015) of trabecular bone volume in the distal femoral region compared to sham controls (Figure 4A). To measure *in vivo* whole gut permeability, mice were gavaged with 4 kD FITC-dextran four hours prior to sacrifice. (Figure 4B). OVX mice had a significantly lower FITC flux (42%, p=0.0227) from the intestinal tract to the serum relative to sham mice. Using Pearson's correlation analysis we identified that whole intestinal permeability as measured by FITC in the serum was significantly and positively correlated with bone density (p=0.0017, r^2=0.4478) (Figure 4C).

Past studies indicated that changes in permeability may occur in the colon, however to our knowledge no information exists on the status of small intestinal permeability in estrogen deficient mice. To examine regional differences in intestinal permeability, paracellular permeability was measured in individual sections *ex vivo* using Ussing chambers. No statistical differences were observed in *ex vivo* FITC (Figure 5A-C) or RITC (data not shown) flux in the duodenum, jejunum or the ileum. However, OVX mice had significantly less colonic paracellular permeability (CPP) than sham operated mice (62%, p=0.0294) and this decrease in CPP was significantly correlated with bone volume (p=0.0001, r^2=0.6629, Figure 5D and F). Additionally, transepithelial electrical

resistance (TER), a measure of tissue integrity and barrier function, was increased in OVX animals, confirming a less permeable intestinal barrier with respect to sham animals (Figure 5E).

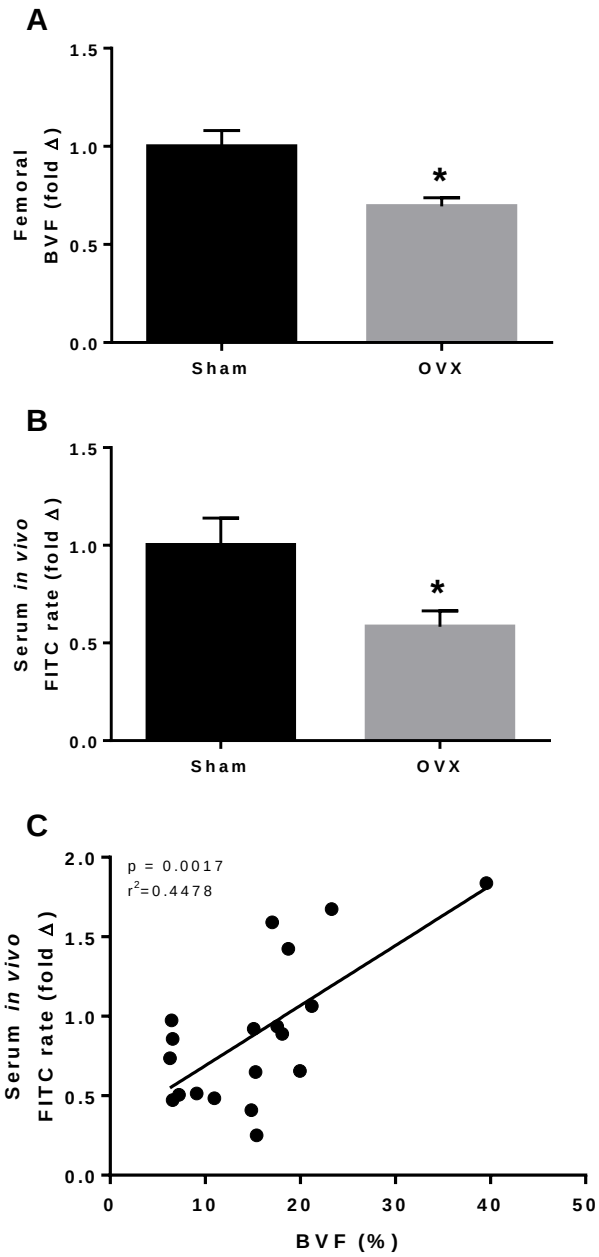

Figure 4. Ovariectomy-Induced Bone Loss is Correlated with Decreased Intestinal Permeability

Female balb/c 11 week old mice were sham operated or ovariectomized (OVX) and at 15 weeks of age serum and femur collected. Trabecular bone volume fraction (BVF) at the distal femur in sham or ovariectomized mice analyzed by microcomputed tomography (A) (n = 22, p = 0.0015). Intestinal permeability was measured by gavaging mice with 300 mg/kg of FITC and measuring serum fluorescence 4 hours later (B) (n = 9-10, p = 0.0227). *In vivo* flux of FITC was correlated with bone volume (C) (p = 0.0017, r^2 = 0.4478). Values represent the mean ± standard error. *p < 0.05 with respect to sham control.

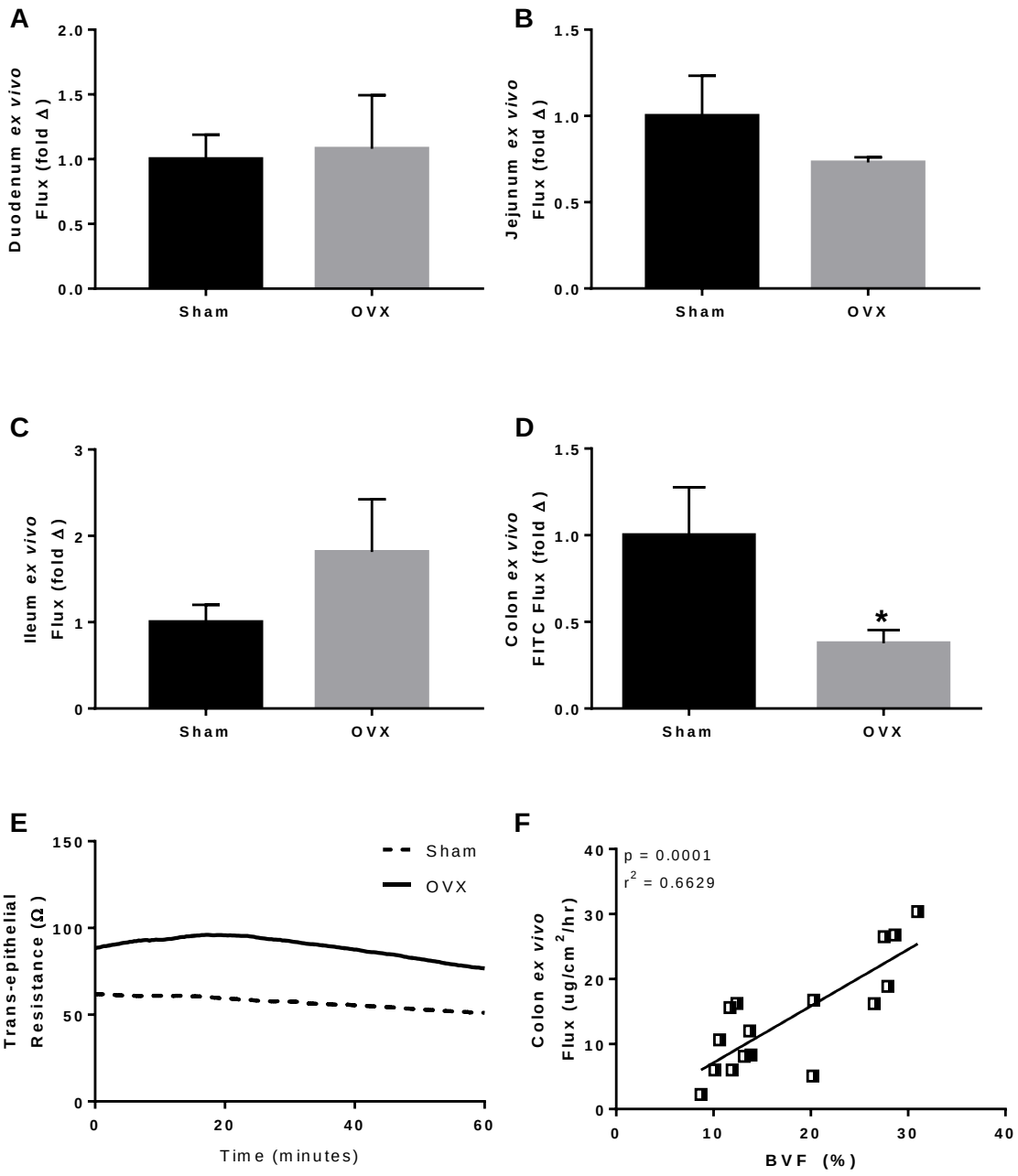

Figure 5. Decreased Intestinal Permeability is Due to Decreased Colonic Paracellular Permeability

Female balb/c 11 week old mice were sham operated or ovariectomized (OVX) and at 15 weeks of age intestinal sections isolated. A-D) Sections of the duodenum, jejunum, ileum and colon were analyzed *ex vivo* FITC permeability in Ussing chambers. (n = 5 – 8). E) Transepithelial electrical resistance was measured over the course of the *ex vivo* experiment. E) Colonic paracellular permeability was correlated with bone volume (F, $p = 0.0001$, $r^2 = 0.6629$). Values represent the mean ± standard error. *$p < 0.05$ with respect to sham control.

2.4.2. Estrogen Increases Colonic Paracellular Permeability

Because OVX causes a reduction in both estrogen and progesterone, to establish a role specifically for estrogen in regulating intestinal permeability, OVX mice were implanted with a subcutaneous slow release (0.25mg/day) 17 β estradiol pellet at the time of ovariectomy (OVX+E). Consistent with a role for estrogen in regulating permeability, *in vivo* intestinal permeability assays revealed that estrogen treatment increased OVX mouse intestinal permeability to levels seen in intact sham mice. Thus, serum FITC levels were higher in the serum of sham and OVX+E compared to OVX mice ($p=0.0083$ and $p=0.0508$, respectively, Figure 6A). Next, we tested the effect of *in vivo* estrogen supplementation specifically on colonic paracellular permeability by measuring *ex vivo* FITC flux. Similar to the in vivo analysis, OVX mice had significantly less FITC flux into the serosal chamber than either sham or OVX+E mice (Figure 6B; $p=0.0027$ and $p=0.0231$, respectively). In other words, estrogen treatment restored OVX mouse colon permeability to the levels observed in intact sham mice. To further confirm that estrogen directly increases colon permeability, segments of distal colon from sham and OVX mice (without subcutaneous estrogen pellet) were placed in the Ussing chambers and 50 nM of exogenous estrogen was added to both the mucosal and serosal chambers (concentration based on dose curve experiment, data not shown). FITC flux measurements revealed that vehicle treated colons from OVX mice had significantly lower paracellular flux than vehicle treated sham colons (Figure 6C, $p=0.0503$). Addition of estrogen to the chambers caused OVX colons to have significantly increased FITC flux in comparison to untreated OVX colons (Figure 3C, $p=0.04$), indicating that estrogen directly increases colon permeability.

Since male mice produce low levels of estrogen similar to OVX mice, we wanted to determine whether the addition of estrogen to male colons *ex vivo* could also increase colonic paracellular flux similar to OVX mice. Distal colons of male mice treated with estrogen (50 nM) in the Ussing chamber had significantly increased FITC levels in the serosal chamber when compared with controls treated with vehicle (Figure 6D, $p < 0.05$).

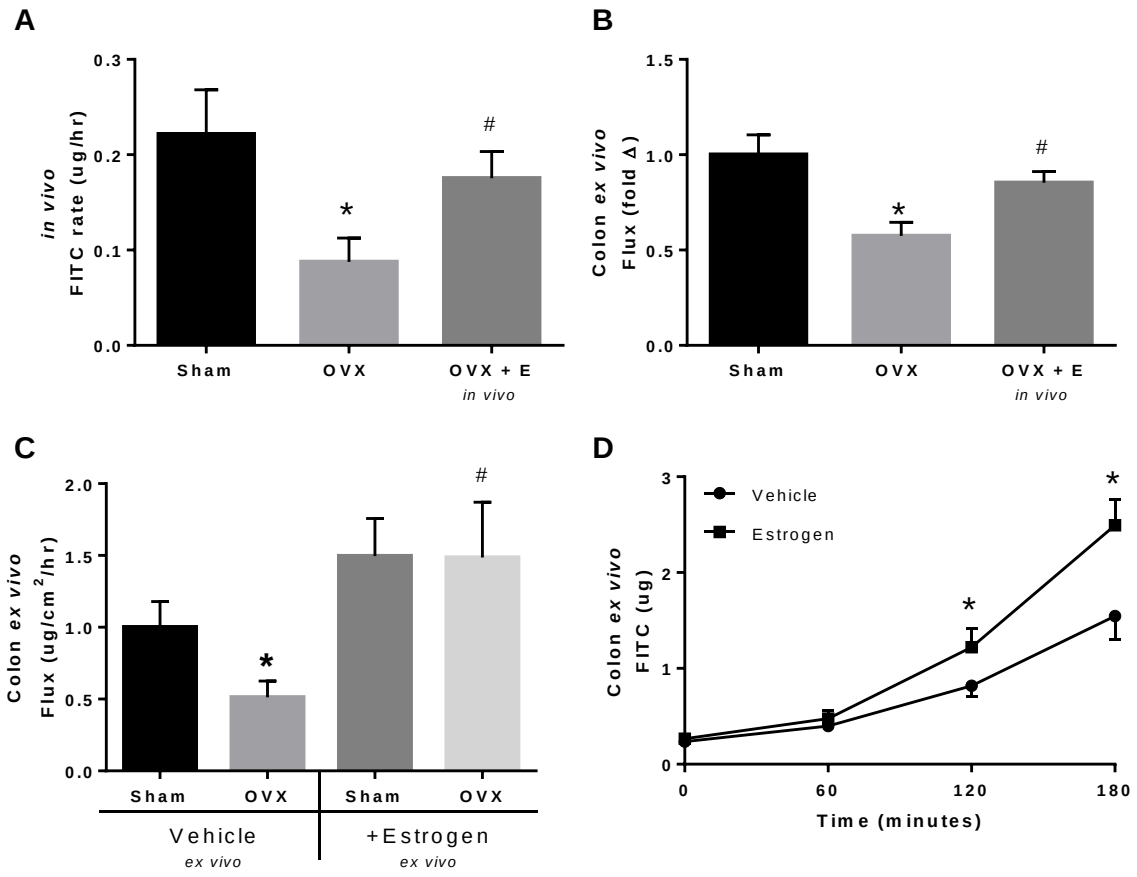

Figure 6. Estrogen Supplementation Prevents OVX-Induced Decrease in Intestinal Permeability

16 week old balb/c sham, OVX, OVX+E and male mice were evaluated for intestinal permeability both *in vivo* and *ex vivo*. Quantification of FITC rate into the serum after *in vivo* oral gavage (A). Flux of FITC across colonic tissue *ex vivo* in Ussing chambers (B). *Ex vivo* measurement of FITC flux across colon tissue with either vehicle (EtOH) or 50 nM of estrogen in sham and OVX mice (C) or male mice (D). Values represent the mean ± standard error. *$p < 0.05$ with respect to sham control and # represents $p < 0.05$ with respect to OVX.

2.4.3. Paracellular Flux is Regulated by Estrogen *in vitro*

To understand how estrogen influences colon permeability, we first sought to examine which estrogen receptors (ER) are expressed in the colon. Of the two nuclear receptors (ERα and ERβ), past studies have indicated low levels of ERα and a key role of ERβ in the intestine (134,135). As expected expression of ERα and ERβ were significantly decreased in OVX and male mice compared to sham controls (ERα - Figure 7A, p= 0.0057 and 0.0066, respectively; ERβ – Figure 7B, p = 0.0031 and p = 0.0152, respectively). Finally, the more recently discovered g-protein coupled transmembrane estrogen receptor, GPR30 was found to be expressed in the colon in all groups, however there was no statistical difference between sham and OVX (Figure 7C). Surprisingly, male mice had significantly less colonic mRNA expression than either sham (p = 0.0064) or OVX (p = 0.0435) mice (Figure 7C).

To determine how estrogen exerts its effect on paracellular permeability, the HT-29 MTX E12 cell line was used. This colonic cell line is able to produce mucus and polarized epithelial layers when grown under semi-wet conditions, and more importantly expresses estrogen receptors (133). Cells were treated for 14 days with 10nM of 17-β estradiol, ICI (ERα and β antagonist), PHTPP (ERβ antagonist), MPP (ERα antagonist), G15 (GPR30 antagonist), or combinations of these drugs. Treatment of the cells with 17-β estradiol (E) significantly increased FITC flux across the cell monolayer with respect to vehicle (EtOH) controls (Figure 8A, p = 0.0009). When the cells were grown with any of the ER antagonists alone, there was no significant difference when compared to the EtOH control except when G15 was combined with ICI (G15+ICI, Figure 8A, p = 0.0333). When cells were treated with a combination of E and the ER antagonists (Figure 8B), the

following treatments were significantly decreased with respect to treatment with E alone: E+PHTPP ($p = 0.0005$), E+MPP ($p = 0.0435$), E+G15 ($p < 0.0001$) and E+G15+ICI ($p < 0.0001$) (Figure 5B). Furthermore, E+PHTPP, E+G15 and E+G15+ICI were significantly lower when compared to E+ICI ($p = 0.0038$, 0.0026 and 0.0013, respectively) and when compared to E+MPP ($p = 0.0112$, 0.0076 and 0.0038, respectively) (Figure 8B).

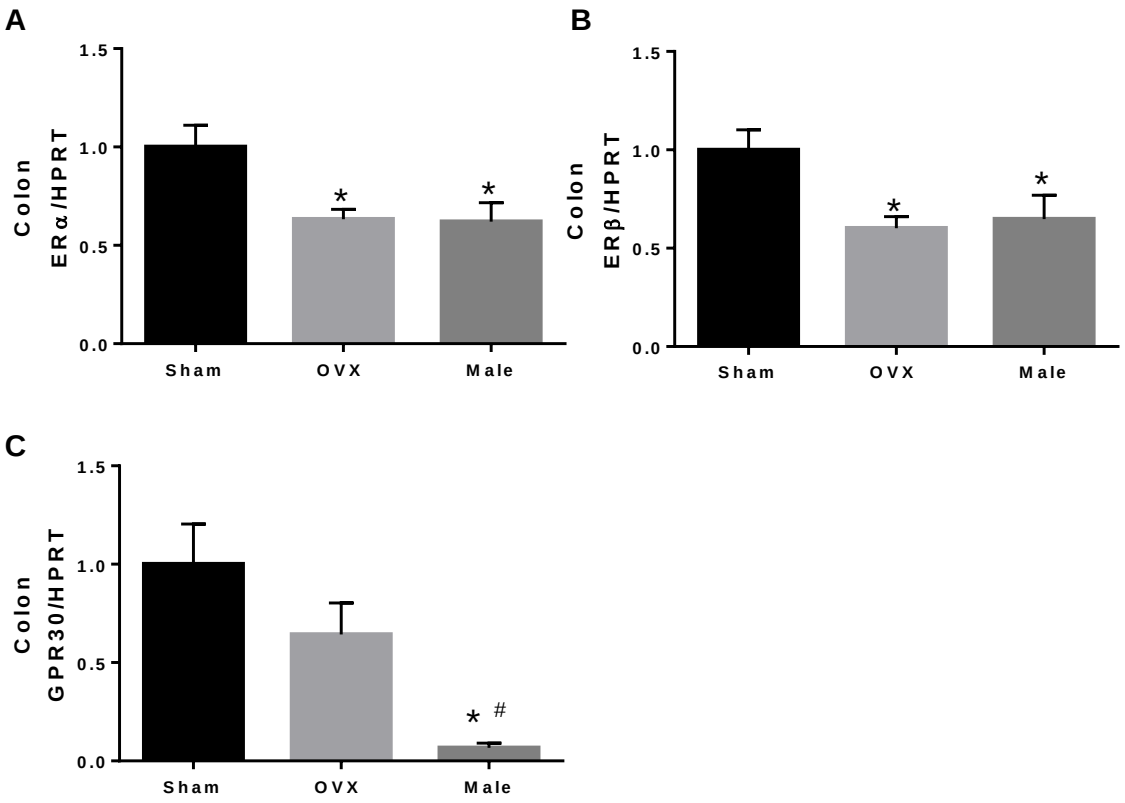

Figure 7. OVX and Male Mice Have Decreased Colonic Estrogen Receptor Expression

Colon tissue from 16 week old mice was examined for mRNA expression of estrogen receptor (ER) α (A), ERβ (B) and GPR30 (C). Genes are expressed relative to the housekeeping gene HPRT. Values represent the mean ± standard error. *$p < 0.05$ with respect to sham control and # represents $p < 0.05$ with respect to OVX.

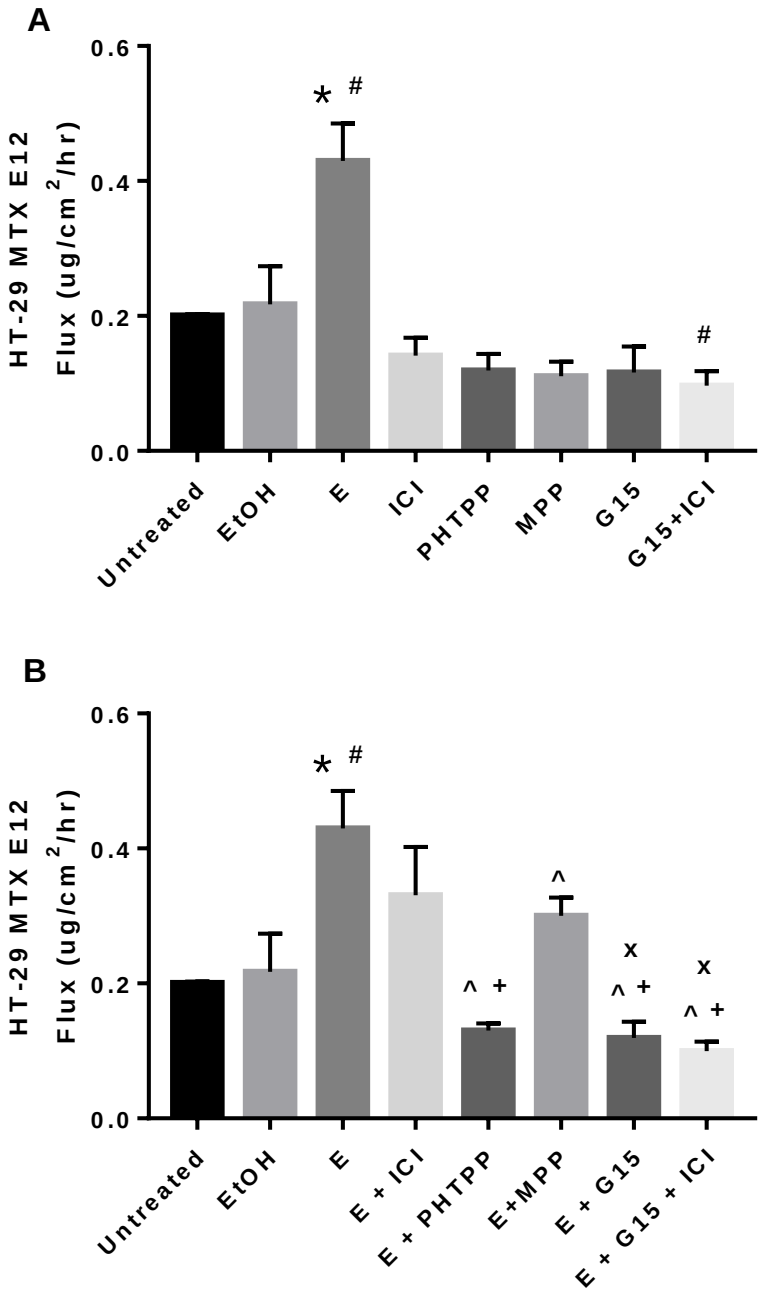

Figure 8. Estrogen Increases Permeability *in vitro*

HT-29 MTX E12 cells were grown in the presence of the various estrogen receptor (ER) antagonists. EtOH was the vehicle for estrogen (E) and the ER antagonist. ICI – ERα and ERβ antagonist; PHTPP – ERβ antagonist, MPP – ERα antagonist, G15 – GPR30 antagonist. Values represent the mean ± standard error. *$p < 0.05$ with respect to untreated cells, #$p<0.05$ with respect to vehicle (EtOH) control, ^ represents $p < 0.05$ with respect to estrogen treated cells, +$p<0.05$ with respect to E+ICI cells, X$p<0.05$ with respect to E+MPP.

2.4.4. Estrogen Deficiency Decreases Colon Epithelial Cell Proliferation

Estrogen has been shown to play a role in cell turnover which is important for normal intestinal function (135).To determine the role of epithelial cell proliferation on colonic permeability, the expression of proliferating cell nuclear antigen (PCNA) was measured by rtPCR. With respect to sham operated mice, OVX significantly decreased the expression of PCNA. However, PCNA expression was significantly increased in OVX mice treated with exogenous estradiol (via subcutaneous pellet) with respect to OVX mice (Figure 9A, $p = 0.0134$, $p = 0.0500$, respectively). Furthermore, colon sections stained for Ki67, a marker of cellular proliferation showed a similar trend with OVX mice having a significantly lower number of Ki67 positive cells per crypt with respect to sham controls and OVX+E mice (Figure 9B, $p = 0.0078$, $p = 0.0047$, respectively; representative images shown in 6D). Interestingly, this decrease in cellular turnover was positively correlated with the *in vivo* flux of FITC from the intestine to the serum (Figure 9C, $p = 0.0022$, $r^2 = 0.4751$).

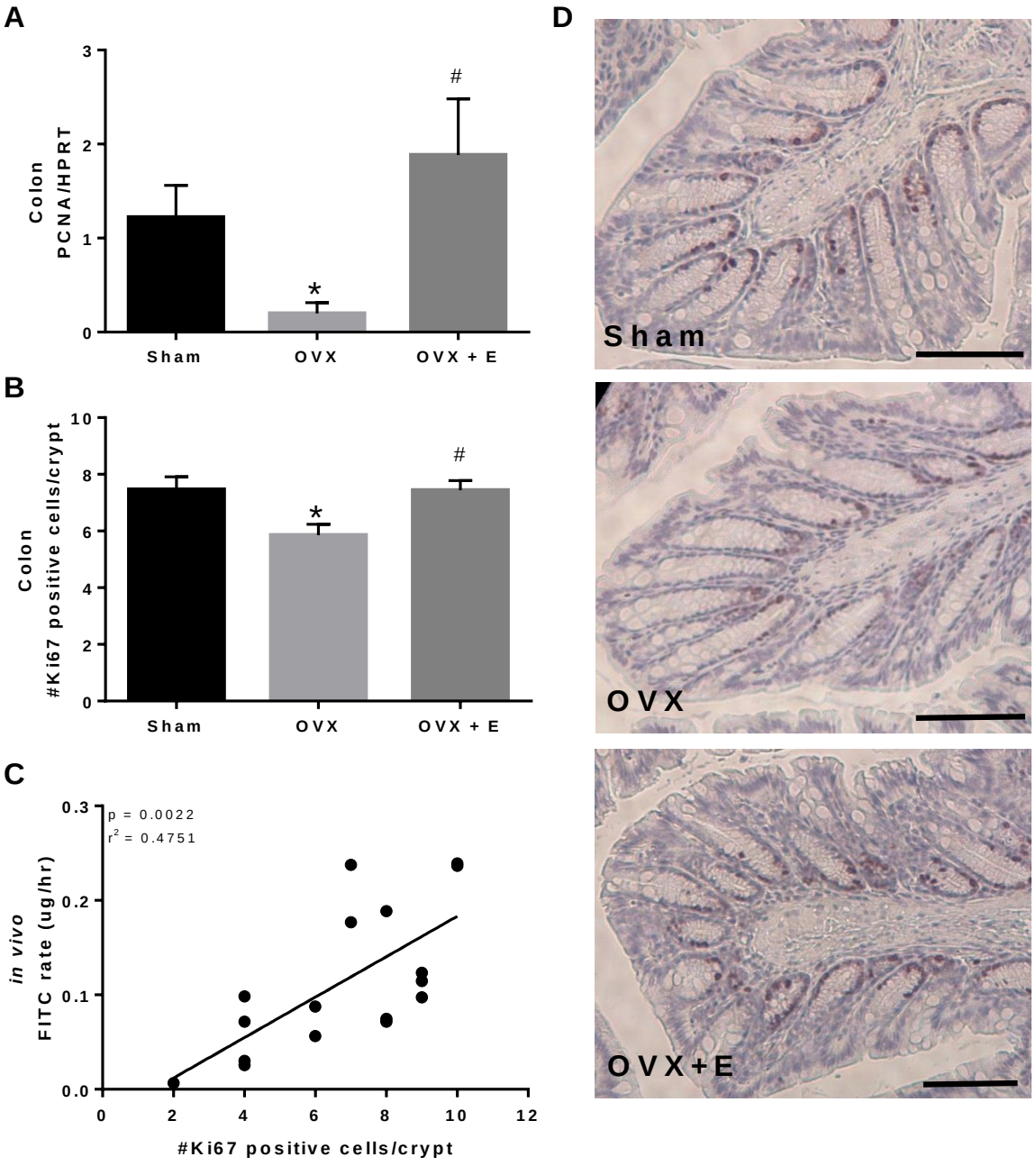

Figure 9. OVX Decreases Colon Cell Proliferation

To determine how intestinal cell turnover effects intestinal permeability colon expression of PCNA and Ki67 were analyzed by rtPCR and immunohistochemistry. mRNA expression of PCNA normalized to HPRT (A). Quantification of Ki67 positive cells in intact colon villi (B) and representative images in D. Correlation between intestinal permeability and the number of Ki67 positive cells. Values represent the mean ± standard error. *$p < 0.05$ with respect to sham control and # represents $p < 0.05$ with respect to OVX.

2.5. DISCUSSION

Menopause is an inevitable life event for all women and as such it is important to understand physiologic changes which occur during estrogen deficiency. As an increasing amount of evidence is revealing a link between intestine and bone health, we found it prudent to investigate changes in the intestine in our model of osteoporosis.

There is evidence to suggest that estrogen alters intestinal barrier integrity by altering intestinal permeability. In a previous study using ovariectomized Wistar rats, colonic paracellular permeability was increased and was observed to decrease dose-dependently with estrogen treatment (oestradiol benzoate) (136). Consistent with this, colonic paracellular permeability decreases during the oestrus (high levels of estrogen) phase of the rat estrogen cycle when compared to the dioestrus (low levels of estrogen) phase (136). Estrogen receptor β (ERβ) is the predominant estrogen receptor in the intestinal tract. Thus, it is not surprising that whole body ERβ knockout mice display altered intestinal cell proliferation, decreased apoptosis and abnormal villus/crypt architecture throughout the intestine (134). One potential mechanism that could account for estrogen effects on the intestine is through its alterations in tight junction and adhesion molecules which would alter intestinal permeability. In models of inflammatory bowel disease (IL-10 deficient mice and HLA-B27 rats), ERβ mRNA levels were decreased and colonic permeability increased (95). Similarly, treatment of cell culture models of intestinal epithelial layers (HT-29, T84, Caco-2) with estrogen receptor antagonists increases permeability while estrogen treatment prevents this outcome (95,136).

Consistent with the previous studies, we found that changes in intestinal permeability during estrogen deficiency are a result of altered colonic permeability.

Surprisingly, however, we saw the opposite result with intestinal permeability decreasing following ovariectomy rather than increasing. Animal models used in previous studies included Wistar rats, HLA-B27 rats and IL-10 knock out mice (bred on the 129 Sv/Ev background) and thus there may be a difference in outcomes based on the animal model and the strain of mouse used. So far, this is the first study to our knowledge which use balb/c mice to investigate the role of estrogen in intestinal permeability. Balb/c mice have been shown to have differences in emotional stress response as well as differences in their immune system when compared with other strains (137). As the intestine houses a large immune cell population, it is possible that the differences seen in our study are attributed to changes in immune response. It will be crucial in future studies to examine the how the intestinal immune system impacts intestinal permeability in different animal models and mouse strains.

For estrogen to exert its effects, the various estrogen receptors (ERs) must be expressed. Consistent with other studies examining estrogen receptor in the intestine, we found that OVX and male mice have decreased expression of both ERα and β (86,138). This is the first study, to our knowledge, showing that the G-protein coupled estrogen receptor, GPR30 is expressed in the colon in both sham and OVX mice but expressed significantly lower in male mice. To further examine how ERs play a role in colonic permeability we chose to use the HT-29 MTX E12 (E12) cell line due to its ability to express ERs, form polarized epithelial layers, as well as possessing goblet cells able to produce mucus (133,139). While previous studies have shown that *in vitro* treatment with 17-β estradiol (E) leads to a decrease in FITC flux across the monolayer, we found that E treatment in E12 cells actually increases paracellular FITC flux (93,95). This difference

in monolayer permeability could be attributed to the difference in cell line along with the length of time the cells were grown and the length of E treatment prior to permeability measurements. To ensure the formation of the polarized monolayer, E12 were grown to confluency and then placed on a nutator with semi-wet conditions for 14 days with E being added when cells were placed on the nutator. Previous studies grew cells to confluency and treated them with E over a shorter span (8 hours).

Interestingly, contrary to previous studies, we observed no difference in permeability when cells were treated with ER antagonists without the addition of E (93,95). This again can be attributed to the difference in cell line, growth time and duration of treatment. When we added E concurrently with ER antagonist, we observed no difference in permeability in the E+ICI treated cells with respect to cells treated with E. This finding was surprising as E12 cells primarily express ERβ and ICI is an antagonist at this receptor (as well as ERα). This is even more surprising considering that E+PHTPP, an ERβ antagonist, lead to a significant decrease in FITC flux. We believe that the lack of change in flux in the E+ICI treated cells is due to the fact that ICI can act as an agonist at the recently discovered G-coupled protein receptor GPR30 (140). This finding is further explained by inhibiting GPR30 with the antagonist G15. Cells treated with either E+G15 or E+G15+ICI lead to a significant decrease in FITC flux across the monolayer indicating a role for both ERβ and GPR30 in the health of the intestinal epithelial barrier.

In addition to changes in intestinal barrier function after ovariectomy, we have shown that estrogen deficiency leads to a decrease in cellular proliferation. This finding is in agreement with a study by Javid et al, 2005 which found that ovariectomy leads to a decrease in BrdU migration up the colon crypt, indicating a decrease in turnover (141).

Cell turnover in the intestine is important for rapid replacement of damaged cells along the villi/crypt (via infection, trauma, cell death, etc…). Proliferation and migration of the enterocytes is tightly regulated to maintain both functional and structural integrity of the epithelial barrier. Interestingly, ERβ knock out mice have an increase in colonic BrdU migration, a decrease in apoptosis, decreased adherens junction protein expression as well as abnormalities in tight junctions and desmosomes (134). However, during this whole body knock-out of ERβ, estrogen was still being produced in these mice and therefore could be exerting its effects on other receptors (ERα and GPR30) which may have a different effect on cellular proliferation than ERβ . More studies are needed to determine the effect of estrogen as a whole on intestinal cell turnover.

The present study shows an interesting role for estrogen in maintaining intestinal health. Contrary to previous studies, estrogen deficiency in balb/c mice leads to a decrease in colonic permeability. Furthermore, this decrease in paracellular permeability is positively correlated with decreased bone density seen in OVX mice. It could be, that by altering both the cellular turnover and barrier function, estrogen deficiency is decreasing preventing nutrient (primarily calcium) absorption that is critical for healthy bone remodeling. Evidence for the regulation of calcium absorption by estrogen has been shown in several studies where decreased intestinal and renal calcium absorption have been observed following estrogen deficiency (142–147). Though the exact mechanism is not well understood, it is thought that estrogen deficiency leads to down regulation of the expression of transcellular calcium transport proteins plasma membrane calcium pump 1b (PMCA1b), transient receptor potential cation channel subfamily V member 5 (TRPV5) and calbindin-D 28K (CaBP28k) (142). Furthermore, estrogen has been found to increase

vitamin D receptor (VDR) gene and protein expression as well as $1,25(OH)_2D_3$ activity in the colon indicating an indirect role of estrogen in calcium regulation (148,149). In addition to the transcellular uptake of calcium, calcium can also be absorbed paracellularly (150). In fact, the primary route of calcium uptake in the intestine is via the passive, paracellular route (151). A decrease in paracellular flux could lead to decreased intestinal absorption of calcium leading to decreased bone density as seen during estrogen deficiency.

Taken together, our studies indicate a role for estrogen in the proper maintenance of the intestinal epithelial barrier and that intestinal permeability is correlated to bone loss. Understanding how estrogen deficiency alters intestinal health can lead to prevention strategies or the development of new therapies for post-menopausal osteoporosis.

CHAPTER 3

3. MDY PREVENTS ESTROGEN DEFICIENCY - INDUCED BONE LOSS

3.1. ABSTRACT

Osteoporotic fractures are estimated to occur in 1 in 2 women and can result in devastating consequences. As current therapeutics are lacking, prevention and new therapy targets are essential. One new target of interest is the intestine as recent research has elucidated a role for the gut-bone axis in maintaining bone density. Estrogen deficiency leads to changes in intestinal function including calcium absorption as well as altered intestinal permeability. As estrogen has been shown to decrease cervical mucus, we wanted to determine if it can also alter intestinal mucus, an important part of the epithelial barrier and intestinal health. We report for the first time that estrogen deficiency (OVX) leads to a decrease in intestinal mucus production and that this is prevented with *in vivo* estrogen supplementation. We treated sham and OVX balb/c mice with MDY, a high molecular weight polymer which can integrate into and maintain the intestinal mucus layer. Treatment with MDY lead to an increase in MUC2 expression and an increase in the area of mucus staining in colon sections in OVX mice. Further examination of the main goblet cell products in the colon (MUC3 – glycocalyx and TFF3 – epithelial cell restitution) revealed a decrease in OVX animals which was prevented with MDY treatment. OVX also lead to a decrease in overall epithelial cell proliferation as well as decreased levels of the transcription factor KLF4 which is necessary for goblet cell differentiation both of which were partially prevented by MDY treatment. Permeability studies using Ussing chambers were carried out to identify if MDY treatment altered colonic permeability in OVX mice. FITC flux across tissue sections revealed a decrease

in colonic permeability which was prevented by MDY treatment. Finally, treatment with MDY was able to prevent bone loss in OVX mice, indicating the role of intestinal health and mucus production in maintaining bone density.

3.2. INTRODUCTION

Over 2 million osteoporosis-associated fractures occur annually in the United States. Postmenopausal, estrogen-deficient women are particularly at risk. One out of two postmenopausal women will fracture a bone, which can lead to increased dependence, depression and mortality (>20% will die within one year of a fracture). While many drugs are available to treat osteoporosis, the disease has yet to be successfully prevented or cured. New therapeutic targets and treatments are needed in this area, given that the National Osteoporosis Foundation predicts that by 2025 osteoporosis will be responsible for approximately 3 million fractures and $25.3 billion in costs annually in the United States. The impact of menopause/estrogen deficiency on bone loss has been a key focus of research for decades (11,12,152,153) and accordingly the majority of therapeutics have been developed to directly target bone and its cells. However, estrogen deficiency also affects other organs that could play a role in regulating bone density (142,149). One organ signaling pathway that has recently received a lot of attention is the gut-bone axis. Recent studies support a role for intestinal health in the prevention of bone loss. Decreasing intestinal inflammation or altering the gut microbiome leads to the prevention of bone loss in models of inflammatory bowel disease, ovariectomy and surgery and can even increase bone in healthy male mice (70–74,119). Understanding the role of estrogen in the intestine could lead to identification of future therapeutics to target bone health.

The intestinal epithelium maintains the barrier between the body and the luminal contents. The integrity and function of this barrier is essential for proper nutrient absorption and protection from pathogenic species and disease (131,132,154).

Surprisingly few studies have characterized changes in the intestine after menopause and during estrogen deficiency. These studies indicate changes in barrier function, calcium absorption and cell turnover (93,94,135,155–157). An essential element of the intestinal epithelial barrier is the mucus layer (158). The goblet cells of the intestinal tract produce mucins which form both the loose, outer layer which houses the microbiome and the thick, adherent inner layer which works to prevent bacteria from gaining access to the epithelial layer (158–161). In addition to mucins, goblet cells also produce anti-microbial peptides and trefoil factors to aid in barrier function (158). Past studies indicate that estrogen can modify mucus production in the cervix and one study suggests a role for estrogen in mucus regulation in intestinal cells *in vitro* (155,162).

MDY-1001 (MDY) is a high molecular weight polymer that can act as a mucus supplement and is neither absorbed nor metabolized by the intestinal tract. High molecular weight polymers similar to MDY, such as polyethylene glycol (PEG) have been shown to have a wide array of benefits to the intestine. Pretreatment with PEG was shown to decrease intestinal radiation damage in the intestines of rats as well as prevent adherence and infection by *Pseudomonas aeruginosa* a common pathogen following radiation treatment (163–165). PEG treatment has also been shown to preserve intestinal grafts better than the current preservation treatments (166–168). These studies indicate a role for polymers in maintaining tissue integrity/health by decreasing permeability, increasing tight junction protein expression, decreasing tissue inflammation, decreasing bacterial pathogenesis and decreasing apoptosis (163–168).

The present study investigates the role of estrogen in regulating intestinal mucus production in the mouse colon. We found that estrogen deficiency leads to a decrease in

mucus production both *in vivo* and *in vitro*. To determine how changes in intestinal mucus following ovariectomy impact bone density we restored intestinal mucus production and identified a reduction in estrogen-deficiency bone loss. Consistent with a role for mucus and barrier function for maintaining bone density, we found goblet cell area and mucus production are positively correlated with bone density.

3.3. MATERIALS AND METHODS

3.3.1. Mice

Female 10 week old Balb/c mice were purchased from Jackson, allowed to acclimate for one week and either sham operated or ovariectomized (OVX) at 11 weeks of age. Mice with estrogen supplementation (OVX+E) were subcutaneously implanted behind the shoulder with a slow release 17 β estradiol pellet at the time of surgery (Innovative Research, FL). Mice were given Teklad 2019 chow (Madison, WI) ad libitum, provided with either normal water or water containing 1% MDY and maintained on a 12-hour light/dark cycle. Food and water intake as well as body mass were monitored throughout the experiment. In addition, MDY treated mice were gavaged with 2 mg/kg body weight of MDY in sterile water 3 times a week. Control animals were gavaged with water. Animals were harvested after 4 full weeks of treatment. All animal procedures were approved by the Michigan State University Institutional Animal Care and Use Committee and NIH guidelines.

3.3.2. RNA Analysis

Immediately following euthanasia intestine segments were flushed with PBS, snap frozen in liquid nitrogen and stored at -80°C. Samples were crushed under liquid nitrogen conditions and RNA was isolated using TriReagent (Molecular Research Center, Cincinnati, OH). RNA integrity was verified via formaldehyde-agarose gel electrophoresis. cDNA was then synthesized by reverse transcription using Superscript II Reverse Transcriptase Kit and oligoDT (12-18) primers (Invitrogen, Carlsbad, CA) and amplified

by real-time PCR with iQ SYBR Green Supermix (BioRad, Hercules, CA) and amplified gene specific primers (synthesized by Integrated DNA Technologies, Coralville, IA). In order to verify that all samples have the same concentration, the housekeeping gene hypoxanthine guanine phosphoribosyltransferase (HPRT) was used as an internal control. Real-time PCR was carried out for 40 cycles using the iCycler (BioRad) and data were evaluated using iCycler software. Each cycle consisted of 95°C for 15 seconds, 60°C for 30 seconds and 72°C for 30 seconds. Samples lacking cDNA were used as controls to verify no production of amplicons without cDNA present.

3.3.3. Immunohistochemistry

Intestine sections were fixed in formalin, transferred to 70% ethanol after 24 hours, processed, embedded in paraffin and sectioned on a rotary microtome at 4 – 5 μm's. Sections were placed on charged slides and dried at 56°C overnight. Slides were subsequently depariffinized and placed in Tris buffered saline (TBS) pH 7.4 (Scytek Labs – Logan, UT) for pH adjustment. Slides were stained with periodic acid and Schiff's reagent (PAS) as indicated by manufacturer (Sigma). Slides were then counterstained in hematoxylin (Sigma), followed by dehydration, clearing and mounting with synthetic mounting media. At least 5 pictures of each slide were taken and analyzed blinded via ImageJ software. Using a color deconvolution plugin, regions of interest of each of the main colors were selected and subsequently separated. The separated PAS stain was them quantified as the average PAS stain area over the total area of tissue.

3.3.4. Permeability Studies

In order to determine the permeability of the whole intestinal tract *in vivo,* mice were gavaged 4 hours prior to harvest with 300 mg/kg of 4 kD fluorescein isothiocyanate dextran (FITC). At the time of harvest, serum was collected and fluorescence was measured on a Tecan Infinite M1000 plate reader at an excitation wavelength of 485nm and an emission wavelength of 530 nm. Ussing chambers (Physiologic Instruments) were used to measure paracellular permeability *ex vivo*. Whole-thickness intestinal sections (mucosa, submucosa, muscular layer and serosa) were flushed with PBS, cut along the mesenteric border, mounted on 0.3 cm^2 aperture inserts and placed between two chambers. Each chamber was filled with 5mL Krebs bicarbonate buffer (Sigma). The buffer was maintained at 37°C and continuously oxygenated with 95% O_2 and 5% CO_2. After a 20-minute equilibration period, 2.2 mg/mL FITC was added to the mucosal chamber half. 0.55 mg/mL of 10 kD rhodamine isothiocyanate dextran (RITC) was also added to the mucosal chamber as a control for holes in the tissue. Samples from both chambers were taken in triplicate at 0 and 60 minutes and fluorescence was measured at 485/530nm for FITC and 595/615 nm for RITC on a Tecan Infinite M1000 plate reader

Differences in paracellular permeability and measurement of tissue viability were performed by measuring the transepithelial electrical resistance (TER). This was calculated by dividing successive measurements of the potential difference across the tissue by the transepithelial current (which was obtained by measuring the current necessary to clamp the offset potential to zero and normalized to the surface area of the insert).

3.3.5. Cell Culture Studies

The human intestinal cell line HT-29 MTX-E12 cells (E12) was used for all studies for their ability to differentiate into goblet cells, produce mucus and form polarized epithelial layers. E12 cells were grown on porous membranes (0.4 µm) with a 12 mm diameter (Snapwell™ insert, Corning, USA) that are supported by a detachable ring. Cultures were started by seeding 8 x 10^4 cells in 200 uL of αMEM media on the apical side of the membrane and 4mL of αMEM media to the basolateral compartment. E12 cells were grown in this way until confluent, with media being changed every other day (αMEM media with 10% FBS and 1% (v/v) penicillin-streptomycin). After reaching confluency, a semi-wet interface was used to produce a polarized epithelial layer and encourage mucous production. This was achieved by using 100 uL of αMEM media in the apical compartment, 1 mL in the basolateral compartment and placing cell culture plates on a nutator in the incubator for mechanical stimulation.

Treatment of cells with MDY consisted of adding 5% MDY to αMEM media. To determine the role of estrogen receptors in intestinal permeability, cells were cultured as stated above with the addition, to the media of both apical and basolateral compartments, of either 10 nM of vehicle (ethanol) or 17-β estradiol (E, Sigma) and/or ICI, PHTPP, MPP, G15, ICI+G15, ICI+MDY, PHTPP+MDY, MPP+MDY, G15+MDY and ICI+G15+MDY (unless otherwise noted, reagents were purchased from Caymen). Cells were treated for 10 days under semi-wet interface conditions. To quantify mucus production, cells were fixed in 4% formaldehyde in PBS for 1 hour and subsequently stained with a periodic acid Schiff stain (PAS) per the manufacturers protocol (Sigma). At least 3 images of each well

were taken at 10X and blindly scored for PAS area over the total cell area using ImageJ software.

3.3.6. Microcomputed Tomography

At the time of death, femurs were fixed in formalin and transferred to 70% ethanol after 24 hours. A GE Explore Locus microcomputed tomography system was used to scan the femurs. Beam strength was set at 80 peak KV and 450 µA with an angle increment of 0.5. 720 views were taken with a voxel resolution of 20 µm. A phantom bone was used with each scan in addition to bones from each experimental group, to maintain consistency throughout scans. A fixed threshold of 782 was used to separate bone from bone marrow. The length of the femur was measured and 1% of the total length, starting at the distal metaphysis and extending toward the diaphysis was measured for trabecular bone. Bone parameters were computed using GE healthcare MicroView software. Vertebral trabecular bone was measured in a similar fashion as the femur in the 3rd lumbar vertebra by selecting the trabecular bone within the body. Cortical measurements were performed using a 2 x 2 x 2 mm cube centered midway down the bone and using a threshold of 1360 to separate bone from marrow.

3.3.6. Statistical Analysis

Unless otherwise noted, all data is presented as a mean value +/- the standard error. Student t-tests or one-way ANOVA analysis (using Fishers Test for multiple

comparisons) was performed via GraphPad Prism Software. Data was considered significant when p-values were less than 0.05.

3.4. RESULTS

3.4.1. Estrogen Deficiency Decreases MUC2 Expression and Goblet Cell Area

Estrogen has been shown to regulate cervical mucus (162) and mucus production *in vitro* (155), however the role of estrogen in regulating intestinal mucus production *in vivo* has yet to be established. Given that intestinal mucus production is highest in the colon (77), colon tissue from sham operated intact female mice as well as ovariectomized (OVX) and OVX mice with estrogen supplementation (OVX+E) mice were analyzed for the expression of MUC2, the main gel-forming mucin in the intestine. While estrogen deficiency (OVX) significantly lower expression of MUC2 with respect to sham controls ($p = 0.0198$), treatment with estrogen restored expression levels to that of sham mice (Figure 10A). MUC2 is produced by goblet cells, therefore we examined if estrogen affects goblet cells in the colon. We quantified the mucus glycoproteins within goblet cells by staining with the periodic acid Schiff (PAS) stain. Measurement of the area of PAS stain, or goblet cell area was decreased in OVX mice compared to sham mice and that estrogen treatment was able to prevent goblet cell changes (Figure 10B). Pearson's correlation analyses indicated that goblet cell area positively correlates with femur trabecular bone volume (Figure 10C, $p = 0.0006$, $r^2 = 0.4867$). (NOTE: Goblet cell number will be quantified prior to publication).

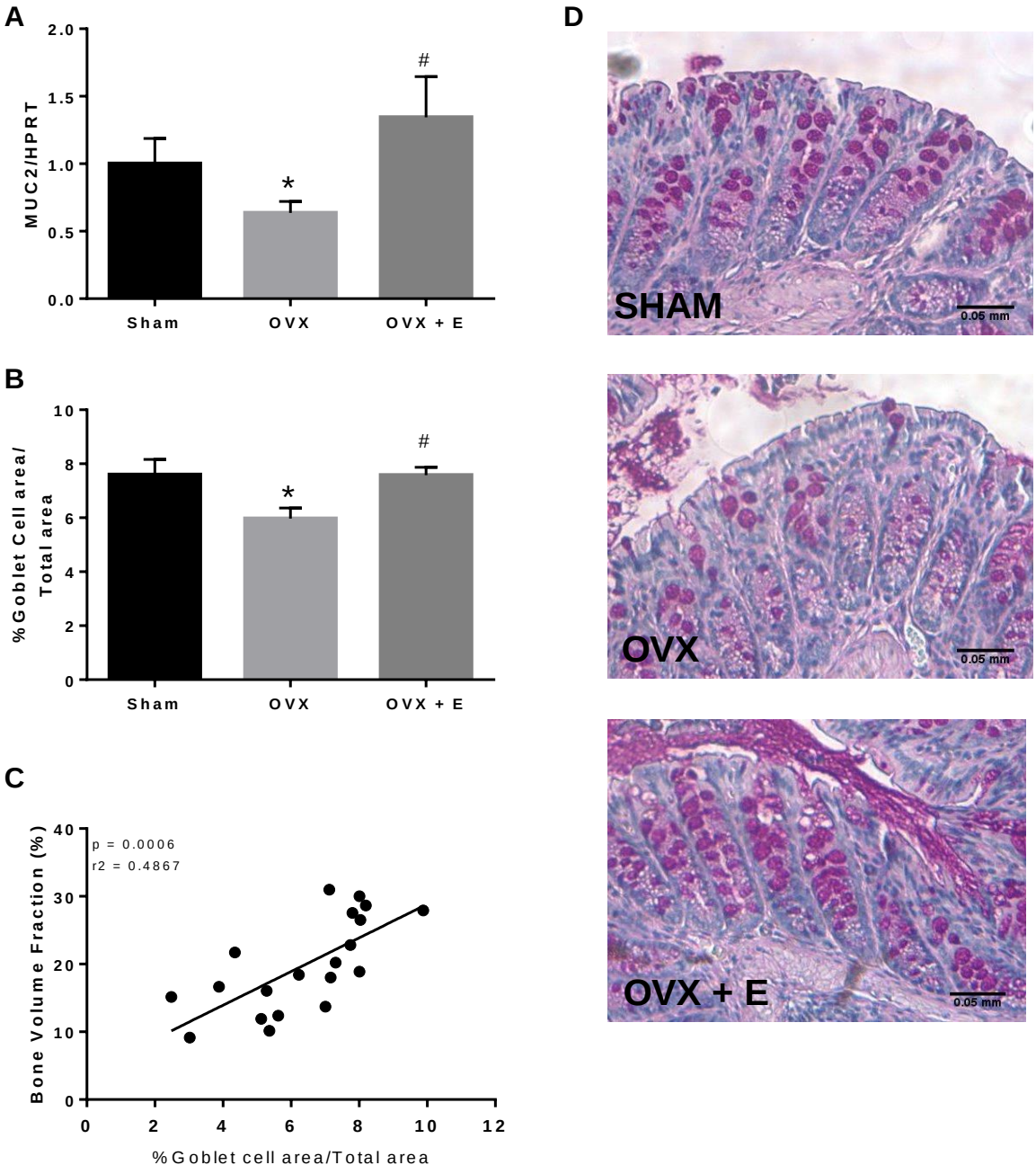

Figure 10. Estrogen Deficiency Decreases MUC2 Expression and Goblet Cell Area

To examine the role of estrogen in intestinal mucus production, colons from sham, OVX and OVX+E mice were analyzed for MUC2 expression (A) via qPCR and goblet cell area via PAS staining (B and D). Goblet cell area was correlated with bone volume fraction (C). Values represent the mean +/- the standard error (n = 5 – 10). *p<0.05 with respect to sham control. #p<0.05 with respect to OVX control.

3.4.2. MDY Increases Mucus Production which is Correlated with Bone Volume

To test the role of the reduced mucus production (seen in estrogen deficient mice) in the regulation of bone density, we used a surrogate mucus, MDY, which is a high molecular weight polymer that is neither absorbed or metabolized (Figure 11) by the intestinal tract. Following sham or OVX surgery, mice were treated for 4-weeks with MDY and colon segments were collected. As previously shown, OVX significantly decreased MUC2 expression in the colon when compared to sham controls (Figure 12A, $p = 0.0269$). Interestingly, OVX animals treated with MDY had significantly increased MUC2 expression with respect to OVX controls (Figure 12A, $p = 0.0041$). Similarly, PAS staining for mucus glycoproteins found in goblet cells revealed that MDY treatment prevented the decrease seen in OVX animals (Figure 12B). In agreement with supplementation of endogenous estrogen, Pearson's correlation revealed a positive correlation between goblet cell area and BVF (Figure 12C, $p = 0.0224$, $r^2 = 0.3404$).

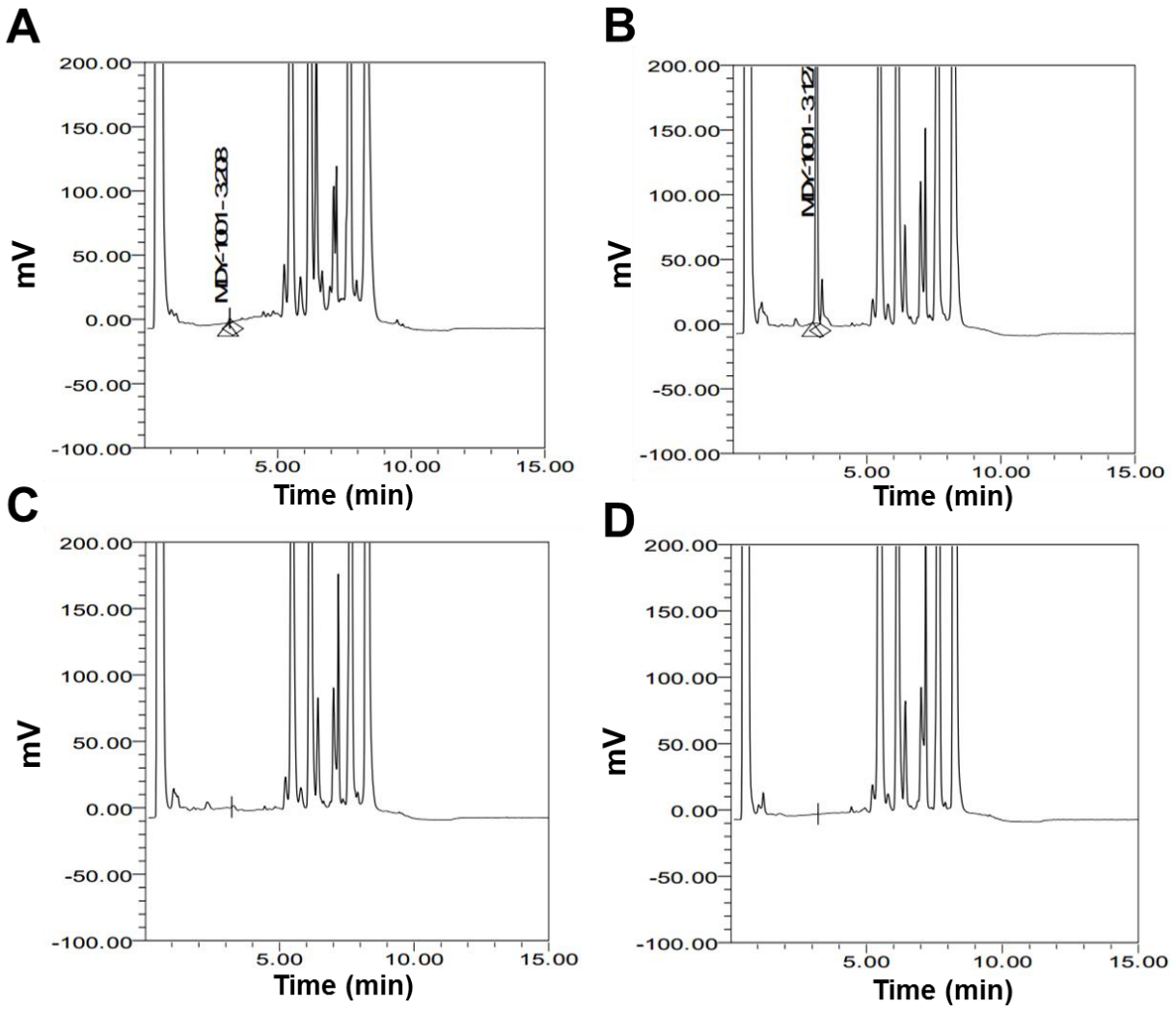

Figure 11. MDY is Not Present in Blood Following Administration

High performance liquid chromatographic (HPLC) determination of MDY presence in the serum of treated rats. A) Representation of the lower limit of quantitation 5.0 µg/mL. B) Representation of the upper limit of quantitation 50 µg/mL. C) Representation of an unspiked (blank) sample. D) Representation of rat dosed at 500 mg/kg/day for 7 days (all samples from all dosing groups were found to be below the lower limit of quantitation.

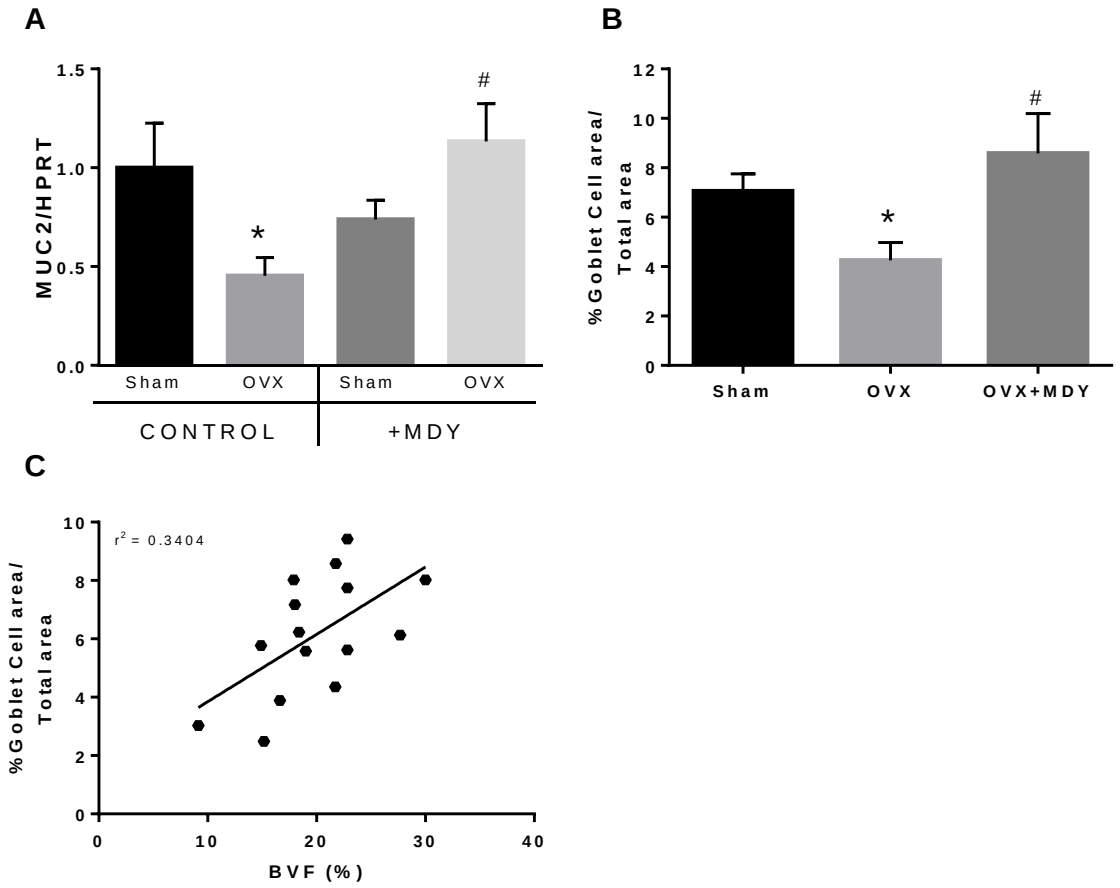

Figure 12. MDY Supplementation Increases MUC2 Expression and Goblet Cell Area in Estrogen Deficient Mice

Colon mRNA expression of MUC2 via rtPCR (A). Goblet cell area, measured by PAS staining (B). Goblet cell area was correlated with bone volume (C). Values represent the mean +/- the standard error (n = 5 – 12). *p<0.05 with respect to sham control. #p<0.05 with respect to OVX control.

3.4.3. MDY Increases Estrogen Receptor β Expression and Mucus Production

To begin to address the mechanism for MDY effects on MUC2 and goblet cells, we considered the finding that both estrogen and MDY supplementation increased the area of glycoproteins in goblet cells as well as MUC2 expression. Therefore, we first examined how MDY affects colonic estrogen receptor (ER) expression. mRNA analysis of ERα, ERβ and GPR30 identified a significant decrease in ERα and ERβ and a decreasing trend of GPR30 in the colon of OVX mice compared with sham controls (Figure 13A-C, $p<0.05$). Interestingly, MDY treatment significantly increased expression of ERβ in OVX mice (Figure 13B, $p<0.05$). To further investigate how MDY and estrogen affect mucus production, HT-29 MTX E12 (E12) colon cells were grown in the presence of MDY and various ER antagonists for 14 days and then stained for glycoproteins present in mucus using the PAS stain. Estrogen (E), MDY and MDY+MPP (an ERα antagonist) treatment significantly increased the stained mucus with respect to both untreated and vehicle controls (Figure 13D). Treatment with MDY+G15 (an inhibitor of GPR30) trended to increase mucus in E12, but was not significant. Interestingly, the combination of MDY+ICI (an ERα and β antagonist) as well as MDY+PHTPP (an ERβ antagonist) significantly decreased the effect of MDY on mucus area (Figure 13D), indicating a role for ERβ in the production of mucus in E12 colon cells.

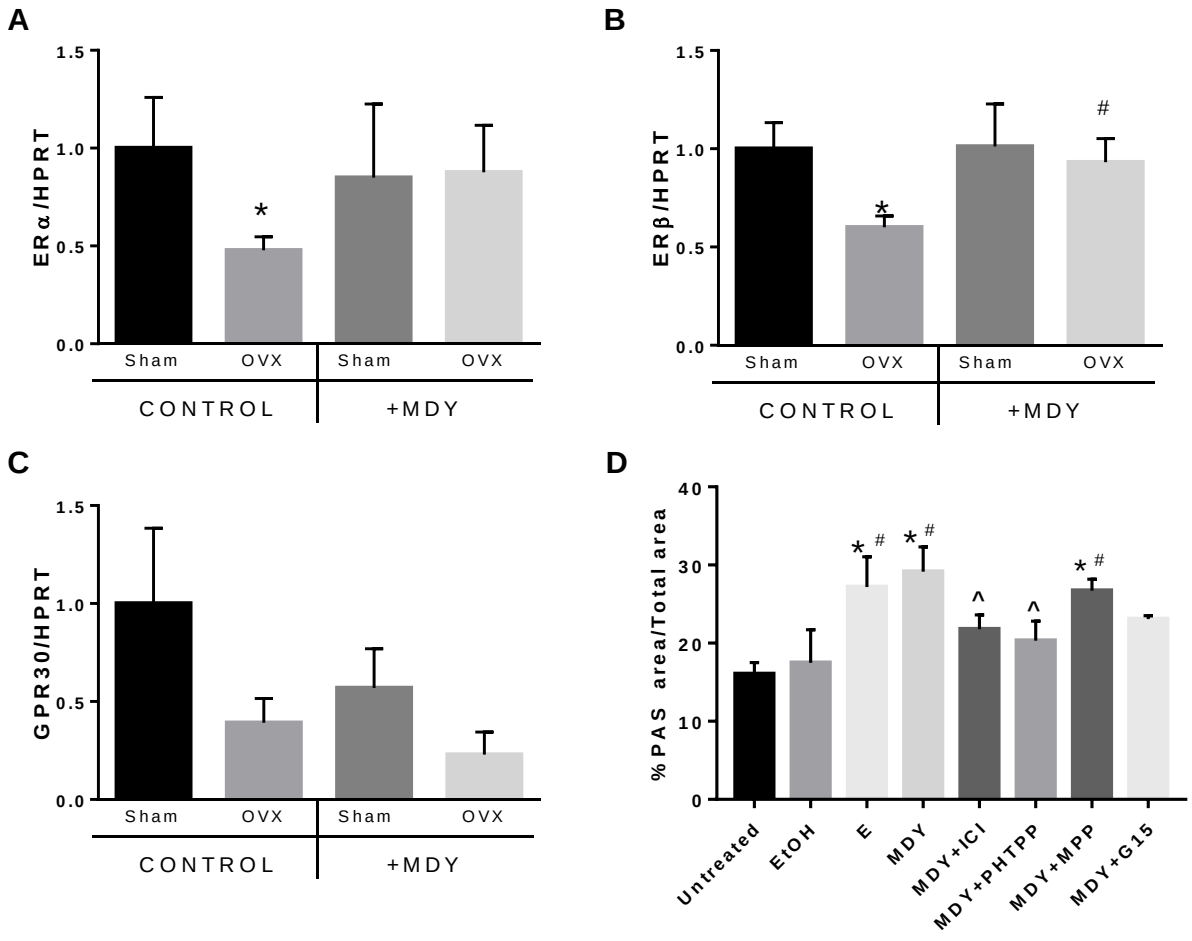

Figure 13. MDY Increases Colonic Expression of ERβ and Goblet Cell Area in HT-29 MTX E12 Cells

Estrogen receptor mRNA expression (ERα (A), ERβ (B) and GPR30 (C)) was measured in mouse colon tissue. HT-29 MTX E12 cells treated with MDY and various ER antagonists were stained with the PAS stain and the area of mucus was quantified (D). Values represent the mean +/- the standard error (n = 5 – 12). *p<0.05 with respect to sham control. #p<0.05 with respect to OVX control in A-C. In D, *p<0.05 with respect to untreated cells, #p<0.05 with respect to EtOH controls and ^p<0.05 with respect to MDY treated cells.

3.4.4. MDY Prevents Estrogen Deficiency Decreases in Goblet Cell Differentiation and Activity

In addition to the secretion of MUC2, goblet cells secrete other mucins and trefoil peptides which play an important role in intestinal health. Therefore, we examined if estrogen deficiency or MDY treatment affected expression of other goblet cell factors. MUC3 is the most prevalent transmembrane mucin and the main component of the enterocyte glycocalyx (158,169). Colonic MUC3 mRNA expression was significantly decreased by OVX as well as MDY treatment in both sham and OVX mice (Figure 14A). Trefoil factor 3 (TFF3) is the second most abundantly secreted protein of goblet cells (after MUC2) and is the only trefoil factor produced in the intestine (TFF1 and 2 are secreted in the gastric epithelium) (158,169). TFF3 is involved in the migration of intestinal epithelial cells to areas of damaged or apoptosed cells to maintain intestinal barrier function (170). Colon mRNA expression of TFF3 was found to be significantly decreased in OVX mice with respect to sham mice and this was prevented by treatment with MDY (Figure 14B).

As TFF3 is required for restitution of a damaged epithelial layer, we wanted to examine if there were differences in cellular proliferation or apoptosis in the colon. To do this, we measured the expression of proliferating cell nuclear antigen (PCNA) and used immunohistochemistry to analyze colon tissue for cell death using the terminal deoynucleotidyltransferase dUTP nick end labeling (TUNEL) stain. PCNA was significantly decreased in both nontreated and MDY treated OVX colons (Figure 14C). However, while OVX+MDY expression of PCNA was significantly decreased compared

to sham, it was also significantly increased when compared to untreated OVX mice (Figure 14C). TUNEL staining revealed no difference between groups (data not shown).

Because overall cell proliferation is decreased in OVX mice (as measured by PCNA expression and Ki67 staining (Chapter 2)), we wanted to determine how the differentiation of goblet cells was affected. Kruppel-like factor 4 (KLF4) is a transcription factor necessary for the terminal differentiation of goblet cells (171). Interestingly and consistent with goblet cell area and MUC2 expression, KLF4 was significantly decreased in OVX animals with respect to both sham and OVX+MDY mice (Figure 14D).

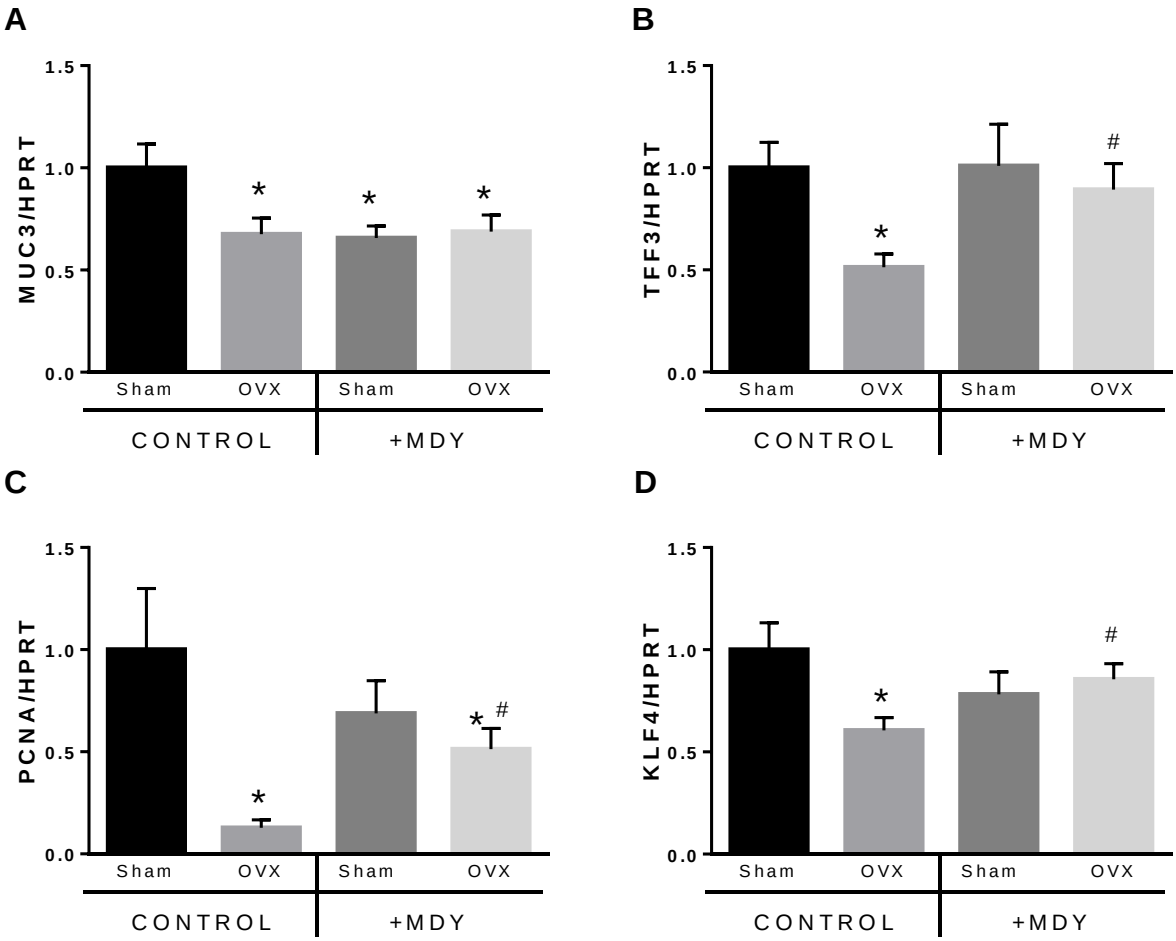

Figure 14. Estrogen Deficiency Decreases Expression of Goblet Cell Products and Decreases Proliferation

Colons were analyzed for mRNA expression of MUC3 (A), TFF3 (B), PCNA (C) and KLF4 (D). Values represent the mean +/- the standard error (n = 8 – 12). *p<0.05 with respect to sham control. #p<0.05 with respect to OVX control.

3.4.5. MDY Increases Intestinal Permeability and Transepithelial Resistance

Previous work in the lab has indicated a role for estrogen in colonic paracellular permeability which is correlated to bone volume (Chapter 2). To determine if MDY treatment alters intestinal permeability in sham and OVX mice, we measured the flux of FITC across the intestinal epithelial barrier *ex vivo*. To do this, sections of distal colons were placed in Ussing chambers for *ex vivo* permeability measurements. As previously shown (Chapter 2) estrogen deficiency lead to decreased colonic paracellular permeability when compared to sham controls (Figure 15A). Interestingly OVX + MDY colons had significantly increased FITC flux when compared to OVX controls (Figure 5A). Another measure of intestinal barrier integrity is the transepithelial resistance (TER) across the tissue; a measure of tissue and barrier integrity. The TER in OVX mice was significantly higher than sham control and OVX + MDY mice (Figure 15B), indicating a barrier that is less permeable.

As changes in barrier function can be due to alterations in the junctional proteins which keep the barrier intact at both the apical and basolateral junctions, we wanted to examine if OVX or MDY could alter these. Occludin is a transmembrane protein found in the apical tight junction complex (172). Along with the family of claudin proteins, occludin works to maintain barrier function. While we did not see a difference in mRNA expression of occludin in OVX mice, OVX mice treated with MDY had significantly less expression of occludin in the colon (Figure 15C, $p<0.05$). We also examined the expression of E-cadherin, the main protein in the adherens junction which is basolateral to the tight junction. E-cadherin was significantly increased in OVX animals with respect to sham

controls and treatment with MDY decreased expression significantly compared to OVX control mice (Figure 15D, $p<0.05$).

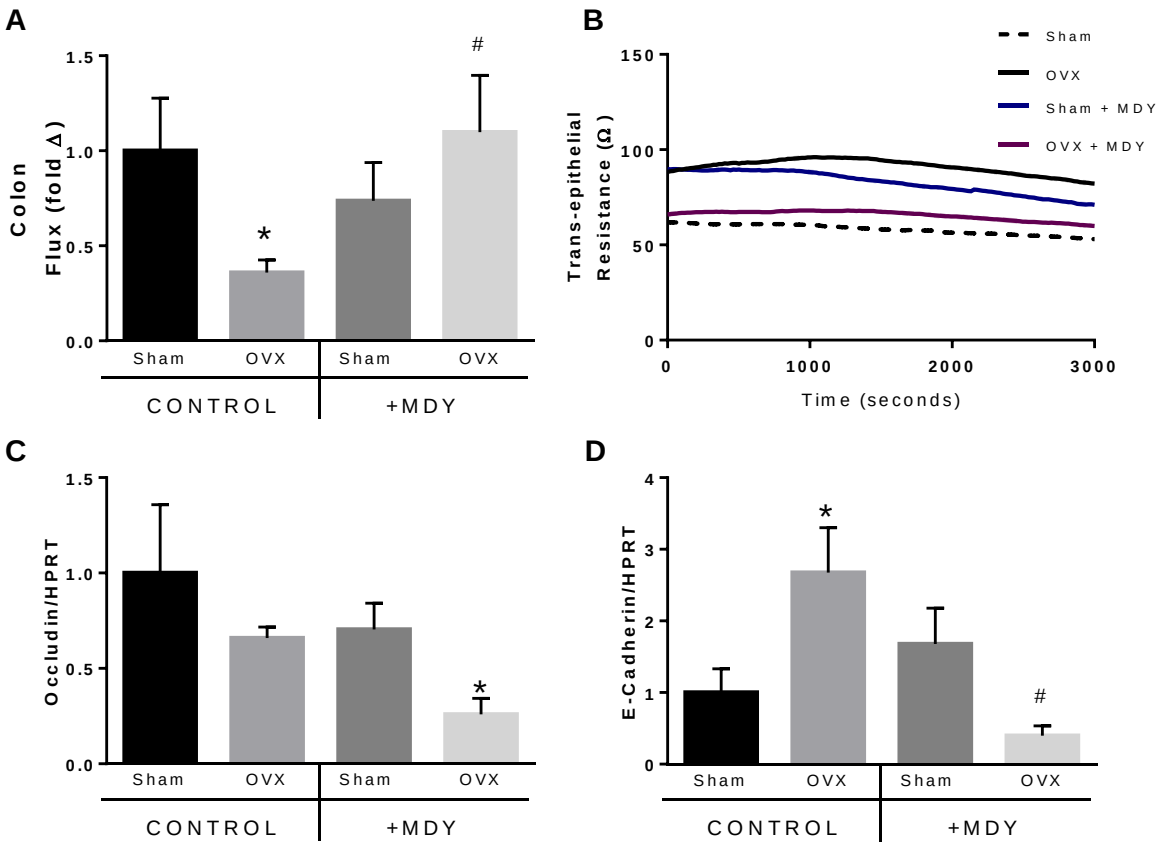

Figure 15. MDY Increases Intestinal Permeability and Transepithelial Resistance

Sham and OVX mice treated with and without MDY were evaluated for intestinal FITC flux *ex vivo.* Colonic paracellular flux (A) and transepithelial electrical resistance (B) was measured using Ussing chambers. Colonic mRNA expression of the tight junction protein occludin (C) and E-cadherin (D). Values represent the mean +/- the standard error (n = 5 – 12). *p<0.05 with respect to sham control. #p<0.05 with respect to OVX control.

3.4.6. Treatment with the Mucus Supplement MDY Prevents OVX-Induced Bone Loss

Previous work has shown that altering intestinal health with probiotics yields a beneficial effect on bone density (72–74,119,124). We wanted to determine if treatment with the mucus supplement, MDY changed bone parameters. Surprisingly, 4 weeks after treatment with 1% of MDY in the drinking water and 2mg/kg gavage of MDY three times a week, OVX-induced bone loss was prevented in the femur (Table 1, Figure 16A). Representative isosurface images of the distal femoral trabecular region are shown in Figure 6B. In addition to significantly increasing the bone volume fraction (BVF) in the femur with respect to OVX controls, MDY treatment increased bone mineral density (BMD), trabecular thickness (Tb. Th.), trabecular number (Tb. N.) and decreased trabecular spacing (Tb. S.) (Table 1). There were no changes in cortical bone analysis between groups (Table 1).

Femoral Parameters	Control		OVX	
	-	+MDY	-	+MDY
Trabecular				
BV/TV	21.8 ± 1.5	22.8 ± 2.7	14.9 ± 1.1**	20.4 ± 1.8#
BMD (mg/cc)	215 ± 8	214 ± 13	174 ± 7**	204 ± 10#
BMC (mg)	0.35 ± 0.01	0.36 ± 0.03	0.27 ± 0.01**	0.33 ± 0.02
Tb. Th. (um)	50.7 ± 2.1	44.6 ± 1.9*	37.2 ± 1.0**	40.8 ± 1.8**
Tb. N. (1/mm)	4.32 ± 0.20	5.07 ± 0.48	3.96 ± 0.22	4.94 ± 0.37#
Tb. Sp. (um)	185 ± 12	168 ± 21	224 ± 16	170 ± 17#
Cortical				
Tt. Ar. (mm2)	1.50 ± 0.03	1.55 ± 0.04	1.51 ± 0.02	1.53 ± 0.02
Ct. Ar. (mm2)	1.00 ± 0.02	1.02 ± 0.03	0.98 ± 0.02	1.01 ± 0.02
Ma. Ar. (mm2)	0.50 ± 0.02	0.52 ± 0.01	0.54 ± 0.02	0.52 ± 0.01
Thickness (mm)	0.29 ± 0.00	0.29 ± 0.01	0.28 ± 0.01	0.29 ± 0.01
Inner P. (mm)	2.68 ± 0.05	2.73 ± 0.03	2.77 ± 0.04	2.70 ± 0.03
Outer P. (mm)	4.53 ± 0.05	4.60 ± 0.06	4.58 ± 0.03	4.58 ± 0.03

Table 1. MDY Prevents OVX-Induced Trabecular Bone Loss in the Femur

µCT analysis of femoral trabecular and cortical bone. Values represent the mean +/- the standard error (n = 8 – 12). *p<0.05 with respect to sham control. #p<0.05 with respect to OVX control.

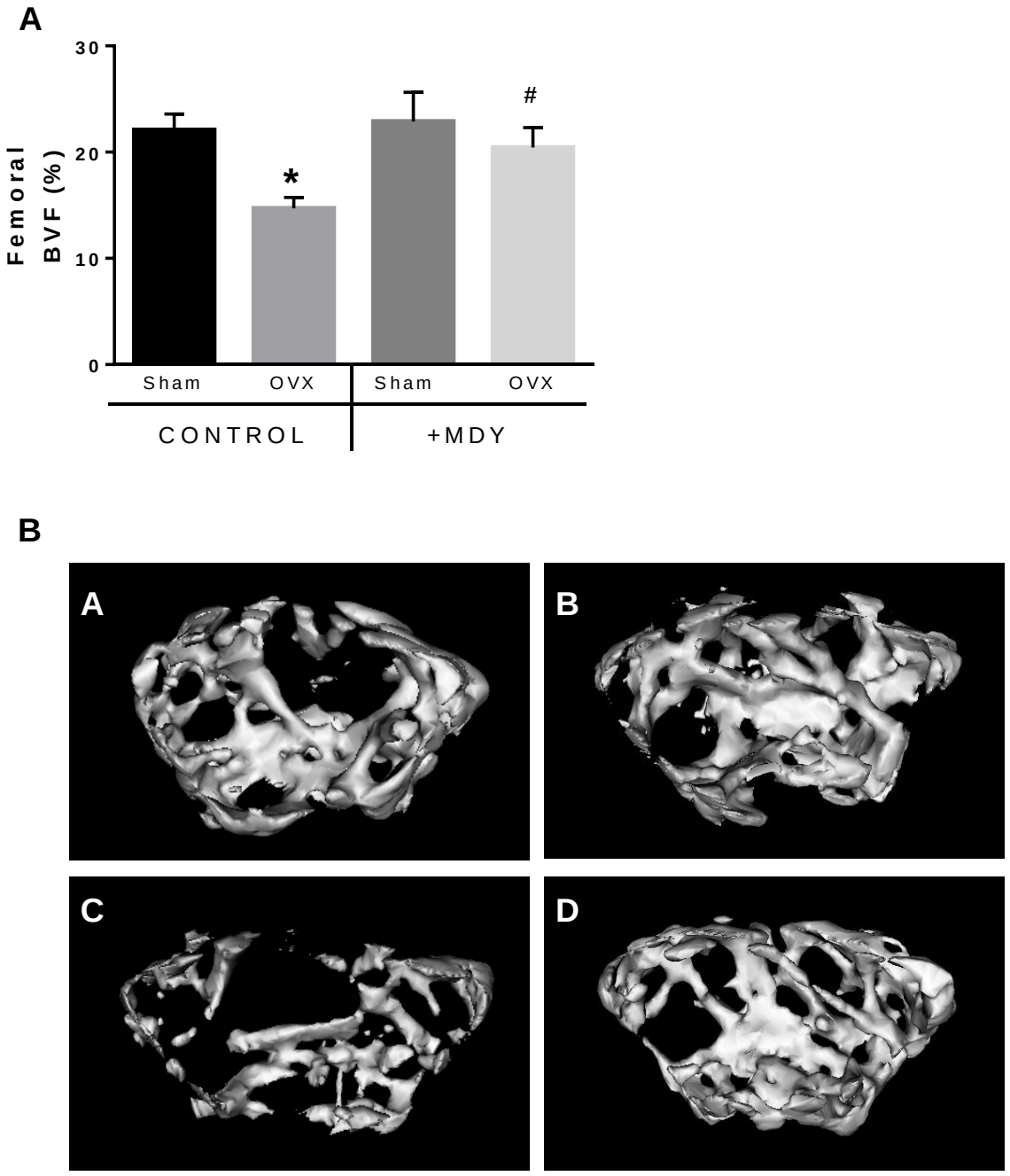

Figure 16. MDY Treatment Increases Trabecular Bone in the Femur and Vertebra

Microcomputed tomography was used to examine the effect of MDY treatment on bone density in the femur and vertebra of sham and OVX mice +/- MDY. Femoral trabecular bone volume (A). Representative isosurface images are shown in Figure 6B. Values represent the mean +/- the standard error (n = 8 – 12). *p<0.05 with respect to sham control. #p<0.05 with respect to OVX control.

3.5. DISCUSSION

For the first time *in vivo*, we have shown that estrogen deficiency or OVX leads to a decrease in intestinal mucus production. This finding is not surprising as estrogen plays a key role in the production of mucus in the reproductive tract as well in addition to recently being found to increase bronchial mucus production in the respiratory tract (155,162,173,174). Intestinal mucus production is greatest in the colon, which coincides with the colon housing the largest population of intestinal microbiota, and serves as the first line of defense in the gastrointestinal tract (77,158,169). Goblet cells in the colon secrete MUC2, the large and highly glycosylated gel-forming mucin, which forms the inner and tightly adherent mucus layer that prevents bacterial invasion. MUC2 expression as well as mucus glycoprotein staining was found to be decreased in OVX mice and this was prevented by estrogen supplementation. Interestingly, treatment with MDY was also able to prevent the decrease in mucus production in OVX mice.

MDY is a high molecular weight polymer which has been shown to maintain barrier function during intestinal graft preservation. Interestingly, preservation of intestinal segments in high molecular weight polymers (such as polyethylene glycol) attenuated epithelial cell apoptosis as well as preserved the number of goblet cells present in the tissue compared with other preservation techniques (167). Preservation of the mucus layer aided in preventing the invasion of bacteria from the microbiota layer through the epithelial barrier, a common problem in intestinal transplantation (167). Although we did not observe a difference in epithelial cell apoptosis (via TUNEL) with either OVX or MDY treatment, we did find that OVX leads to a significant decrease in cellular proliferation (as measured by PCNA mRNA expression) as well as a decrease in the transcription factor

necessary for goblet cell differentiation (KLF4). MDY was able to partially prevent the decrease in PCNA expression in treated OVX mice as well as prevent the decrease in KLF4 which agrees with the quantification of mucus in colon sections. It has been suggested that high molecular weight polymers may act as an artificial mucin, but they may also exert their effects by the stabilization of membrane lipids which enhance the epithelial barrier, leading to normal production of mucus (163,166–168). In both cases, due to restitution of the mucus barrier the epithelial barrier is protected from bacterial invasion and damage which may lead to an inflammatory response in the intestine which can then cause bone loss (70,71).

In line with increased mucus production, we found that barrier function in OVX mice, measured by FITC paracellular flux and transepithelial resistance in Ussing chambers was restored to control levels after MDY treatment. MUC2 knock out animals have increased intestinal permeability which makes them more susceptible to the development of dextran sodium sulphate (DSS) induced colitis, highlighting the importance of the mucus in epithelial barrier function (78). It is interesting to note that we find a decrease in intestinal permeability in estrogen deficient mice which is restored to control levels with MDY treatment. This could be due to a compensatory mechanism in junctional proteins following a decrease in mucus production which causes the barrier to tighten. This hypothesis is consistent with our findings that the adherens junction protein E-cadherin, is significantly elevated in OVX mice. Restitution of the mucus barrier by MDY treatment lead not only to a decrease in E-cadherin expression, but also occludin expression, a transmembrane protein found in the more apical tight junction. Future

studies examining the junctions between epithelial cells in response to decrease mucus production will help reveal the mechanism behind OVX-induced decreased permeability.

It is interesting to note that MDY treatment decreased permeability and transepithelial resistance in sham treated animals. If MDY is in fact acting as an artificial mucus, it could be that the addition of the MDY to a functional mucus layer causes a decrease in permeability. As no studies examining the additive effect of mucus layers have been performed (to our knowledge), we can only speculate that too much mucus may not necessarily be a good thing.

In order to determine how estrogen acts to increase mucus production, we utilized the HT-29 MTX E12 (E12) cell line. Unlike other intestinal cell lines, E12 cells grown in semi-wet conditions are able to form a polarized epithelial layer, capable of forming tight and adherens junctions and contain goblet cells which produce mucus making them more representative of the intestinal epithelial barrier. Consistent with our *in vivo* results, E12 cells growth with either estrogen (E) or MDY increased the area of PAS stain of the mucus glycoproteins. Additionally, cells treated with MDY and MPP (an ERα antagonist) had mucus levels similar to E or MDY treatment alone, significantly increased with respect to vehicle control treated cells. Interestingly, treating cells with a combination of MDY and ICI (ERα and ERβ antagonist) or MDY and PHTPP (ERβ antagonist) resulted in a decrease in stained mucus indicating a role for ERβ in intestinal mucus production. Treatment with MDY and G15, a GPR30 antagonist was neither significantly increased compared to vehicle controls or decreased to MDY treatment.

It is not surprising that estrogen works through ERβ to increase mucus production as ERβ is the most prominent ER in the intestine (138). Surprisingly, MDY treatment

increased ERβ expression in the colon. As MDY is not taken up by cells and ERβ is a nuclear receptor we are not sure if this increase is due to a change in barrier function or if MDY can initiate a signal from outside the cell. Future studies are necessary to understand how MDY can influence ERβ signaling.

We and others have demonstrated that the ingestion of probiotics or prebiotics reduces intestinal inflammation, alters the gut microbiome and increases bone density in healthy and T1D male mice as well as in estrogen-deficient female mice (72,74,106–108,119,175). Both probiotics and prebiotics act on the intestinal microbiome to elicit their beneficial effect. While these products do not leave the intestine, both of these factors are either metabolized or can produce metabolites which could be mediating the downstream effects on bone health. In this study we utilized a compound (MDY) which modifies the intestinal barrier, yet does not get metabolized and therefore its effects are only through its beneficial effects on barrier integrity. This is the first study, to our knowledge which has identified that the intestinal barrier alone can prevent bone loss which is not due to a secreted factor by bacteria or a metabolite from the breakdown of prebiotics.

Taken together, our results highlight the role for estrogen in the production of mucus. MDY, a high molecular weight polymer works to increase mucus levels which restore barrier function and can prevent bone loss in estrogen deficient mice. As MDY is not absorbed or metabolized, this research reveals the role of intestinal barrier function in the maintenance of bone health and provides a potential therapeutic for the prevention of osteoporosis.

CHAPTER 4

4. MDY WORKS THROUGH THE INTESTINE TO PREVENT TYPE 1 DIABETES INDUCED BONE LOSS

4.1. ABSTRACT

Type 1 diabetes is the most prevalent type of diabetes diagnosed in children. As a result of long-term glycemic dysregulation, secondary complications such as osteoporosis, are common. As osteoporosis treatments are expensive and can lead to detrimental side effects, it is important to develop new therapeutic targets. One such target is the intestine as more research has shown a link between intestinal and bone health. To examine how the intestine can influence bone health in type 1 diabetes (T1), *Ins2*$^{+/-\ Akita}$ mice were used. *Ins2*$^{+/-\ Akita}$ mice develop T1D spontaneously around 3-5 weeks of life with a pathogenesis similar to human disease. *Ins2*$^{+/-\ Akita}$ diabetic mice exhibited increased intestinal motility and permeability, consistent with previous reports in other rodent models and humans. In addition to this, *Ins2*$^{+/-\ Akita}$ diabetic mice had increased intestinal inflammation. To prevent inflammation and increase intestinal barrier health and integrity, *Ins2*$^{+/-\ Akita}$ diabetic mice and wild-type littermate controls were treated for 4 weeks with the intestine supplement, MDY. MDY is a high molecular weight polymer that is neither absorbed or metabolized and has been shown to decrease inflammation and increase intestinal health in rats exposed to radiation. MDY treatment led to a decrease in inflammation as measured by serum endotoxin and colon mRNA expression of TNFα. Furthermore, MDY treatment was able to prevent T1D induced bone loss. These findings reveal a role for intestinal health in the prevention of osteoporosis and may lead to the development of new therapeutic targets.

4.2. INTRODUCTION

Type 1 diabetes (T1D) is characterized by hyperglycemia and hypoinsulinemia and requires treatment with exogenous insulin therapy. While insulin therapy has increased the overall health and lifespan of T1D patients, perfect glycemic control is difficult and long-standing diabetes can result in several secondary complications including retinopathy, nephropathy, microvascular complications as well as osteoporosis (176). Osteoporosis due to T1D results from an anabolic defect characterized by suppression of osteoblast number and activity as well as an increase in bone marrow adipogenesis (60,62,65,177,178). T1D is the most commonly diagnosed form of diabetes in children, and therefore is chronic lifetime disease that predisposes the young patients to increased fracture risk that lasts a lifetime. Thus, there is a need for new therapeutics (drugs and targets) to treat or prevent the T1D pathological changes which lead to bone loss (176).

Recently the intestinal tract has been implicated in the pathogenesis of T1D (179,180). In addition, T1D induced changes in intestinal health and function have been suggested to contribute to further T1D complications (108). Intestinal changes that have been reported to precede or be caused by T1D include increased intestinal permeability, changes in the intestinal microbiota as well as altered intestinal motility (98,99,102,179,181–184). Previous studies have shown that prior to the onset of T1D, biobreeding rats (prone to develop T1D) have increased intestinal permeability to lactulose and mannitol and decreased expression of the tight junction claudin protein (179). In addition, humans genetically predisposed to developing T1D have an altered intestinal barrier and abnormal intestinal sugar permeability tests indicating the role for a “leaky” barrier in the pathogenesis of T1D (98,99,102,181–184). While permeability

studies have been done in rats, microbiome studies have focused on the T1D predisposed male NOD mouse. These studies suggest that the intestinal microbiome contributes to T1D onset, is sex related and that healthy fecal transplant (from females) can protect mice from disease onset (185–192). While the most common gastrointestinal complaint of T1D patients is diarrhea (193), diabetic patients can also display decreased motility as a consequence of neuropathy. Thus, intestinal motility (increased or decreased) is another factor that could also contribute to T1D complications, including those just discussed (microbiome dysregulation and intestinal permeability).

Surprisingly studies utilizing the mouse model to examine the role of intestinal health in T1D and its complications are limited and focus mainly on the role of the microbiome as the trigger of an autoimmune response leading to diabetes (185–191). In fact, few studies examine the link between T1D intestinal health and bone health (our Zhang ref). A number of T1D models exist (ref our papersINS2, NOD, STZ) but the *Ins2*$^{+/-\ Akita}$ mouse serves as a good model to study T1D intestinal-bone signaling for several reasons: 1) expression of a mutant form of insulin causes ER stress in beta-cells of the pancreas causing them to die in a similar way to T1D, without the need for pharmacologic agents that could affect the intestine , 2) the mice develop T1D in their youth, similar to humans and 3) the model has been used in a number of T1D studies so comparsions can be made (65,108,178).

In these studies, we show for the first time that *Ins2*$^{+/-\ Akita}$ diabetic mice have increased intestinal motility, permeability and inflammation compared to littermate controls. We further confirmed bone loss in the *Ins2*$^{+/-\ Akita}$ diabetic mice. To test if the increase in intestinal permeability plays a role in the T1D bone loss, we treated mice with

MDY-1001 (MDY), a unabsorbed high molecular weight polymer that has been shown to prevent intestinal bacterial adhesion and invasion under conditions of weak intestinal barrier function (163,164). Treatment with MDY blocked intestinal inflammation in the *Ins2*$^{+/-\ Akita}$ mice and was able to partially prevent T1D-induced bone loss. These results indicate the role for intestinal permeability and inflammation in the development of T1D osteoporosis and provide a potential new drug target and therapeutic for the prevention of T1D-induced fractures.

4.3. MATERIALS AND METHODS

4.3.1. Mice

Age matched male *Ins2*$^{+/-\ Akita}$ mice (C57BL/6 background) and wildtype (WT) C57BL/6 mice were purchased from Jackson Laboratory (Bar Harbor, Maine). *Ins2*$^{+/-\ Akita}$ mice become spontaneously diabetic at approximately 4 weeks of age. All mice were kept on a 12-hour light/dark cycle and received 2019 chow (Teklad) ad libitum. Both WT and *Ins2*$^{+/-\ Akita}$ littermates were randomly placed into control and treatment groups. Control animals received water ad libitum while treatment groups received 1.25% MDY in the water ad libitum for 4 weeks. Food and water consumption were recorded weekly. At 8 weeks of age, mice were euthanized. Animal studies were conducted in accordance with the Michigan State University Committee on Animal Use and Care and NIH.

4.3.2. Microcomputed Tomography Bone Analysis

At the time of death, femurs and vertebra were fixed in formalin and subsequently transferred to 70% ethanol after 24 hours. Bones were scanned using a GE Explore Locus microcomputed tomography system. The beam strength was set at 80 peak kV and 450 uA with an angle increment of 0.5. 720 views were taken at a voxel resolution of 20um. Each scan consisted of bones from each experimental group and contained a phantom bone used for calibration to maintain consistency throughout all the scans. In order to separate bone from marrow area, a threshold of 997 was used for all bones analyzed. A defined region of interest was analyzed in the distal femur and consisted of 1% of the total length of bone, starting at the growth plate and extending toward the diaphysis. The

growth plate and outer cortical bone was excluded from trabecular bone analysis (bone mineral content, bone volume fraction, trabecular thickness, spacing and number) as computed by GE healthcare MicroView software. The third/fourth lumbar vertebral body trabecular bone was analyzed in a similar fashion. Cortical measurements were performed by using a 2 x 2 x 2 mm cube centered midway down the length of the bone and using a threshold of 1825 to separate bone from marrow.

4.3.3. Motility Studies

Whole gut transit was measured by orally gavaging 200uL of 6% carmine red dye (Sigma) in 0.5% methylcellulose. Mice were individually caged and the time of gavage was noted. The time of the appearance of the first red stool (transit time) was noted for all mice. Mice were gavaged with 300mg/kg body weight with 4kD fluorescein isothiocyanate dextran (FITC) to measure both the transit of FITC in the serum (to be described below) and the stool. Stool samples were collected every half an hour until the time of death (4 hours after the time of gavage). Stool samples were weighed, suspended in 250uL of PBS, spun down to remove solid fragments and the supernatant was analyzed for the presence of FITC via a Tecan Infinite M1000 fluorescent plate reader at an excitation/emission wavelength of 485/530nm.

4.3.4. Permeability Studies

For whole intestinal permeability *in vivo*, mice were gavaged with 300mg/kg of FITC in sterile PBS. Blood was collected either via the saphenous vein from live mice or

cardiac puncture at the time of death. Serum was allowed to sit at room temperature for 5 minutes and was then spun down at 10,000 RCF for 10 minutes. The serum was then analyzed for fluorescence via a Tecan Infinite M1000 fluorescent plate reader at an excitation/emission wavelength of 485/530nm. The time of gavage and the time of blood collection was taken and the rate of FITC into the serum was calculated and normalized to the WT control for each day of the experiment.

Ussing chambers (Physiologic Instruments) were used to measure paracellular permeability *ex vivo*. Whole-thickness, 1.5 cm intestinal sections, (midway down the jejunum and ileum in the small intestine and the distal colon; whole thickness including the mucosa, submucosa, muscular layer and serosa) were flushed with PBS, cut along the mesenteric border, mounted on 0.3cm^2 aperture inserts and placed between two chambers. Each chamber was filled with 5mL Krebs bicarbonate buffer (Sigma). The buffer was maintained at 37°C and continuously oxygenated with 95% O_2 and 5% CO_2. After a 20-minute equilibration period, 2.2mg/mL FITC was added to the mucosal chamber. 0.55mg/mL of 10kD rhodamine isothiocyanate dextran (RITC) was also added to the mucosal chamber as a control for tissue integrity. Samples from both chambers were taken in triplicate at 0 and 60 minutes and fluorescence was measured at 485/530nm for FITC and 595/615nm for RITC on a Tecan Infinite M1000.

Serum endotoxin was measured by collecting sterile blood via cardiac puncture, allowing blood to sit at room temperature for 5 minutes and then spin down at 10,000 RCF for 10 minutes. Serum was frozen at -80C and not allowed to go through more than one freeze/thaw. The HEK-Blue™ LPS Detection Kit (InVivoGen, California) was used as described in protocol to analyze serum for endotoxin.

4.3.5. RNA Analysis

Immediately following euthanasia intestine segments were flushed with PBS, snap frozen in liquid nitrogen and stored at -80C. Samples were crushed under liquid nitrogen conditions and RNA was isolated using TriReagent (Molecular Research Center, Cincinnati, OH). RNA integrity was verified via formaldehyde-agarose gel electrophoresis. cDNA was then synthesized by reverse transcription using Superscript II Reverse Transcriptase Kit and oligoDT (12-18) primers (Invitrogen, Carlsbad, CA) and amplified by real-time PCR with iQ SYBR Green Supermix (BioRad, Hercules, CA) and amplified gene specific primers (synthesized by Integrated DNA Technologies, Coralville, IA). In order to verify that all samples have the same concentration, the housekeeping gene hypoxanthine guanine phosphoribosyltransferase (HPRT) was used as an internal control. Real-time PCR was carried out for 40 cycles using the iCycler (BioRad) and data were evaluated using iCycler software. Each cycle consisted of 95C for 15 seconds, 60C for 30 seconds and 72C for 30 seconds. Samples lacking cDNA were used as controls to verify no production of amplicons without cDNA present.

4.3.6. Flow Cytometry

Following euthanasia femora were cleaned of muscle and bone marrow (BM) cells isolated by centrifugation (n = 10–18 per group). $1x10^6$ cells were incubated with Fc block (BD Pharmingen, CA, USA) for 15 min. Cells were stained with anti-mouse CD3-AlexaFluor 700 (500A2, eBioscience), anti-mouse CD4-FITC (RM 4–5, eBioscience), anti-mouse CD8a-PE-Cyanine5.5 (5–6.7, eBioscience), anti-mouse F4/80-APC

eFlour780 (BM8, eBioscience) and anti-mouse CD11c-APC (N418) for 30 minutes before fixing in formaldehyde. Data were acquired on a BD LSRII (Becton Dickinson, Franklin Lakes, NJ) and analyzed with FlowJo (Version 10; FlowJo, LLC, Ashland OR).

4.3.7. Statistics

Unless otherwise noted, all data is presented as a mean value +/- the standard error. Student t-tests or one-way ANOVA analysis (using Fishers Test for multiple comparisons) was performed via GraphPad Prism Software. Data was considered significant when p-values were less than 0.05.

4.4. RESULTS

4.4.1. Early Stages of Type 1 Diabetes Increases Intestinal Motility and Causes Time Dependent Changes in Permeability Measures

To determine if T1D *Ins2*$^{+/-\ Akita}$ mice display increased intestinal changes 4 weeks after developing T1D, we measured both intestinal motility and permeability *in vivo*. Intestinal transit was measured by gavaging mice with carmine red dye and tracking the time of its appearance in the stool. Compared to nondiabetic WT mice, T1D *Ins2*$^{+/-\ Akita}$ mice displayed a significantly faster transit time (Figure 17A, $p<0.0001$). To examine permeability, we first measured in vivo whole intestinal permeability by gavaging mice with FITC-dextran (4 kD size) and measuring the amount of FITC in the serum after 4 hours. Interestingly, diabetic *Ins2*$^{+/-\ Akita}$ mice had significantly lower amounts of serum FITC when compared with control mice, which suggested a decrease in intestinal permeability (Figure 17B, $p<0.0018$). Because the transit time was increased in diabetic mice, we further examined the influence of motility on FITC appearance in the stool. We found that T1D *Ins2*$^{+/-\ Akita}$ mice had a high concentration of stool FITC sooner after gavage (150 min.) than control mice (Figure 17C, $p<0.0015$). Due to the increase in motility, we wanted to verify if the serum FITC levels also increased in diabetic mice at an earlier time point than 4 hours (a conventional time point for this assay). Serum FITC concentration was greater at one-hour post gavage in T1D *Ins2*$^{+/-\ Akita}$ mice when compared with controls, while nondiabetic control mice had greater serum FITC levels after 4 hours than *Ins2*$^{+/-\ Akita}$ mice (Figure 17D, $p<0.05$). Thus, differences in motility can impact permeability measures making it critical to do a time course.

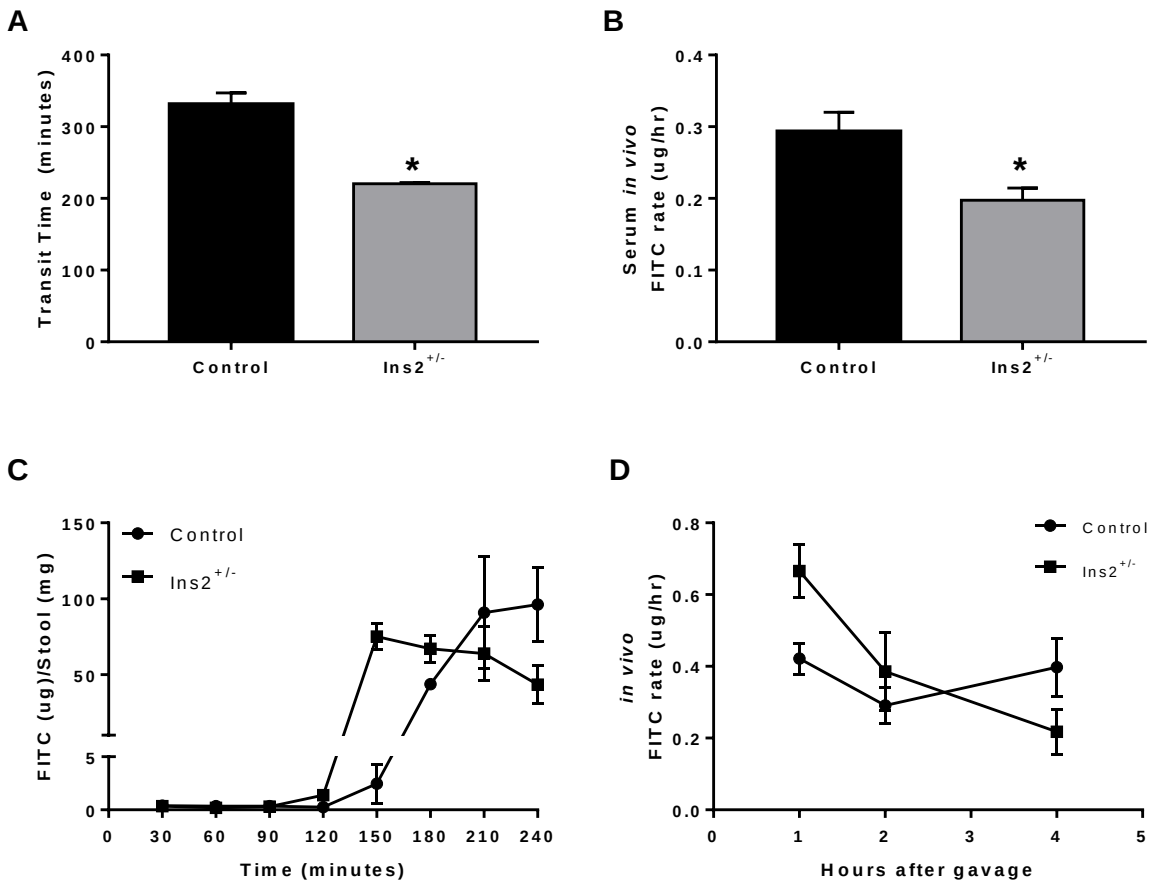

Figure 17. T1D Leads to Increased Intestinal Motility and Permeability

8-10 week old C57Bl/6 WT or *Ins2*$^{+/-\ Akita}$ mice were examined for motility changes as well as whole gut permeability. Carmine red dye intestinal transit time (A). Serum FITC concentrations 4 hours after oral gavage (B). Time course of FITC in stool samples (C). Time course of FITC in serum after oral gavage (D). Values represent the mean +/- the standard error (n = 3 - 5). *p<0.05 with respect to WT control.

4.4.2. MDY Decreases Intestinal Inflammation

To address the role of intestinal permeability and inflammation on our primary outcome measure, bone density, we treated control and T1D mice with MDY, a high molecular weight polymer that has been shown to reduce gut inflammation, integrate with and fortify the intestinal mucus layer and affect permeability. First we assessed the effects of MDY on general mouse parameters and found that treatment did not significantly alter body mass or blood glucose (Figure 18A and B). To assess intestinal inflammation and permeability, serum endotoxin and colon RNA analysis was performed. The T1D *Ins2*$^{+/-\ Akita}$ mice had significantly higher levels of endotoxin than control mice supporting the FITC data demonstrating that T1D increases permeability. Interestingly, MDY treatment was able to partially reduce the T1D elevation in serum endotoxin (Figure 19A, $p<0.05$). RNA analysis of colonic expression of tumor necrosis factor α (TNFα) and interleukin-10 (IL-10) revealed a trend in *Ins2*$^{+/-\ Akita}$ mice to have an increased TNFα to IL-10 ratio, indicating a pro-inflammatory environment which was significantly decreased in *Ins2*$^{+/-\ Akita}$ +MDY mice (Figure 19B, $p<0.05$). Because increased intestinal inflammation is often linked with changes in intestinal permeability and because of the observed increase in serum FITC from in vivo permeability studies (Figure 17), we wanted to determine if there was an increase in intestinal permeability *ex vivo*. Surprisingly, Ussing chambers did not reveal a significant difference in FITC flux in the jejunum, ileum or the colon in any of the conditions (Figure 19C-E).

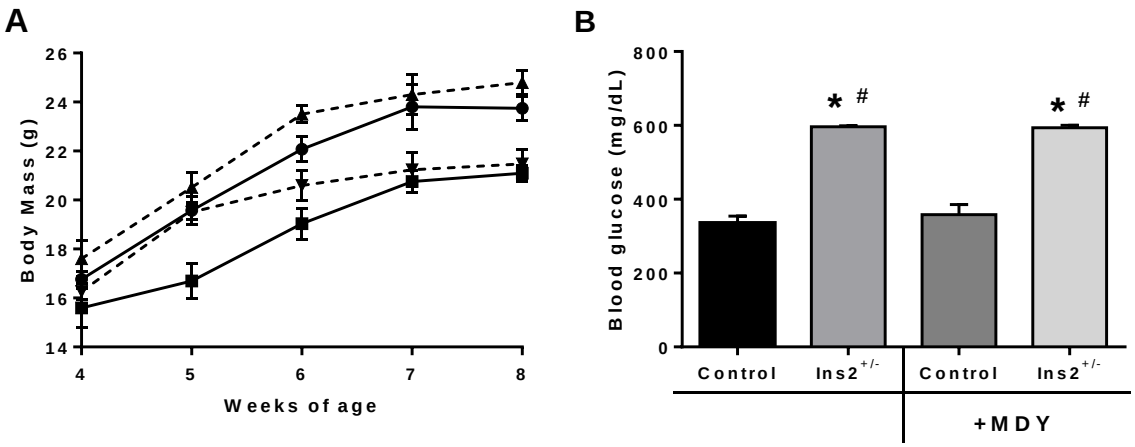

Figure 18. MDY Treatment Does Not Alter Body Weight or Blood Glucose

To examine how the mucus supplement, MDY, can affect intestinal and bone health, mice received 1.25% of MDY in their water for 4 weeks. MDY treatment did not significantly alter body weight or blood glucose in animals treated. Values represent the mean +/- the standard error (n = 8 - 12). *p<0.05 with respect to WT control. #p<0.05 with respect to WT+MDY mice.

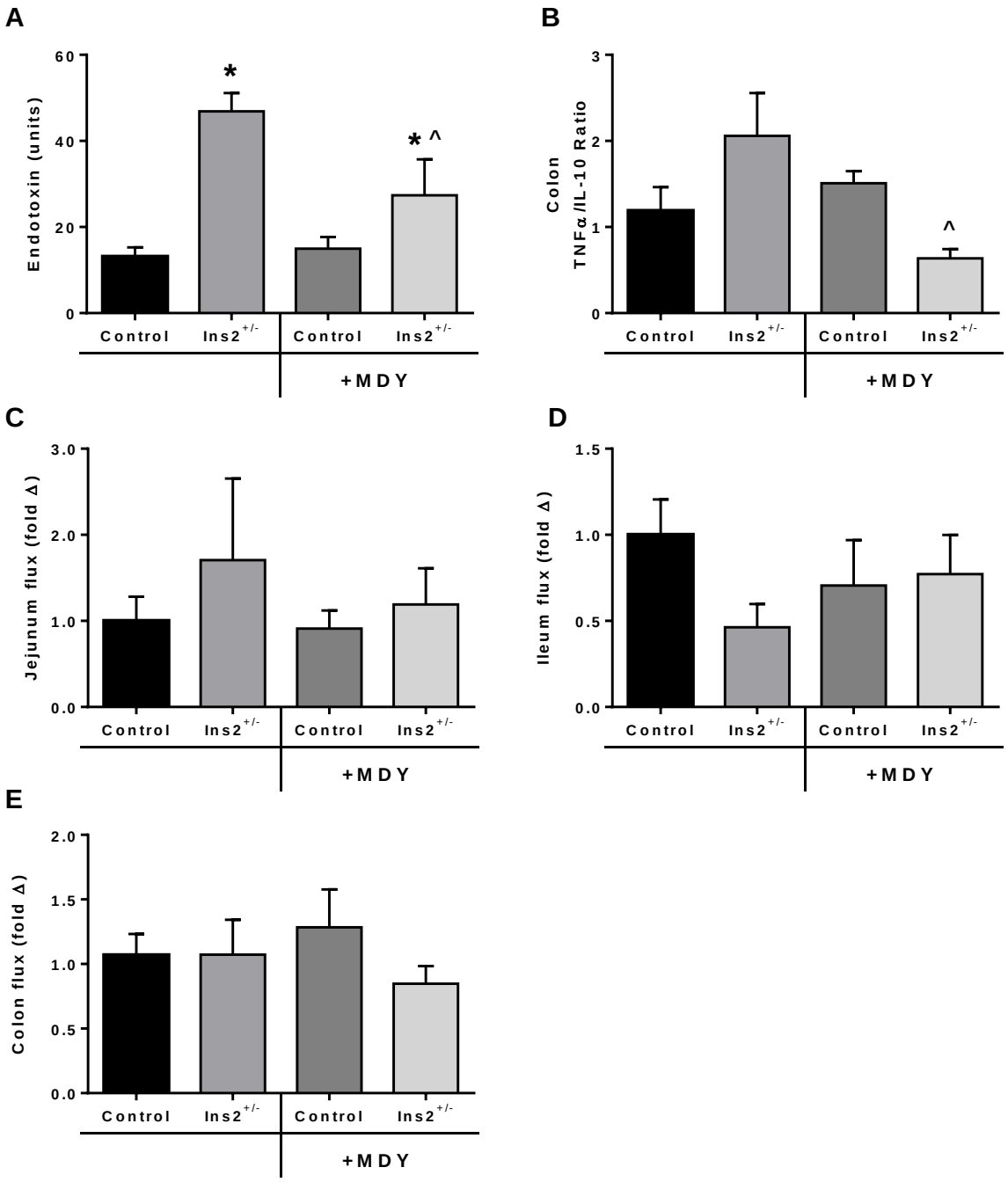

Figure 19. MDY Decreases Serum Endotoxin Levels and Inflammatory Cytokines

To examine how MDY alters intestinal health, serum endotoxin, colon RNA and *ex vivo* permeability was examined. Serum endotoxin levels (A). Colon mRNA analysis of the TNFα to IL-10 ratio (B). Sections of jejunum, ileum and colon were analyzed for FITC flux across the tissue in Ussing chambers (C-E). Values represent the mean +/- the standard error (n = 5 - 8). *p<0.05 with respect to WT control. #p<0.05 with respect to WT+MDY mice.

4.4.3. MDY Prevents T1D Induced Bone Loss

Previous studies have shown that decreasing intestinal inflammation leads to increased bone density. To determine if the effects of MDY which is non-absorble, on the intestine could affect T1D bone loss, we examined femurs and vertebra by microcomputed tomography. As expected, distal femurs of the T1D *Ins2*$^{+/-\ Akita}$ mice had significantly less trabecular bone density than control mice. Excitingly, treatment with MDY was able to partially prevent this effect (Figure 20A, $p<0.05$). Analysis of trabecular parameters indicated that MDY treatment in *Ins2*$^{+/-\ Akita}$ mice significantly prevented the T1D decreases in BMC, BMD, Tb.Th., Tb.N. and increased Tb.Sp. (Figure 20A-F, $p<0.05$). Analysis of cortical bone parameters revealed no difference between the groups (data not shown).

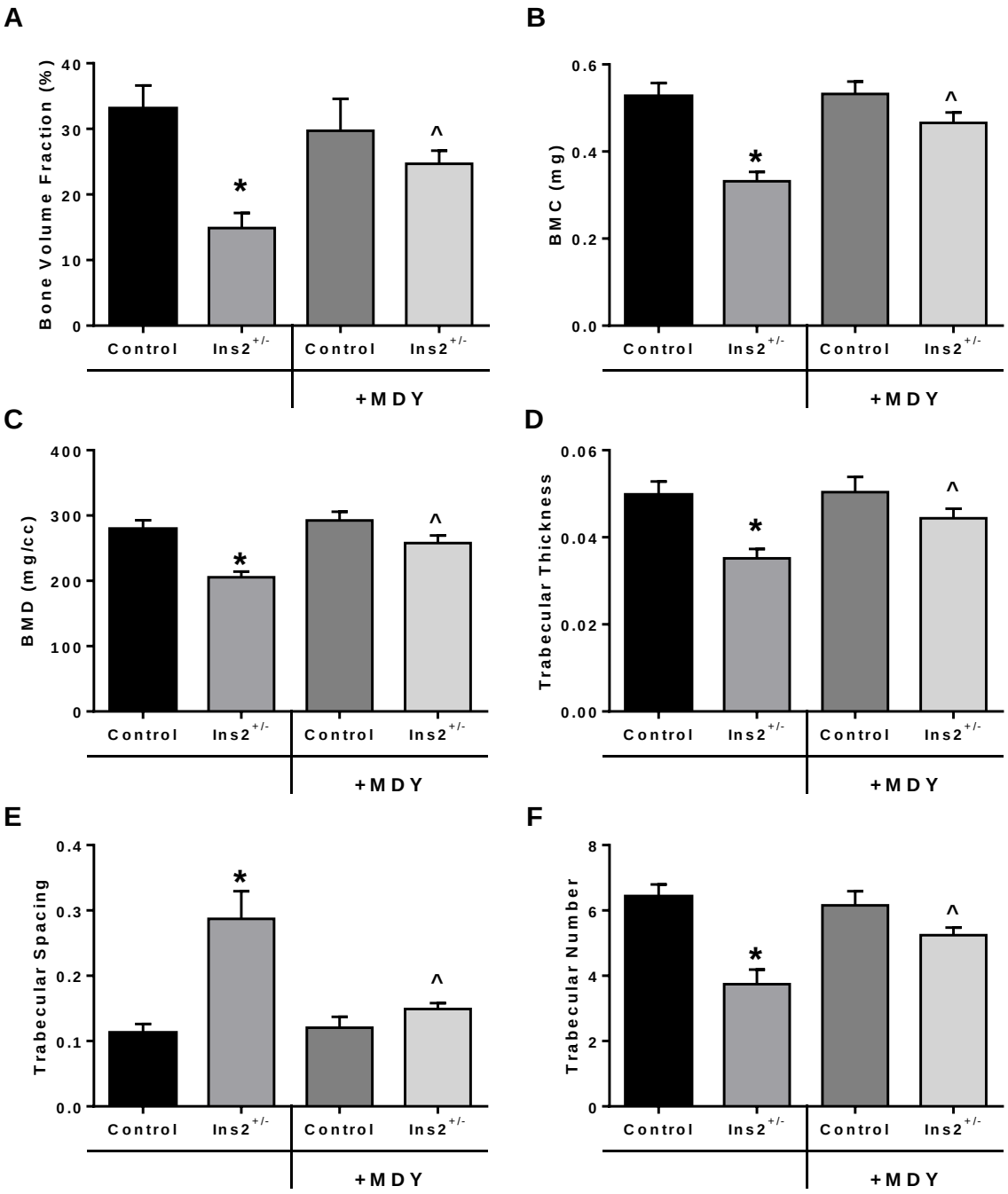

Figure 20. MDY Prevents T1D-Induced Bone Loss

8-week old WT and *Ins2*$^{+/-\ Akita}$ littermates were treated for 4 weeks with MDY. Femurs were analyzed via microcomputed tomography. BVF (A), BMC (B), BMD (C), Tb. Th. (D), Tb. Sp. (E) and Tb. N. (F). Values represent the mean +/- the standard error (n = 8 – 12). *p<0.05 with respect to WT control. ^p<0.05 with respect to *Ins2*$^{+/-\ Akita}$ control mice.

4.4.4. MDY Does Not Alter Immune Cell Population in the Bone Marrow

T1D is an autoimmune disease and therefore contains an altered immune system which may affect both intestinal and bone health. As both the intestine and the bone marrow house a large population of immune cells we wanted to determine if MDY altered immune cell population in the bone marrow as changes in the bone marrow can lead to decreased bone density (194–196). To determine if MDY affects the immune system in the intestine to elicit its beneficial role on bone health, we examined the different populations of immune cells in the bone marrow of the mice. Interestingly, we saw no difference in CD4+, CD8+, macrophage or dendritic cell number between any of the conditions (Figure 21A-D). Furthermore, when mice lacking mature B and T cells were treated with MDY, there was no difference in bone volume, indicating that MDY does not alter the immune system to prevent bone loss in T1D (Figure 21E).

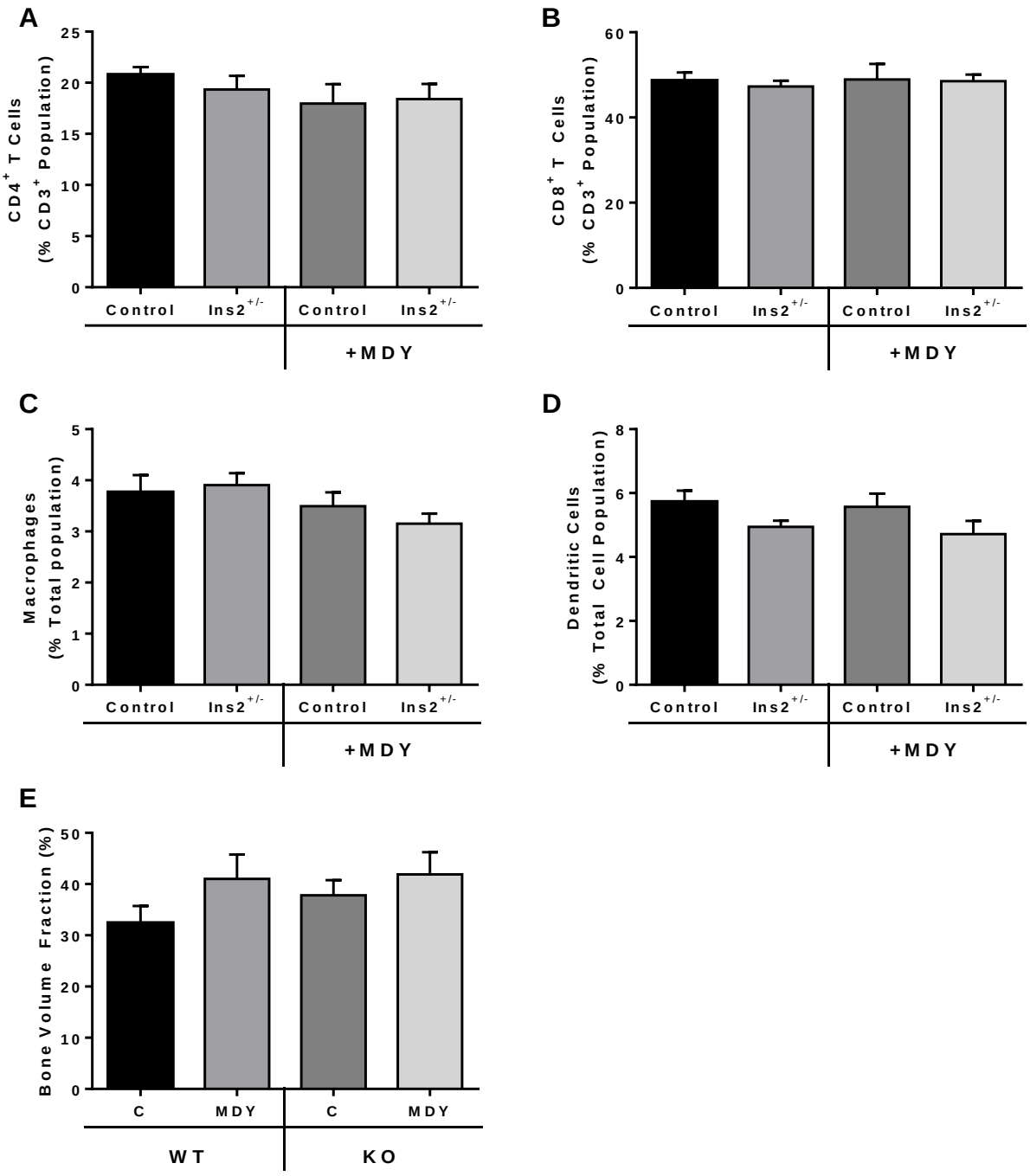

Figure 21. MDY Does Not Alter the Immune System in T1D

To determine if MDY alters immune cell population the bone marrow was analyzed for the relative number of different immune cells. Quantification of CD4+ cells (A), CD8+ cells (B), macrophages (C) and dendritic cells (D). RAGKO mice treated with and without MDY bone volume fraction (E). Values represent the mean +/- the standard error (n = 8-12).

4.5. DISCUSSION

The health of the intestinal epithelial barrier is essential for the prevention of disease as well as proper nutrition absorption (154). Recent studies have implicated a breakdown in the barrier, called “leaky gut” in the pathogenesis of type 1 diabetes (T1D) (179,180). As intestinal permeability and inflammation has been linked to bone loss, we wanted to examine how intestinal health is altered in the juvenile mouse model of diabetes, the *Ins2*$^{+/-\ Akita}$ mice. *Ins2*$^{+/-\ Akita}$ mice develop diabetes similar to the pathogenesis of type 1 diabetes (T1D) in humans. Consistent with the finding that the most common gastrointestinal complaint of patients with T1D is diarrhea, we found that *Ins2*$^{+/-\ Akita}$ mice had a faster whole gut transit time as measured by the appearance of red dye in the stool after gavage (197).

When we initially examined intestinal permeability *in vivo* we used a commonly published method of gavaging mice with FITC and measuring the amount of FITC in the serum after 4 hours. Surprisingly, when we did this, we found that *Ins2*$^{+/-\ Akita}$ mice had decreased FITC in their serum with respect to WT littermate controls. As this was not consistent with the literature on barrier function in T1D, we performed a time course experiment to determine if FITC in the serum spiked before 4 hours. We did in fact see an increase in serum FITC concentration at an earlier time point in *Ins2*$^{+/-\ Akita}$ mice highlighting the importance of doing a time course study. Additionally, we measured the amount of FITC in the stool every 30 minutes for 4 hours so that we could determine if the difference in serum FITC was due to the increase in transit time. We found an increase in FITC concentration in stool after 150 minutes whereas WT mice had similar FITC levels after 210 minutes. Thus we concluded that *Ins2*$^{+/-\ Akita}$ diabetic mice have both increased

intestinal motility and intestinal permeability which can lead to alterations in intestinal health.

Interestingly, although we observed an increase in serum FITC in *Ins2*$^{+/-\ Akita}$ diabetic mice, we were unable to locate the intestinal region responsible for the change in *in vivo* permeability measurements. It is possible that the *ex vivo* measurements in the Ussing chambers are not conclusive as we only measured a 1.5 cm piece of intestine from each section and previous work in our lab has shown differences in permeability in different regions of the same intestinal segment (unpublished). In addition to this, the main changes in permeability may occur earlier in the pathogenesis of T1D and may require us to look at younger mice as the mice we examined were 8 weeks old and had high blood glucose levels (>300 mg/dL) for at least 4 weeks. Previous work supports this as increased intestinal permeability is thought to precede the onset of diabetes and may be the initiating factor which triggers an autoimmune response (80,97,182,198).

To examine how altered intestinal barrier function can affect T1D induced bone loss, we utilized MDY, a high molecular weight polymer which is not broken down by the intestine and does not get absorbed into the blood stream (Figure 11). A polymer similar to MDY, has been shown to decrease radiation induced mucosal damage, increase intestinal graft health after preservation and prevent the adherence and penetration of intestinal microbiota past the barrier (163,164,166,168,199). *Ins2*$^{+/-\ Akita}$ had elevated serum levels of endotoxin as well as an increased ration of TNFα to IL-10, indicative of a decrease in intestinal barrier function. Interestingly, MDY was able to decrease both the raise in serum endotoxin as well as the TNFα to IL-10 ratio. As MDY has been suggested to be an artificial mucus, it may be able to exert these effects by preventing the passage

of intestinal bacteria past the epithelial layer. However, the levels of intestinal mucus production in T1D has not yet been characterized so it is unknown if an artificial mucus would be beneficial or not. MDY has also been shown to alter intestinal tight junction proteins and decrease epithelial cell apoptosis (166,167). It is possible that treatment with MDY decreased serum endotoxin levels by repairing junctional proteins and stabilizing the epithelial barrier. Future studies are necessary to elucidate the role of MDY in the treatment of altered intestinal health.

Consistent with our finding in estrogen deficient mice, treatment with MDY prevented T1D induced bone loss indicating the role of the intestinal epithelial barrier in bone health. Previously in the lab, we have shown that treatment with the probiotic *Lactobacillus reuteri* prevents bone loss in T1D mice (108) and can increase bone density in healthy mice (107). It was observed that *L. reuteri* lead to a decrease in intestinal inflammation. As intestinal inflammation has been shown to cause bone loss (70,71), it is not surprising that both *L. reuteri* and MDY treatment, which decrease intestinal inflammation preserved bone mass in T1D. While *L. reuteri* may secrete products which could affect the bone directly to exert its anti-inflammatory effects, MDY is not broken down by the intestine and its effects are limited to the intestine. This is the first study which shows that maintenance of the intestinal epithelial barrier leads to beneficial bone effects.

The intestine houses a large population of immune cells which can become activated and travel to the bone to elicit an effect on the bone. As increased inflammation in the bone marrow leads to decreased bone, we used flow cytometry to measure the different populations of immune cells present in the bone marrow. We hypothesized that

increased intestinal inflammation would lead to an increase in immune cell population in the bone marrow of *Ins2*$^{+/-\ Akita}$ mice. However, we saw no changes in CD4+, CD8+, macrophages or dendritic cell populations in the bone marrow of *Ins2*$^{+/-\ Akita}$ mice. Furthermore, we saw no difference in immune cell population with MDY treatment, further indicating that MDY works primarily at the intestinal epithelial barrier. Additionally, MDY treatment of mice with no mature T or B cells (RAGKO) lead to no changes in bone density, further showing that MDY does not alter the systemic immune system to have an effect on bone density.

Taken together, our data indicate that T1D in *Ins2*$^{+/-\ Akita}$ mice lead to an increase in intestinal motility and permeability which cause dysfunction of the intestinal epithelial barrier as measured by serum endotoxin. Interestingly, treatment with MDY was able to decrease serum endotoxin levels as well as pro-inflammatory cytokine expression in the colon. MDY prevented T1D induced bone loss, although there was no change in bone marrow immune cell population, indicating the role of the intestinal epithelium in maintaining bone health. These studies point to the intestine as a target for future therapeutics to prevent bone loss and fractures in T1D patients.

CHAPTER 5

5. ESTROGEN DEFICIENCY EXACERBATES TYPE 1 DIABETIC INDUCED BONE LOSS

5.1. ABSTRACT

Estrogen deficiency following menopause is associated with rapid bone loss, osteoporosis and increased fracture risk. Type 1 Diabetes (T1D), characterized by little or no insulin secretion and hyperglycemia, is also associated with bone loss and increased fracture risk. With better treatment options, T1D patients are living longer and therefore the number of patients having both T1D and estrogen deficiency is increasing. Little is known about the impact of type 1 diabetes and estrogen deficiency on bone health and density. To investigate this, 11 week old mice were ovariectomized (OVX) and T1D was induced by multiple low dose streptozotocin injection. MicroCT analysis of both distal femur and lumbar vertebrae trabecular bone indicated significant bone volume fraction (BVF) losses in all groups. However, while OVX and T1D mice lost roughly 50% BVF, the combination of T1D and OVX led to a BVF loss of 82% in the distal femur. A similar response was seen in the vertebrae. 2-way ANOVA analyses indicated a significant interaction between T1D and OVX resulting in greater bone loss. mRNA analysis of bone remodeling markers revealed an increase in osteoclast markers and decreased osteoblast markers of differentiation and activity in T1D-OVX mice with respect to T1D-sham or OVX mice. Histology revealed a decrease in total osteoblast number, an increase in osteoblast cell death (as measured by TUNEL) and a decrease in the ratio of osteoblasts to osteoclasts in mice with both T1D and OVX. Taken together, our results show that T1D combined with estrogen deficiency can have a profound effect on bone

health. Understanding the additive effects of estrogen deficiency and T1D on bone health is essential for fracture prevention in this patient population.

5.2. INTRODUCTION

Osteoporosis is characterized by decreased bone density and impaired bone architecture (11). While osteoporosis is a secondary manifestation to many diseases, it is primarily caused by the cessation of estrogen production in menopausal women. It is estimated that 1 in 2 women over the age of 50 will experience an osteoporotic fracture in their lifetime leading to dependence, depression, and decreased health and life expectancy (National osteoporosis foundation). Secondary osteoporosis can be caused by metabolic diseases and disturbances, organ dysfunction, poor nutrition and lifestyle habits as well as being a side effect of various medications (200). Because treatments for chronic diseases are becoming more effective, as the female population ages there is an increased risk of bone loss from not only menopause but from existing chronic diseases. This is an under-investigated area and thus it is important to identify if there are additive effects of estrogen-deficiency induced osteoporosis with chronic disease induced bone loss. Type 1 diabetes (T1D) is one chronic disease that causes bone loss and as individuals with T1D are now living longer we sought to determine the combinatory role of T1D and estrogen deficiency on bone density.

T1D is an autoimmune disease in which the beta cells of the pancreas are destroyed, resulting in a hypoinsulinemic and hyperglycemic environment (201). While current patients have a longer lifespan due to exogenous insulin therapy, maintaining normal blood glucose levels remains difficult, even under therapeutic vigilance (202,203), thus patients still suffer from a number of complications associated with the long-term dysregulation of glucose, including cardiovascular disease, retinopathy, nephropathy, neuropathy and bone loss (201). Studies in both animal and human models have

demonstrated that T1D results in decreased trabecular and cortical bone density and increased fracture risk (204,205). This reduction in bone health is primarily due to effects on the selection, maturation and activity of osteoblasts (6,62,206) as evidenced by decreased levels of osteoblast markers of maturity and activity such as alkaline phosphatase and osteocalcin (53,60,65,207–212). Bone formation is linked with metabolic control, as formation markers are inversely proportional to glycosylated hemoglobin levels (62,213,214). In T1D mouse models, bone marrow adiposity is also increased indicating that mesenchymal stem cells preferentially differentiate into adipocytes rather than osteoblasts (59,60). The role of osteoclasts in T1D bone loss, is not well established with reports showing no change, decrease or increase in number and activity (53–56,215). Due to the increasing lifespan of T1D patients it is important not only to investigate the long-term effects of T1D on bone (216), but also examine T1D in combination with the condition of menopause as both lead to pathological bone loss and osteoporosis, albeit via different mechanisms.

Menopause is characterized by the loss of estrogen and is preceded by several years of declining ovarian estrogen production (11). Estrogen is effective at inhibiting osteoclast bone resorption. During the first few years after menopause the rapid decline in estrogen production results in increased osteoclast (bone resorption) and osteoblast (bone formation) activities (217). These processes, however, are no longer balanced and bone resorption outweighs bone formation leading to net bone loss and osteoporosis (152,218,219). Estrogen-deficiency during menopause also increases production of inflammatory cytokines such as tumor necrosis factor α (TNFα). TNFα stimulates osteoclast activity and decreases osteoclast apoptosis in addition to inhibiting osteoblast

differentiation and activity (220–222). Taken together, estrogen-deficiency favors an osteoclast environment, promoting bone loss.

While both causes of osteoporosis, T1D and estrogen deficiency, have been researched independently, we sought to identify the impact of both T1D and menopause on bone. Our results indicate that the combination of T1D and estrogen deficiency caused by ovariectomy (OVX) leads to a decrease in bone volume in both the femur and vertebra that is greater than either T1D or OVX alone. The combined conditions decreased osteoblast activity and viability while increasing osteoclast activity and bone marrow adipogenesis. Taken together, our data suggest that post-menopasual women with T1D could be at increased risk for bone loss.

5.3. MATERIALS AND METHODS

5.3.1. Experimental Design

Female 11 week old balb/c mice were purchased from Jackson Laboratories and allowed to acclimate to the animal facilities for 1 week. Mice were randomly assigned to groups and subsequently either ovariectomized or sham operated (n = 5 – 10 mice per group). To induce T1D, one week after surgery, mice were intraperitonally injected with 50 mg/kg body weight of streptozotocin (STZ) for 5 consecutive days and blood glucose levels measured on the 5^{th} day. Mice with blood glucose over 300mg/dL were considered diabetic and mice with levels under 300mg/dL were given a single extra dose of STZ at 80 mg/kg body weight. Mice that lost 15% of initial body weight were given daily injections of 0.5 mU/g of insulin. Mouse bones were harvested and imaged 4 weeks after the induction of diabetes. Mice were given Teklad 2019 chow and water ad libitum and were maintained on a 12-hour light/dark cycle. Food and water intake were monitored during the experiment. All animal procedures were approved by the Michigan State University Institutional Animal Care and Use Committee and conformed to NIH guidelines.

5.3.2. Serum Measurements

Blood was collected at the end of the study and was either placed in EDTA tubes to prevent clotting or allowed to clot at room temperature for 5 minutes. Clotted blood was centrifuged at 10,000 RCF for 10 minutes. Serum was removed, snap frozen in liquid nitrogen and stored at -80ºC. Serum went through no more than two freeze/thaw cycles. Serum TRAP5b (n = 5 - 10) and Osteocalcin (n = 5 - 10) were measured using a Mouse

TRAP and OC assay kits (SB-TR103, Immunodiagnostic Systems Inc., Fountain Hills, AZ and BT – 470, Biomedical Technologies Inc., Stoughton MA, respectively) according to the manufacturer's protocol. Whole blood in EDTA tubes was used to measure HbA1C levels (n = 5 - 10) (Crystal Chem, Downers Grove, IL) according to the manufacturer's protocol.

5.3.3. Microcomputed Tomography Bone Imaging

Femurs were fixed in formalin and transferred to 70% ethanol after 24 hours. Bones were scanned using a GE Explore Locus microcomputed tomography (µCT) system with a voxel resolution of 20 µm obtained from 720 views. Beam strength was set at 80 peak kV and 450 µA with a beam angle increment of 0.5. Each scan consisted of bones from all experimental groups and a calibration phantom bone in order to maintain consistency throughout the scans. A fixed threshold of 792 was used to separate bone from bone marrow. A region of interest in the distal femur was analyzed and defined as 1% of the total length proximal to the growth plate and extending 2 mm toward the diaphysis excluding the outer cortical bone. Trabecular bone mineral content (BMC), bone volume fraction (BVF), thickness (Tb. Th.), spacing (Tb. Sp.) and number (Tb. N) values were computed by a GE healthcare MicroView software application for visualization and analysis of volumetric image data. The third lumbar vertebral body was analyzed for trabecular bone as described above. Cortical measurements were performed in a 2 x 2 x 2 mm cube centered midway down the length of the bone using a threshold of 1200 to separate bone from marrow.

5.3.4. Femur Histomorphometry and Dynamic Measures

Femurs were fixed in formalin and transferred to 70% ethanol after 24 hours. Fixed samples were processed on an automated Thermo Electron Excelsior tissue processor for dehydration, clearing, and infiltration using a routine overnight processing schedule. Samples were embedded in Surgipath-embedding paraffin on a Sakura Tissue Tek II-embedding center. Paraffin blocks were sectioned at 5 µm on a Reichert Jung 2030 rotary microtome. Slides were stained for TRAP activity and counterstained with hematoxylin according to manufacturer protocol (n = 5 – 10) (387A-IKT, Sigma, St. Louis, MO). At least 5 images at 40x magnification were taken at the distal metaphysis per section for analysis. The number of osteoclasts per mm of bone surface was calculated using the osteoclast number per mm of bone surface from histologic sections and multiplying that by the bone surface area calculated via the µCT. The ratio of osteoclasts to osteoblasts was found by dividing the calculated number of osteoclasts by the calculated number of osteoblasts (see below) per mm of bone surface. Visible adipocytes (greater than 30µm) were counted in the distal trabecular region and expressed as a percentage of the total area analyzed.

Cell death was determined using a TACS XL Basic In Situ Apoptosis Detection Kit (TUNEL, Trevigen Inc., Gaithersburg, MD) on femur sections (n = 5 - 10). At least 5 images at 40x magnification were taken at the distal metaphysis per section for analysis. TUNEL negative and positive osteoblasts were counted per mm of bone and multiplied by the bone surface area found using the µCT for a calculated number of either total or TUNEL positive osteoblasts per mm of bone surface. Positive controls included slides which were incubated with nuclease.

For dynamic histomorphometric measures of bone formation, mice were injected intraperitoneally with 200 µL of 10mg/mL calcein (Sigma, St. Louis, MO) dissolved in sterile saline at 7 and 2 days prior to harvest. Vertebra were fixed in formalin at the time of harvest and then transferred to 70% ethanol 48 hours later and processed. Vertebra were sectioned and examined under fluorescent light (n = 5 – 10). At least five images at 25x magnification were taken and the distance between the calcein lines (mineral apposition rate) and their lengths along the bone surface (used to calculate bone formation rate) were measured.

5.3.5. mRNA Analysis

Immediately after euthanasia, tibias were dissected and cleaned of muscle and connective tissue and subsequently snap frozen in liquid nitrogen. Frozen tibias were crushed under liquid nitrogen conditions with a Bessman Tissue Pulverizer (Spectrum Laboratories, Rancho Dominguez, CA). RNA was isolated using TriReagent (Molecular Research Center, Cincinnati, OH) and RNA integrity assessed by formaldehyde-agarose gel electrophoresis. cDNA was synthesized by reverse transcription using Superscript II Reverse Transcriptase Kit and oligo dT(12-18) primers (Invitrogen, Carlsbad, CA) and amplified by real-time PCR with iQ SYBR Green Supermix (BioRad, Hercules, CA) (n = 5 – 10). Gene specific primers were synthesized by Integrated DNA Technologies (Coralville, IA). Hypoxanthine guanine phosphoribosyl transferase (HPRT) mRNA levels do not fluctuate between conditions and were used as an internal control. Amplicon specificity was confirmed by melting curve, size, and sequence analysis. Primers for real-time PCR and cycle parameters have been previously described (72).

5.3.6. Statistical Analysis

All measurements are presented as the mean ± SEM. Significant outliers were removed using the Grubb's test for outliers. One-way ANOVA was performed using GraphPad Prism software version 6 (GraphPad, San Diego, CA, USA). *p*-values of ≤ 0.05 were considered significant and values of ≤ 0.01 were considered highly significant.

5.4. RESULTS

5.4.1. Femoral and Vertebral Bone is Significantly Decreased in T1D-OVX Mice Compared to T1D or OVX Alone

To determine if estrogen deficiency and T1D have an additive impact on bone loss, 11 week old mice were ovariectomized (OVX) and T1D was induced. First we examined general body parameters to assess effects on body and fat weight, metabolic dysregulation, and uterine size. As expected, T1D mice, both sham and OVX, had significantly elevated blood glucose and HbA1c levels (indicating metabolic dysregulation) and displayed significantly decreased body and fat pad, inguinal and retroperitoneal, weight compared to control animals (Table 2). In contrast, estrogen deficiency increased body mass and retroperitoneal fat pad mass in sham mice, but not in T1D mice. Interestingly, OVX mice also had increased HbA1c levels, though they were below 7% (what we would consider T1D) and this effect was not additive in T1D mice (since OVX did not further increase HbA1c levels). As expected, all OVX mice displayed decreased uterine mass confirming estrogen deficiency.

Next we examined the mouse bones by microcomputed tomography. Analysis of the distal femoral metaphysis bone volume fraction (BVF) revealed a significant decrease in OVX (52%, $p<0.0001$) and T1D (57%, $p<0.0001$) as expected, but more importantly the BVF in combined T1D-OVX mice (84%, $p<0.0001$) was significantly less compared to mice with either T1D (by 63%, $p<0.0001$) or OVX (by 66%, $p<0.0001$) (Figure 22A and B). Two-way ANOVA identified a highly significant interaction between T1D and OVX ($p<0.0001$). Consistent with this finding, bone mineral density (BMD), bone mineral content (BMC), trabecular thickness (Tb. Th.) and trabecular number (Tb. N.) were all

significantly decreased in OVX as well as T1D animals compared to controls, while T1D-OVX animals were significantly decreased with respect to sham control, OVX and T1D mice (Table 3). Trabecular spacing (Tb. Sp.) was significantly increased in OVX, T1D and T1D-OVX with T1D-OVX being significantly higher than all conditions (Table 3). Femoral cortical analysis revealed no change in OVX mice while significantly decreased BMD and BMC was observed in T1D mice (Table 3). T1D-OVX mice had significantly decreased cortical thickness, outer perimeter, marrow area, cortical area, BMD and BMC compared to controls (Table 3).

To determine if the observed femur changes were apparent in other bone sites, the 3rd lumbar vertebrae was examined. While OVX did not alter vertebral trabecular BVF compared to sham control mice, a significant decrease was observed in T1D mice compared to controls (24%, $p<0.05$) and in T1D-OVX animals compared to control (51%, $p<0.0001$), OVX (47%, $p<0.0001$) and T1D (35%, $p<0.01$) (Figure 22C). Though, 2-way ANOVA did not indicate an interaction between T1D and OVX at this site. In addition, BV/TV, BMD, Tb. Th. and Tb. N were significantly decreased and Tb. Sp. increased in T1D-OVX mice (Table 3).

Dynamic histomorphometry was used to assess if changes in osteoblast activity contributed to the identified bone loss. In correlation with the bone density analyses, OVX, T1D and T1D-OVX mice had significantly decreased mineral apposition rate with respect to control animals (MAR, $p<0.01$) (Figure 22D and E). Both T1D groups (sham and OVX) had significantly lower MAR in comparison to OVX animals (Figure 22D and E, $p<0.01$). Calculation of bone formation rate (BFR) indicated a decrease in both the T1D

and T1D-OVX groups with respect to the sham control (Figure 22D and F, $p<0.05$), but no change was observed in the OVX groups.

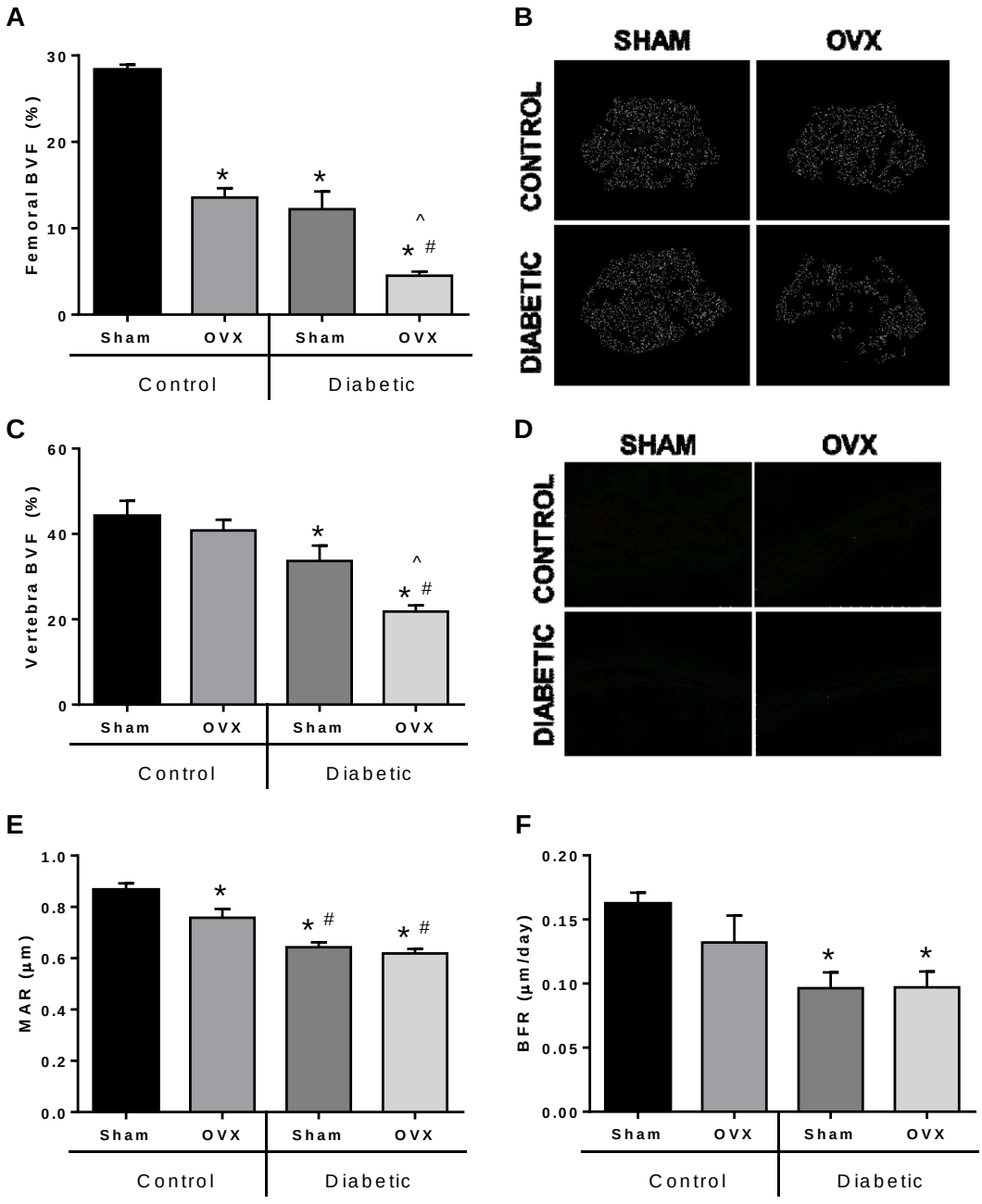

Figure 22. The Combination of T1D and OVX Impacts Bone More than Either T1D or OVX Alone

Microcomputed tomography analysis of the distal femoral bone volume fraction (A). Representative isosurface images of femoral trabecular bone (B). Vertebral bone volume fraction (C). Representative images of calcein labeling used to measure MAR (E) and BFR (F). Bars represent the mean ± standard error (n = 6-12 per group). *p < 0.05 with respect to sham control; #p < 0.05 with respect to OVX control; ^ p < 0.05 with respect to T1D-sham.

	CONTROL		DIABETIC	
	Sham	OVX	Sham	OVX
Body Mass (g)	21.8 ± 0.7	23.4 ± 0.4*	18.5 ± 0.7*	18.2 ± 0.6*#
Blood Glucose (mg/dL)	290 ± 20	254 ± 19	489 ± 40*	441 ± 20*#
HbA1c	3.6 ± 0.3	4.7 ± 0.2*	7.8 ± 0.7*	8.4 ± 0.5*#
Subcutaneous fat (%BM)	0.92 ± 0.06	1.015 ± 0.04	0.45 ± 0.04*	0.40 ± 0.03*#
Retroperitoneal Fat (%BM)	0.26 ± 0.02	0.37 ± 0.04*	0.09 ± 0.01*	0.11 ± 0.02*#
Uterus (%BM)	0.58 ± 0.11	0.10 ± 0.01*	0.40 ± 0.11	0.10 ± 0.01*^

Table 2. General Mouse Parameters

Values represent the mean ± standard error (n = 6-12 per group). *p < 0.05 with respect to sham control; #p < 0.05 with respect to OVX control; ^ p < 0.05 with respect to T1D-sham.

	CONTROL		DIABETIC	
	Sham	OVX	Sham	OVX
Femur Trabecular				
BVF	28.3 ± 1.0	13.4 ± 1.0*	12.4 ± 2.2*	4.4 ± 0.4*#^
BMD (mg/cc)	293.9 ± 4.9	209.0 ± 7.8	195.2 ± 16.7*	136.7 ± 6.52*#^
BMC (mg)	0.43 ± 0.01	0.35 ± 0.01*	0.33 ± 0.02*	0.24 ± 0.01*#^
Tb. Th. (um)	56.2 ± 1.1	42.1 ± 1.0*	40.7 ± 2.9*	31.6 ± 1.0*#^
Tb. N. (1/mm)	5.03 ± 0.13	3.17 ± 0.18*	2.93 ± 0.35*	1.38 ± 0.11*#^
Tb. Sp. (um)	143.1 ± 5.1	286.0 ± 19.1*	331.4 ± 55.3*	754.0 ± 71.1*#^
Vertebral Trabecular				
BVF	44.6 ± 4.6	40.4 ± 2.3	32.0 ± 4.3	21.6 ± 1.4*#^
BMD (mg/cc)	307.2 ± 15.3	284.9 ± 9.9	253.1 ± 22.9	200.6 ± 6.1*#^
BMC (mg)	0.44 ± 0.07	0.45 ± 0.04	0.35 ± 0.04	0.37 ± 0.03
Tb. Th. (um)	63.2 ± 4.9	56.8 ± 2.8	48.5 ± 4.7	37.4 ± 1.3*#^
Tb. N. (1/mm)	7.04 ± 0.51	7.10 ± 0.19	6.45 ± 0.26	5.72 ± 0.23*#
Tb. Sp. (um)	81.8 ± 11.8	84.9 ± 4.9	107.2 ± 10.7	141.3 ± 9.1*#
Femur Cortical				
Mean Thickness (mm)	0.248 ± 0.003	0.261 ± 0.004	0.237 ± 0.051	0.229 ± 0.004*#
Inner Perimeter (mm)	2.80 ± 0.05	2.76 ± 0.02	2.89 ± 0.04	2.84 ± 0.03
Outer Perimeter (mm)	4.36 ± 0.06	4.40 ± 0.03	4.39 ± 0.02	4.29 ± 0.03#
Marrow Area (mm2)	0.56 ± 0.02	0.54 ± 0.01	0.59 ± 0.01	0.58 ± 0.01#
Cortical Area (mm2)	0.85 ± 0.02	0.89 ± 0.02	0.82 ± 0.01	0.78 ± 0.02*#
BMD (mg/cc)	1066 ± 17	1053 ± 12	998 ± 14*	984.9 ± 17*#
BMC (mg)	0.018 ± 0.000	0.019 ± 0.000	0.016 ± 0.000*	0.016 ± 0.000*#

Table 3. Femoral and Vertebral Bone Parameters

Values represent the mean ± standard error (n = 6-12 per group). *p < 0.05 with respect to sham control; #p < 0.05 with respect to OVX control; ^ p < 0.05 with respect to T1D-sham.

5.4.2. T1D-OVX Mice Have Increased Osteoblast Death and Decreased Markers of Osteoblast Maturation Compared to T1D Alone

Previous work has shown that T1D decreases osteoblast (OB) lineage selection, maturation and viability (6,62,178,223–225). Therefore, we examined the impact of T1D in combination with OVX on osteoblast parameters. We measured osteoblast gene expression in tibia, analyzed serum for markers of osteoblast activity, and examined histological preparations of fixed femurs for OB apoptosis. RNA expression analyses revealed a significant decrease in RUNX2 a critical gene for early osteoblast differentiation, in the T1D-OVX animals compared to sham ($p<0.05$) or OVX ($p<0.01$) animals (Figure 23A). Two-way ANOVA analysis indicated an interaction between T1D and OVX in the regulation of RUNX2 expression ($p<0.043$). Osterix, a marker of osteoblast maturation, was significantly decreased in OVX ($p<0.01$), T1D-Sham ($p<0.01$) and T1D-OVX ($p<0.001$) animals with respect to control sham-operated animals (Figure 23B). We also examined osteocalcin expression and serum levels which serve as a marker of osteoblast maturation and activity. Osteocalcin RNA levels in the tibia were significantly decreased in both sham ($p<0.05$) and OVX diabetic ($p<0.05$) conditions in the tibia while serum levels of osteocalcin were significantly lower in the T1D-OVX group compared to the sham ($p<0.001$) or OVX control ($p<0.05$) (Figure 23C and D). Neither measure was affected by OVX. To directly assess osteoblasts in bone, osteoblast number per millimeter of bone surface was counted on femoral histological sections and the total number of osteoblasts per bone surface area was calculated using the bone surface measurement from µCT analysis. Interestingly, there were significantly less osteoblasts per mm of bone in OVX ($p<0.0001$), T1D ($p<0.05$) and T1D-OVX ($p<0.0001$)

conditions with respect to sham controls. Additionally, T1D-OVX had significantly lower total number of osteoblasts than either OVX ($p<0.0001$) or T1D ($p<0.0001$) animals (Figure 23E), which parallels the BVF data. To assess effects on osteoblast viability, we TUNEL stained the femur and found a significant increase in osteoblast apoptosis only in the T1D-OVX animals compared to sham ($p<0.05$), OVX ($p<0.01$) and T1D ($p<0.05$) animals (Figure 23F).

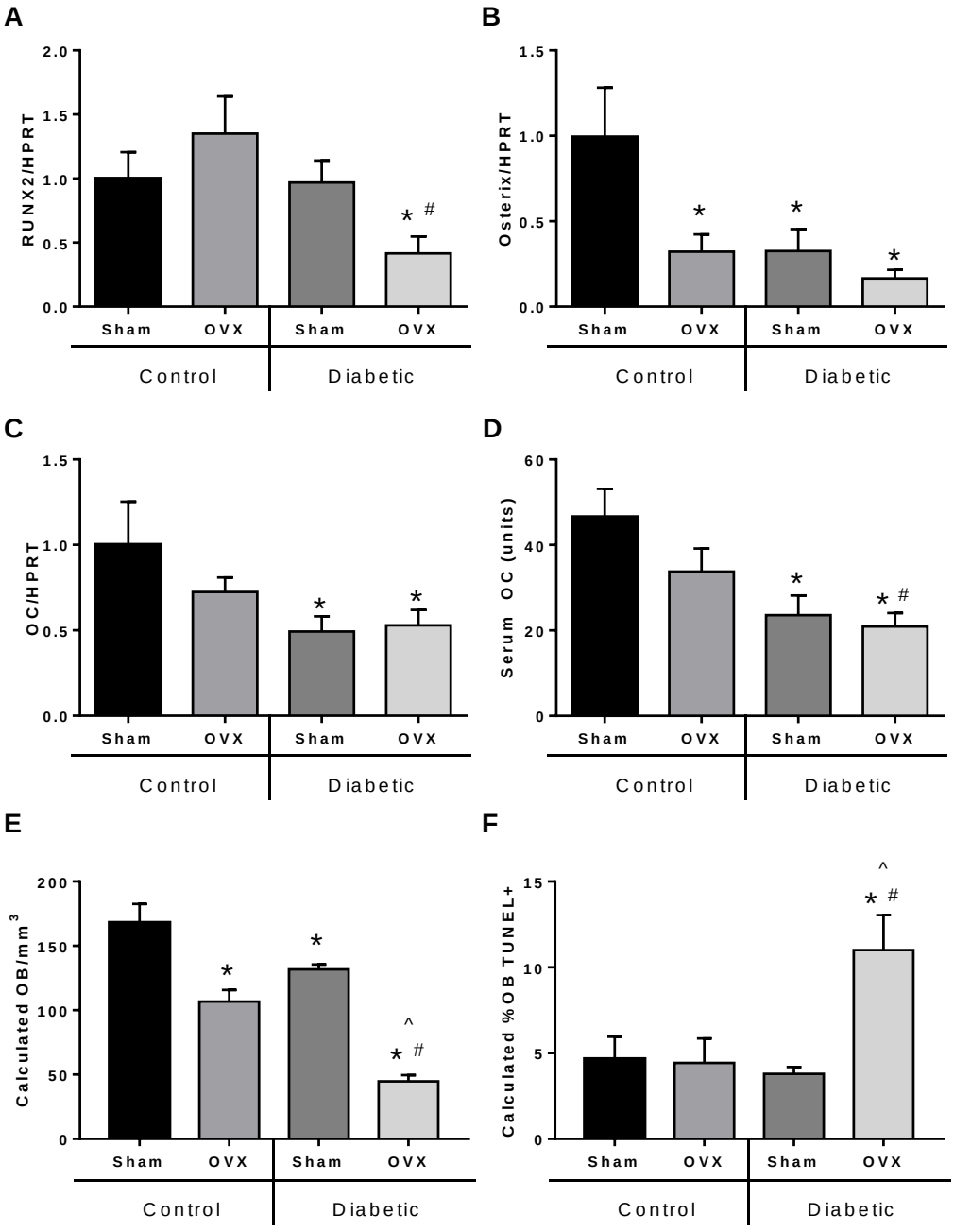

Figure 23. Type 1 Diabetes Decreases Markers of Osteoblast Maturation and Activity and Increases Cell Death When Combined with Ovariectomy

Tibia RNA was isolated and cDNA was analyzed for expression of RUNX2 (A), osterix (B) and osteocalcin (C). Serum osteocalcin levels (D). TUNEL staining was performed on fixed femur sections and total osteoblast number (E) and TUNEL positive osteoblasts were quantified (F). Values represent the mean ± standard error (n = 6-12 per group). *p < 0.05 with respect to sham control; #p < 0.05 with respect to OVX control; ^ p < 0.05 with respect to T1D-sham.

5.4.3. Combination of T1D and OVX Leads to Increased Markers of Osteoclast Activity

While T1D has previously been shown target osteoblast activity, estrogen deficiency has a predominant effect on osteoclasts (152). In order to examine the effect of both T1D and OVX on osteoclast activity we analyzed serum markers, tibia mRNA and femoral histomorphometry. Tibia mRNA expression of tartrate resistant acid phosphatase (TRAP), an enzyme secreted by mature osteoclasts, was significantly decreased in OVX animals compared to controls ($p<0.05$), increased in T1D mice compared to OVX mice ($p<0.01$) and increased in T1D-OVX animals with respect to sham ($p<0.01$) and OVX controls ($p<0.0001$) (Figure 24A). Two-way ANOVA indicated an interaction between T1D and OVX ($p<0.0073$). Interestingly, Serum TRAP5b, an indicator of osteoclast activity, was increased in T1D-Sham and T1D-OVX animals compared to the non-diabetic controls ($p<0.01$) and OVX mice ($p<0.01$) (Figure 24B). We further examined regulators of osteoclast activity and found that the ratio of expression levels of receptor activator of nuclear factor Kappa-B ligand (RANKL, critical in osteoclast differentiation) to osteoprotegrin (OPG, an inhibitor of RANKL) was significantly increased in T1D-OVX animals with respect to sham ($p<0.05$), OVX ($p<0.05$) and T1D ($p<0.01$) animals (Figure 24C). A role for enhanced osteoclast activity is further supported by the ratio of total osteoclast/osteoblast numbers relative to the total bone surface area, which was in T1D-OVX mice with respect to sham ($p<0.05$) and T1D ($p<0.01$) animals (Figure 24D).

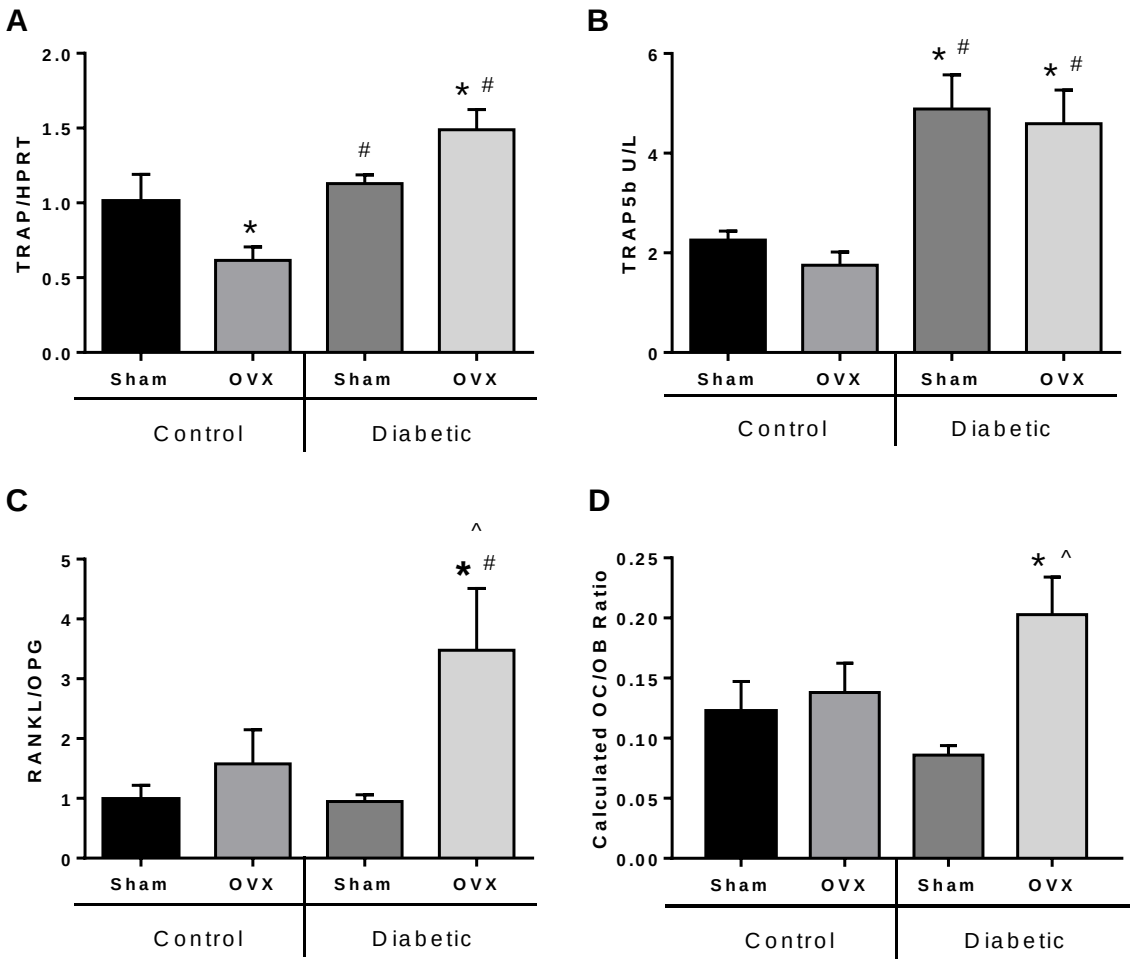

Figure 24. Combination of T1D and OVX Increases Markers of Osteoclast Activity

In order to examine the effect of T1D and OVX on osteoclast activity tibia RNA was extracted and analyzed for osteoclast markers TRAP (A) and RANKL/OPG ratio (C). Serum was collected and analyzed for the osteoclast marker TRAP (B). Femurs were sectioned and TRAP stained for histological analysis of osteoclast number (D). Values represent the mean ± standard error (n = 6-12 per group). *p < 0.05 with respect to sham control; #p < 0.05 with respect to OVX control; ^ p < 0.05 with respect to T1D-sham.

5.4.4. T1D-OVX Mouse Bone Marrow Exhibits Increased Adiposity

Osteoblasts and adipocytes are both derived from mesenchymal stem cells. Selection of adipocytes over osteoblasts will decrease the number of osteoblasts available to remodel bone. Both ovariectomy and T1D have been previously shown increase bone marrow adiposity (59,226), thus, we examined bone marrow adipogenesis in our study by RNA and histomorphometry. Tibia mRNA expression of FABP4 (fatty acid binding protein 4, a marker of adipocyte differentiation), was significantly increased in both T1D-sham and T1D-OVX animals compared to OVX controls ($p<0.01$) (Figure 25A). Histomorphometry further shows an increase in the percentage of adipocyte/total area in both OVX and T1D mice compared to controls but an even greater increase in T1D-OVX animals compared to sham controls ($p<0.001$, Figure 25B and C).

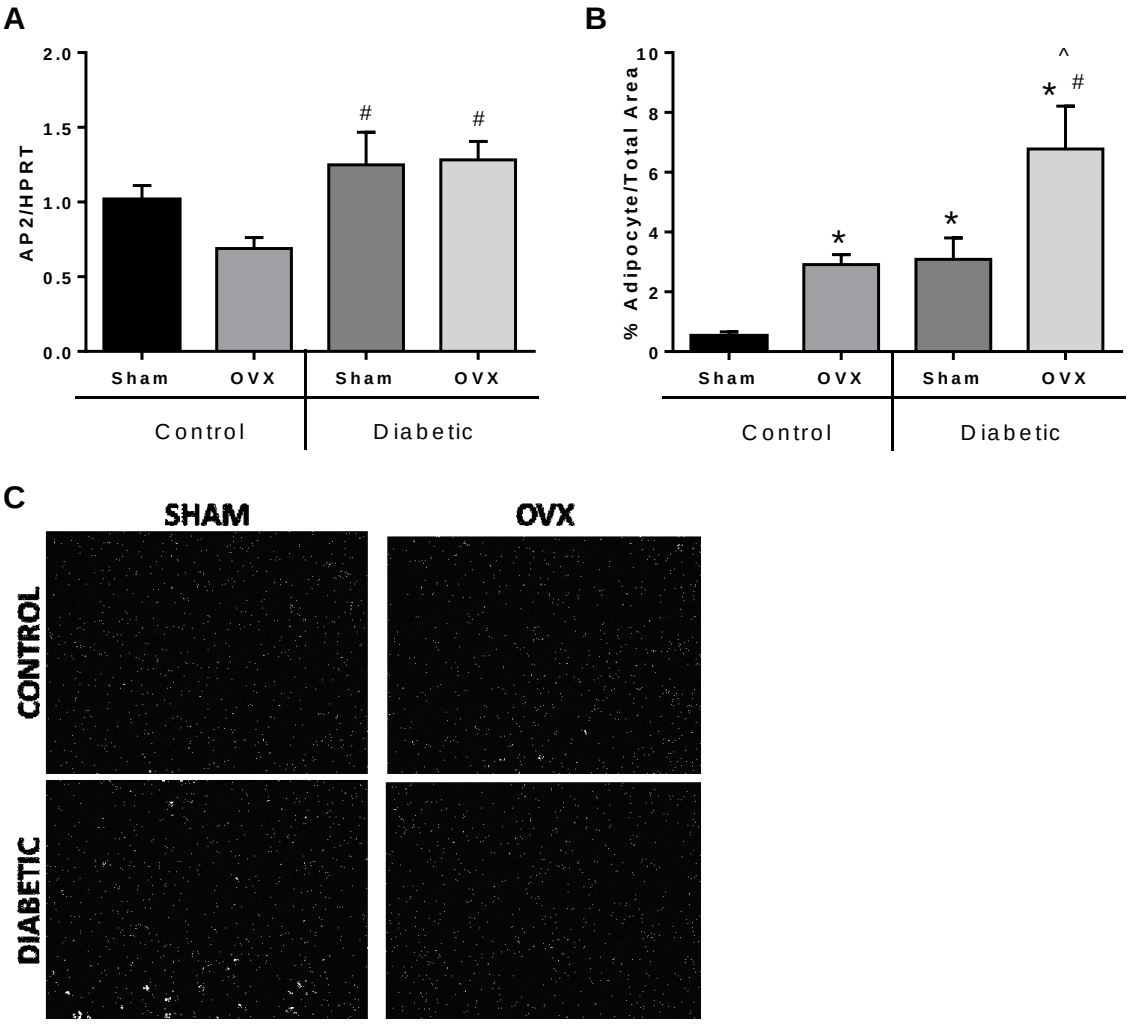

Figure 25. The Bone Marrow of T1D-OVX Mice Exhibits Increased Bone Marrow Adiposity

Tibia RNA was extracted and examined for expression of the adipocyte lineage selection marker AP2 (A). Adipocyte area was quantified from femur histological sections (B). Representative images of the bone marrow are shown in C. Values represent the mean ± standard error (n = 6-12 per group). *$p < 0.05$ with respect to sham control; #$p < 0.05$ with respect to OVX control; ^ $p < 0.05$ with respect to T1D-sham.

5.5. DISCUSSION

T1D patients are living longer due to exogenous insulin therapy resulting in an increase in the number of T1D postmenopausal patients. Therefore, we sought to identify if T1D exacerbates estrogen deficiency induced bone loss. Our findings indicate that indeed the combination/interaction of T1D with OVX leads to a greater femoral BVF loss that is associated with worse trabecular and cortical bone parameters compared to sham or either T1D or OVX alone. The combination of T1D-OVX also shows the greatest decrease in osteoblast markers and viability, while increasing osteoclast parameters and marrow adipocyte area. This is the first study, to our knowledge that shows trabecular bone volume and cortical bone changes as well as dynamic and static histological changes that occur when animals have both T1D and OVX.

Previous studies have examined the effects of either T1D or OVX on bone parameters, with only a few studies that began to look at general effects of T1D-OVX on bone. One study (227) used DEXA to measure femoral BMD in 23 week old rats and found bone loss to have the greatest decreased in T1D-OVX rats (12 weeks T1D), consistent with our finding. Another study examined the effect of T1D-OVX on vertebral bone matrix and found that the combined condition caused a marked reduction in heparin sulfate and chondroitin sulfate (228).

It is logical that T1D and estrogen-deficiency would together induce greater bone loss because they each cause bone loss through different mechanisms. T1D decreases osteoblast lineage selection and differentiation from mesenchymal stem cells as well as decreasing osteoblast activity resulting in reduced bone formation and subsequently bone loss (62). In contrast, estrogen-deficiency induced bone loss as a result of increased

osteoclast activity and lifespan which typically occurs during the first few years after menopause (12). Consistent with this, we demonstrate that the combination of T1D and estrogen deficiency has a negatively additive effect. This effect was due to a combination of increased osteoclast number and activity and a reduction in osteoblast selection, differentiation and activity.

T1D induced bone loss is attributed to decreased osteoblast differentiation from mesenchymal stem cells, decreased osteoblast maturation and bone formation as well as increased bone marrow adiposity. Interestingly, although we found a decrease in RUNX2, a transcription factor necessary for the selection and differentiation of mesenchymal stem cells into osteoblasts, in the T1D-OVX group, we did not see a difference in the T1D-sham animals 4 weeks after the induction of diabetes as seen in previous studies (223,229). We did, however, observe a decrease in osterix and osteocalcin, factors involved in maturation and bone formation respectively, as well as a decrease in the total number of osteoblast cells. In addition, T1D mice showed a decrease in both mineral apposition rate (MAR) and bone formation rate (BFR). These data support the current hypothesis that T1D induced bone loss is primarily due to a defect in bone formation due to decreased numbers and activity of osteoblasts.

While T1D has a predominant effect on bone formation, estrogen deficiency leads to bone loss through increased bone resorption (153). In the present study markers of osteoclast activity (TRAP and RANKL) or the ratio of osteoclast to osteoblast cells in OVX mice were not observed to be increased. However, changes in osteoclast activity typically occur early after ovary removal and so it is highly possible that these changes occurred at an earlier time-point to that looked at in this study. In contrast, the T1D-OVX group had

increased expression of TRAP, in both serum and tibia mRNA expression, RANKL/OPG ratio and an increase in the ratio of osteoclasts to osteoblasts. Although this may be attributed to STZ toxicity, the T1D-sham group only had an increase in serum TRAP and showed no difference in the other markers of osteoclast activity and number. Thus, we hypothesize that the combination of ovariectomy and diabetes exacerbates osteoclast activity which could be attributed to the decrease in osteoblast population. While estrogen deficiency influences osteoclast activity and T1D effects osteoblast activity, both conditions can alter adipogenesis which also impacts bone health.

Both T1D and estrogen deficiency have been shown to cause an increase in bone marrow adipogenesis (41,59,230,231). Consistent with this we found that T1D, OVX and T1D-OVX mice have an increase in the area of adipocytes in the bone marrow compared to sham animals. Only the diabetic conditions showed an increase in AP2, the transcription factor necessary for the selection of adipocytes from mesenchymal stem cells suggesting that the increase in adipocytes during estrogen deficiency may be due to another mechanism. This finding supports a previous report which suggests that although estrogen deficiency leads to an increase in fat mass, it is not a contributing factor to the decline in bone density as OVX mice that are unable to generate bone marrow adipocytes exhibit the same level of bone loss as control OVX mice (232).

Taken together, our data shows that the combination of T1D and OVX leads to increased bone loss compared to either condition alone. We have shown that T1D-OVX decreases osteoblast selection, differentiation, activity and number as well as increasing osteoclast activity and number. Furthermore, T1D and OVX increases bone marrow adiposity. Understanding how T1D and OVX work additively on bone health can lead to

better prevention techniques as well as new therapeutic targets to prevent bone loss and fractures in this patient population.

BIBLIOGRAPHY

BIBLIOGRAPHY

1. Walsh JS. Normal bone physiology, remodelling and its hormonal regulation. Surg (United Kingdom). Elsevier Ltd; 2015;33(1):1–6.

2. Kronenberg H, Williams R. Williams textbook of endocrinology. 11th ed. Saunders/Elsevier, Philidelphia, PA; 2008.

3. Bilezikian J, Raisz L, Rodan G. Principles of bone biology. 2nd ed. ACADEMIC PRESS INC ELSEVIER SCIENCE, 525 B ST, STE 1900, SAN DIEGO, CA 92101-4495 USA; 2002.

4. Sims N a, Gooi JH. Bone remodeling: Multiple cellular interactions required for coupling of bone formation and resorption. Semin Cell Dev Biol. 2008 Oct;19(5):444–51.

5. Baron R, Ferrari S, Russell RGG. Denosumab and bisphosphonates: different mechanisms of action and effects. Bone. ELSEVIER SCIENCE INC, 360 PARK AVE SOUTH, NEW YORK, NY 10010-1710 USA; 2011 Apr 1;48(4):677–92.

6. Khan TS, Fraser LA. Type 1 diabetes and osteoporosis: From molecular pathways to bone phenotype. J Osteoporos. Hindawi Publishing Corporation; 2015;2015.

7. Kearns AE, Khosla S, Kostenuik PJ. Receptor activator of nuclear factor kappaB ligand and osteoprotegerin regulation of bone remodeling in health and disease. Endocr Rev. 2008 Apr;29(2):155–92.

8. Chapurlat RD, Confavreux CB. Novel biological markers of bone: from bone metabolism to bone physiology. Rheumatology. 2016;1–12.

9. Rosen CJ. Clinical practice. Postmenopausal osteoporosis. N Engl J Med. 2005 Aug 11;353(6):595–603.

10. Gabriel SE, Tosteson a N a, Leibson CL, Crowson CS, Pond GR, Hammond CS, et al. Direct medical costs attributable to osteoporotic fractures. Osteoporos Int. 2002;13(4):323–30.

11. Armas LAG, Recker RR. Pathophysiology of Osteoporosis. New Mechanistic Insights. Endocrinol Metab Clin North Am. Elsevier Inc; 2012;41(3):475–86.

12. Manolagas SC, O'Brien C a, Almeida M. The role of estrogen and androgen receptors in bone health and disease. Nat Rev Endocrinol. 2013;9(12):699–712.

13. Garnero P, SornayRendu E, Chapuy M, Delmas P. Increased bone turnover in late postmenopausal women is a major determinant of osteoporosis. J BONE Miner Res. 1996 Mar;11(3):337–49.

14. Martin-Millan M, Almeida M, Ambrogini E, Han L, Zhao H, Weinstein RS, et al. The estrogen receptor-alpha in osteoclasts mediates the protective effects of estrogens on cancellous but not cortical bone. Mol Endocrinol. ENDOCRINE SOC, 8401 CONNECTICUT AVE, SUITE 900, CHEVY CHASE, MD 20815-5817 USA; 2010 Feb;24(2):323–34.

15. Nakamura T, Imai Y, Matsumoto T, Sato S, Takeuchi K, Igarashi K, et al. Estrogen prevents bone loss via estrogen receptor alpha and induction of Fas ligand in osteoclasts. Cell. CELL PRESS, 600 TECHNOLOGY SQUARE, 5TH FLOOR, CAMBRIDGE, MA 02139 USA; 2007 Sep 7;130(5):811–23.

16. Shevde NK, Bendixen AC, Dienger KM, Pike JW. Estrogens suppress RANK ligand-induced osteoclast differentiation via a stromal cell independent mechanism involving c-Jun repression. Proc Natl Acad Sci U S A. NATL ACAD SCIENCES, 2101 CONSTITUTION AVE NW, WASHINGTON, DC 20418 USA; 2000 Jul 5;97(14):7829–34.

17. Huber DM. Androgens Suppress Osteoclast Formation Induced by RANKL and Macrophage-Colony Stimulating Factor. Endocrinology. ENDOCRINE SOC, 4350 EAST WEST HIGHWAY SUITE 500, BETHESDA, MD 20814-4110 USA; 2001 Sep 1;142(9):3800–8.

18. Srivastava S, Toraldo G, Weitzmann MN, Cenci S, Ross FP, Pacifici R. Estrogen decreases osteoclast formation by down-regulating receptor activator of NF-kappa B ligand (RANKL)-induced JNK activation. J Biol Chem. 2001 Mar 23;276(12):8836–40.

19. Robinson LJ, Yaroslavskiy BB, Griswold RD, Zadorozny E V, Guo L, Tourkova IL, et al. Estrogen inhibits RANKL-stimulated osteoclastic differentiation of human monocytes through estrogen and RANKL-regulated interaction of estrogen receptor-alpha with BCAR1 and Traf6. Exp Cell Res. ELSEVIER INC, 525 B

STREET, STE 1900, SAN DIEGO, CA 92101-4495 USA; 2009 Apr 15;315(7):1287–301.

20. Hofbauer LC. Estrogen Stimulates Gene Expression and Protein Production of Osteoprotegerin in Human Osteoblastic Cells. Endocrinology. ENDOCRINE SOC, 8401 CONNECTICUT AVE, SUITE 900, CHEVY CHASE, MD 20815-5817 USA; 1999 Sep 1;140(9):4367–70.

21. Khosla S, Atkinson E, Dunstan C, O'Fallon W, Riggs B. Estrogen and testosterone have opposite effects on circulating OPG levels following induction of hypogonadism and aromatase inhibition in normal elderly men: Potential mechanism for differential effects of estrogen versus testosterone on bone resorption. J BONE Miner Res. 2001 Sep;16:S146–S146.

22. MANOLAGAS S, JILKA R. MECHANISMS OF DISEASE - BONE-MARROW, CYTOKINES, AND BONE REMODELING - EMERGING INSIGHTS INTO THE PATHOPHYSIOLOGY OF OSTEOPOROSIS. N Engl J Med. MASS MEDICAL SOC, 10 SHATTUCK, BOSTON, MA 02115; 1995 Feb;332(5):305–11.

23. Pacifici R, Brown C, Puscheck E, Friedrich E, Slatopolsky E, Maggio D, et al. Effect of surgical menopause and estrogen replacement on cytokine release from human blood mononuclear cells. Proc Natl Acad Sci. NATL ACAD SCIENCES, 2101 CONSTITUTION AVE NW, WASHINGTON, DC 20418; 1991 Jun 15;88(12):5134–8.

24. Tanaka S, Takahashi N, Udagawa N, Tamura T, Akatsu T, Stanley ER, et al. Macrophage colony-stimulating factor is indispensable for both proliferation and differentiation of osteoclast progenitors. J Clin Invest. ROCKEFELLER UNIV PRESS, 1114 FIRST AVE, 4TH FL, NEW YORK, NY 10021; 1993 Jan;91(1):257–63.

25. Kimble RB, Vannice JL, Bloedow DC, Thompson RC, Hopfer W, Kung VT, et al. Interleukin-1 receptor antagonist decreases bone loss and bone resorption in ovariectomized rats. J Clin Invest. ROCKEFELLER UNIV PRESS, 1114 FIRST AVE, 4TH FL, NEW YORK, NY 10021; 1994 May;93(5):1959–67.

26. Ammann P, Rizzoli R, Bonjour JP, Bourrin S, Meyer JM, Vassalli P, et al. Transgenic mice expressing soluble tumor necrosis factor-receptor are protected against bone loss caused by estrogen deficiency. J Clin Invest. ROCKEFELLER UNIV PRESS, 1114 FIRST AVE, 4TH FL, NEW YORK, NY 10021; 1997 Apr 1;99(7):1699–703.

27. Kitazawa R, Kimble RB, Vannice JL, Kung VT, Pacifici R. Interleukin-1 receptor antagonist and tumor necrosis factor binding protein decrease osteoclast formation and bone resorption in ovariectomized mice. J Clin Invest. ROCKEFELLER UNIV PRESS, 1114 FIRST AVE, 4TH FL, NEW YORK, NY 10021; 1994 Dec;94(6):2397–406.

28. Roggia C, Gao Y, Cenci S, Weitzmann MN, Toraldo G, Isaia G, et al. Up-regulation of TNF-producing T cells in the bone marrow: a key mechanism by which estrogen deficiency induces bone loss in vivo. Proc Natl Acad Sci U S A. 2001 Nov 20;98(24):13960–5.

29. Cenci S, Weitzmann MN, Roggia C, Namba N, Novack D, Woodring J, et al. Estrogen deficiency induces bone loss by enhancing T-cell production of TNF- α. 2000;106(10):1229–37.

30. Kousteni S, Bellido T, Plotkin LI, O'Brien CA, Bodenner DL, Han L, et al. Nongenotropic, Sex-Nonspecific Signaling through the Estrogen or Androgen Receptors. Cell. CELL PRESS, 1050 MASSACHUSETTES AVE, CIRCULATION DEPT, CAMBRIDGE, MA 02138 USA; 2001 Mar;104(5):719–30.

31. Almeida M, Han L, Martin-Millan M, Plotkin LI, Stewart SA, Roberson PK, et al. Skeletal involution by age-associated oxidative stress and its acceleration by loss of sex steroids. J Biol Chem. AMER SOC BIOCHEMISTRY MOLECULAR BIOLOGY INC, 9650 ROCKVILLE PIKE, BETHESDA, MD 20814-3996 USA; 2007 Sep 14;282(37):27285–97.

32. Chiang JL, Kirkman MS, Laffel LMB, Peters AL. Type 1 Diabetes Through the Life Span : A Position Statement of the American Diabetes Association. 2014;37(July):2034–54.

33. Hough FS, Pierroz DD, Cooper C, Ferrari SL. MECHANISMS IN ENDOCRINOLOGY: Mechanisms and evaluation of bone fragility in type 1 diabetes mellitus. Eur J Endocrinol. 2016;174(4):R127–38.

34. Weber DR, Haynes K, Leonard MB, Willi SM, Denburg MR. Type 1 diabetes is associated with an increased risk of fracture across the life span: a population-based cohort study using The Health Improvement Network (THIN). Diabetes Care. 2015 Oct;38(10):1913–20.

35. Nicodemus KK, Folsom AR. Type 1 and type 2 diabetes and incident hip fractures in postmenopausal women. Diabetes Care. 2001 Jul;24(7):1192–7.

36. Miao J, Brismar K, Nyrén O, Ugarph-Morawski A, Ye W. Elevated hip fracture risk in type 1 diabetic patients: a population-based cohort study in Sweden. Diabetes Care. 2005 Dec;28(12):2850–5.

37. Vestergaard P. Discrepancies in bone mineral density and fracture risk in patients with type 1 and type 2 diabetes--a meta-analysis. Osteoporos Int. 2007 Apr;18(4):427–44.

38. Ahmed LA, Joakimsen RM, Berntsen GK, Fønnebø V, Schirmer H. Diabetes mellitus and the risk of non-vertebral fractures: the Tromsø study. Osteoporos Int. 2006 Jan;17(4):495–500.

39. Janghorbani M, Van Dam RM, Willett WC, Hu FB. Systematic review of type 1 and type 2 diabetes mellitus and risk of fracture. Am J Epidemiol. 2007 Sep 1;166(5):495–505.

40. Vestergaard P, Rejnmark L, Mosekilde L. Relative fracture risk in patients with diabetes mellitus, and the impact of insulin and oral antidiabetic medication on relative fracture risk. Diabetologia. 2005 Jul;48(7):1292–9.

41. Rosen CJ, Ackert-Bicknell C, Rodriguez JP, Pino AM. Marrow fat and the bone microenvironment: developmental, functional, and pathological implications. Crit Rev Eukaryot Gene Expr. 2009 Jan;19(2):109–24.

42. Sadie-Van Gijsen H, Crowther NJ, Hough FS, Ferris WF. The interrelationship between bone and fat: from cellular see-saw to endocrine reciprocity. Cell Mol Life Sci. 2013 Jul;70(13):2331–49.

43. Baron R, Kneissel M. WNT signaling in bone homeostasis and disease: from human mutations to treatments. Nat Med. 2013 Feb;19(2):179–92.

44. Fleming HE, Janzen V, Lo Celso C, Guo J, Leahy KM, Kronenberg HM, et al. Wnt signaling in the niche enforces hematopoietic stem cell quiescence and is necessary to preserve self-renewal in vivo. Cell Stem Cell. 2008 Mar 6;2(3):274–83.

45. Poole KES, van Bezooijen RL, Loveridge N, Hamersma H, Papapoulos SE, Löwik CW, et al. Sclerostin is a delayed secreted product of osteocytes that inhibits bone formation. FASEB J. 2005 Nov;19(13):1842–4.

46. van Bezooijen RL, Roelen BAJ, Visser A, van der Wee-Pals L, de Wilt E, Karperien M, et al. Sclerostin is an osteocyte-expressed negative regulator of bone formation, but not a classical BMP antagonist. J Exp Med. 2004 Mar 15;199(6):805–14.

47. Day TF, Guo X, Garrett-Beal L, Yang Y. Wnt/beta-catenin signaling in mesenchymal progenitors controls osteoblast and chondrocyte differentiation during vertebrate skeletogenesis. Dev Cell. 2005 May;8(5):739–50.

48. Kennell JA, MacDougald OA. Wnt signaling inhibits adipogenesis through beta-catenin-dependent and -independent mechanisms. J Biol Chem. 2005 Jun 24;280(25):24004–10.

49. Portal-Núñez S, Lozano D, de Castro LF, de Gortázar a R, Nogués X, Esbrit P. Alterations of the Wnt/beta-catenin pathway and its target genes for the N- and C-terminal domains of parathyroid hormone-related protein in bone from diabetic mice. FEBS Lett. 2010 Jul 16;584(14):3095–100.

50. Pignolo RJ, Kassem M. Circulating osteogenic cells: implications for injury, repair, and regeneration. J Bone Miner Res. 2011 Aug;26(8):1685–93.

51. Eghbali-Fatourechi GZ, Lamsam J, Fraser D, Nagel D, Riggs BL, Khosla S. Circulating osteoblast-lineage cells in humans. N Engl J Med. 2005 May 12;352(19):1959–66.

52. Armas LAG, Akhter MP, Drincic A, Recker RR. Trabecular bone histomorphometry in humans with Type 1 Diabetes Mellitus. Bone. 2012 Jan;50(1):91–6.

53. Kemink SA, Hermus AR, Swinkels LM, Lutterman JA, Smals AG. Osteopenia in insulin-dependent diabetes mellitus; prevalence and aspects of pathophysiology. J Endocrinol Invest. 2000 May;23(5):295–303.

54. Cakatay U, Telci A, Kayali R, Akçay T, Sivas A, Aral F. Changes in bone turnover on deoxypyridinoline levels in diabetic patients. Diabetes Res Clin Pract. 1998 May;40(2):75–9.

55. Bjørgaas M, Haug E, Johnsen HJ. The urinary excretion of deoxypyridinium cross-links is higher in diabetic than in nondiabetic adolescents. Calcif Tissue Int. 1999 Aug;65(2):121–4.

56. Cloos C, Wahl P, Hasslacher C, Traber L, Kistner M, Jurkuhn K, et al. Urinary glycosylated, free and total pyridinoline and free and total deoxypyridinoline in diabetes mellitus. Clin Endocrinol (Oxf). 1998 Mar;48(3):317–23.

57. Rees DA, Alcolado JC. Animal models of diabetes mellitus. Diabet Med. 2005 Apr;22(4):359–70.

58. Szkudelski T. The mechanism of alloxan and streptozotocin action in B cells of the rat pancreas. Physiol Res. 2001 Jan;50(6):537–46.

59. Botolin S, McCabe LR. Bone loss and increased bone adiposity in spontaneous and pharmacologically induced diabetic mice. Endocrinology. 2007 Jan;148(1):198–205.

60. Botolin S, Faugere M-C, Malluche H, Orth M, Meyer R, McCabe LR. Increased bone adiposity and peroxisomal proliferator-activated receptor-gamma2 expression in type I diabetic mice. Endocrinology. 2005 Aug;146(8):3622–31.

61. Atkinson MA, Leiter EH. The NOD mouse model of type 1 diabetes: as good as it gets? Nat Med. 1999 Jun;5(6):601–4.

62. McCabe L, Zhang J, Raehtz S. Understanding the skeletal pathology of type 1 and 2 diabetes mellitus. Crit Rev Eukaryot Gene Expr. 2011 Jan;21(2):187–206.

63. Manavalan JS, Cremers S, Dempster DW, Zhou H, Dworakowski E, Kode A, et al. Circulating osteogenic precursor cells in type 2 diabetes mellitus. J Clin Endocrinol Metab. 2012 Sep;97(9):3240–50.

64. Yoshioka M, Kayo T, Ikeda T, Koizumi A. A novel locus, Mody4, distal to D7Mit189 on chromosome 7 determines early-onset NIDDM in nonobese C57BL/6 (Akita) mutant mice. Diabetes. 1997 May;46(5):887–94.

65. Coe LM, Zhang J, McCabe LR. Both spontaneous Ins2(+/-) and streptozotocin-induced type I diabetes cause bone loss in young mice. J Cell Physiol. 2013 Apr;228(4):689–95.

66. Khosla S, Burr D, Cauley J, Dempster DW, Ebeling PR, Felsenberg D, et al. Bisphosphonate-associated osteonecrosis of the jaw: report of a task force of the American Society for Bone and Mineral Research. J Bone Miner Res. 2007

Oct;22(10):1479–91.

67. Bellido T, Ali AA, Plotkin LI, Fu Q, Gubrij I, Roberson PK, et al. Proteasomal degradation of Runx2 shortens parathyroid hormone-induced anti-apoptotic signaling in osteoblasts. A putative explanation for why intermittent administration is needed for bone anabolism. J Biol Chem. 2003 Dec 12;278(50):50259–72.

68. Keller H, Kneissel M. SOST is a target gene for PTH in bone. Bone. 2005 Aug;37(2):148–58.

69. Gallagher JC, Tella SH. Prevention and treatment of postmenopausal osteoporosis. J Steroid Biochem Mol Biol. Elsevier Ltd; 2013 Oct;1–16.

70. Harris L, Senagore P, Young VB, McCabe LR. Inflammatory bowel disease causes reversible suppression of osteoblast and chondrocyte function in mice. Am J Physiol Gastrointest Liver Physiol. 2009 May;296(5):G1020–9.

71. Irwin R, Lee T, Young VB, Parameswaran N, McCabe LR. Colitis-induced bone loss is gender dependent and associated with increased inflammation. Inflamm Bowel Dis. 2013 Jul;19(8):1586–97.

72. Britton R a, Irwin R, Quach D, Schaefer L, Zhang J, Lee T, et al. Probiotic L. reuteri Treatment Prevents Bone Loss in a Menopausal Ovariectomized Mouse Model. J Cell Physiol. 2014 Nov;229(11):1822–30.

73. McCabe LR, Irwin R, Schaefer L, Britton R a. Probiotic use decreases intestinal inflammation and increases bone density in healthy male but not female mice. J Cell Physiol. 2013 Aug;228(8):1793–8.

74. Collins FL, Irwin R, Bierhalter H, Schepper J, Britton RA, Parameswaran N, et al. Lactobacillus reuteri 6475 Increases Bone Density in Intact Females Only under an Inflammatory Setting. PLoS One. 2016;11(4):e0153180.

75. Barrett KE, Barman SM, Boitano S, Brooks HL. Overview of Gastrointestinal Function & Regulation. Ganong’s Review of Medical Physiology, 25e. New York, NY: McGraw-Hill Education; 2016.

76. Smith K, McCoy KD, Macpherson AJ. Use of axenic animals in studying the adaptation of mammals to their commensal intestinal microbiota. Semin Immunol.

2007 Apr;19(2):59–69.

77. Swidsinski A, Sydora BC, Doerffel Y, Loening-Baucke V, Vaneechoutte M, Lupicki M, et al. Viscosity gradient within the mucus layer determines the mucosal barrier function and the spatial organization of the intestinal microbiota. Inflamm Bowel Dis. 2007 Aug;13(8):963–70.

78. Van der Sluis M, De Koning BAE, De Bruijn ACJM, Velcich A, Meijerink JPP, Van Goudoever JB, et al. Muc2-deficient mice spontaneously develop colitis, indicating that MUC2 is critical for colonic protection. Gastroenterology. 2006 Jul;131(1):117–29.

79. Clayburgh DR, Shen L, Turner JR. A porous defense: the leaky epithelial barrier in intestinal disease. Lab Invest. 2004;84:282–91.

80. Visser J, Rozing J, Sapone A, Lammers K, Fasano A. Tight Junctions, Intestinal Permeability, and Autoimmunity. Ann N Y Acad Sci. 2009;1165(1):195–205.

81. Natividad JMM, Verdu EF. Modulation of intestinal barrier by intestinal microbiota: pathological and therapeutic implications. Pharmacol Res. Elsevier Ltd; 2013 Mar;69(1):42–51.

82. Spiller RC, Jenkins D, Thornley JP, Hebden JM, Wright T, Skinner M, et al. Increased rectal mucosal enteroendocrine cells, T lymphocytes, and increased gut permeability following acute Campylobacter enteritis and in post-dysenteric irritable bowel syndrome. Gut. 2000 Dec;47(6):804–11.

83. Berkes J, Viswanathan VK, Savkovic SD, Hecht G. Intestinal epithelial responses to enteric pathogens: effects on the tight junction barrier, ion transport, and inflammation. Gut. 2003 Mar;52(3):439–51.

84. Wirtz S, Neufert C, Weigmann B, Neurath MF. Chemically induced mouse models of intestinal inflammation. Nat Protoc. 2007 Jan;2(3):541–6.

85. Dahlman-Wright K, Cavailles V, Fuqua SA, Jordan VC, Katzenellenbogen JA, Korach KS, et al. International Union of Pharmacology. LXIV. Estrogen receptors. Pharmacol Rev. 2006 Dec;58(4):773–81.

86. Campbell-Thompson M, Lynch IJ, Bhardwaj B. Expression of estrogen receptor

(ER) subtypes and ERbeta isoforms in colon cancer. Cancer Res. 2001 Jan 15;61(2):632–40.

87. Konstantinopoulos PA, Kominea A, Vandoros G, Sykiotis GP, Andricopoulos P, Varakis I, et al. Oestrogen receptor beta (ERbeta) is abundantly expressed in normal colonic mucosa, but declines in colon adenocarcinoma paralleling the tumour's dedifferentiation. Eur J Cancer. 2003 Jun;39(9):1251–8.

88. Godet PG, May GR, Sutherland LR. Meta-analysis of the role of oral contraceptive agents in inflammatory bowel disease. Gut. 1995 Nov;37(5):668–73.

89. Khalili H, Higuchi LM, Ananthakrishnan AN, Manson JE, Feskanich D, Richter JM, et al. Hormone therapy increases risk of ulcerative colitis but not Crohn's disease. Gastroenterology. 2012 Nov;143(5):1199–206.

90. Khalili H, Higuchi LM, Ananthakrishnan AN, Richter JM, Feskanich D, Fuchs CS, et al. Oral contraceptives, reproductive factors and risk of inflammatory bowel disease. Gut. 2013 Aug;62(8):1153–9.

91. Cornish JA, Tan E, Simillis C, Clark SK, Teare J, Tekkis PP. The risk of oral contraceptives in the etiology of inflammatory bowel disease: a meta-analysis. Am J Gastroenterol. 2008 Sep;103(9):2394–400.

92. Heijmans J, Wielenga MCB, Rosekrans SL, van Lidth de Jeude JF, Roelofs J, Groothuis P, et al. Oestrogens promote tumorigenesis in a mouse model for colitis-associated cancer. Gut. 2014 Feb;63(2):310–6.

93. Braniste V, Leveque M, Buisson-Brenac C, Bueno L, Fioramonti J, Houdeau E. Oestradiol decreases colonic permeability through oestrogen receptor beta-mediated up-regulation of occludin and junctional adhesion molecule-A in epithelial cells. J Physiol. 2009 Jul 1;587(Pt 13):3317–28.

94. Braniste V, Jouault A, Gaultier E, Polizzi A, Buisson-Brenac C, Leveque M, et al. Impact of oral bisphenol A at reference doses on intestinal barrier function and sex differences after perinatal exposure in rats. Proc Natl Acad Sci U S A. 2010;107(1):448–53.

95. Looijer-van Langen M, Hotte N, Dieleman LA, Albert E, Mulder C, Madsen KL, et al. Estrogen receptor-β signaling modulates epithelial barrier function. Am J

Physiol Gastrointest Liver Physiol. 2011 Apr;300(4):G621–6.

96. Fasano A. Leaky gut and autoimmune diseases. Clin Rev Allergy Immunol. 2012 Feb;42(1):71–8.

97. Vaarala O, Atkinson MA, Neu J. The “Perfect Storm” for Type 1 Diabetes: The Complex Interplay Between Intestinal Microbiota, Gut Permeability, and Mucosal Immunity. Diabetes. 2008;57(10):2555–62.

98. Meddings JB, Jarand J, Urbanski SJ, Hardin J, Gall DG. Increased gastrointestinal permeability is an early lesion in the spontaneously diabetic BB rat. Am J Physiol. 1999 Apr;276(4 Pt 1):G951–7.

99. Neu J, Reverte CM, Mackey AD, Liboni K, Tuhacek-Tenace LM, Hatch M, et al. Changes in intestinal morphology and permeability in the biobreeding rat before the onset of type 1 diabetes. J Pediatr Gastroenterol Nutr. 2005 May;40(5):589–95.

100. Todd DJ, Forsberg EM, Greiner DL, Mordes JP, Rossini AA, Bortell R. Deficiencies in gut NK cell number and function precede diabetes onset in BB rats. J Immunol. 2004 May 1;172(9):5356–62.

101. Carratù R, Secondulfo M, de Magistris L, Iafusco D, Urio A, Carbone MG, et al. Altered intestinal permeability to mannitol in diabetes mellitus type I. J Pediatr Gastroenterol Nutr. 1999 Mar;28(3):264–9.

102. Kuitunen M, Saukkonen T, Ilonen J, Akerblom HK, Savilahti E. Intestinal permeability to mannitol and lactulose in children with type 1 diabetes with the HLA-DQB1*02 allele. Autoimmunity. 2002 Aug;35(5):365–8.

103. Wright NC, Looker AC, Saag KG, Curtis JR, Delzell ES, Randall S, et al. The recent prevalence of osteoporosis and low bone mass in the united states based on bone mineral density at the femoral neck or lumbar spine. J Bone Miner Res. 2014;29(S1):2520–6.

104. Hinoi E, Gao N, Jung DY, Yadav V, Yoshizawa T, Kajimura D, et al. An Osteoblast-dependent mechanism contributes to the leptin regulation of insulin secretion. Ann N Y Acad Sci. 2009 Sep;1173 Suppl:E20–30.

105. Yoshizawa T, Hinoi E, Jung DY, Kajimura D, Ferron M, Seo J, et al. The transcription factor ATF4 regulates glucose metabolism in mice through its expression in osteoblasts. J Clin Invest. 2009 Sep;119(9):2807–17.

106. McCabe L, Britton RA, Parameswaran N. Prebiotic and Probiotic Regulation of Bone Health: Role of the Intestine and its Microbiome. Curr Osteoporos Rep. 2015;13(6):363–71.

107. McCabe LR, Irwin R, Schaefer L, Britton R a. Probiotic use decreases intestinal inflammation and increases bone density in healthy male but not female mice. J Cell Physiol. 2013 Aug;228(8):1793–8.

108. Zhang J, Motyl KJ, Irwin R, MacDougald OA, Britton RA, McCabe LR. Loss of bone and Wnt10b expression in male type 1 diabetic mice is blocked by the probiotic Lactobacillus reuteri. Endocrinology. 2015;156(9):3169–82.

109. Weaver CM. Diet, gut microbiome, and bone health. Curr Osteoporos Rep. 2015 Apr;13(2):125–30.

110. Cantini G, Mannucci E, Luconi M. Perspectives in GLP-1 Research: New Targets, New Receptors. Trends Endocrinol Metab. Elsevier Ltd; 2016;27(6):427–38.

111. Gallwitz B. Glucagon-like peptide-1 and gastric inhibitory polypeptide: new advances. Curr Opin Endocrinol Diabetes Obes. 2016 Feb;23(1):23–7.

112. Zofková I, Matucha P. New insights into the physiology of bone regulation: the role of neurohormones. Physiol Res. 2014;63(4):421–7.

113. Gensollen T, Iyer SS, Kasper DL, Blumberg RS. How colonization by microbiota in early life shapes the immune system. Science (80-). 2016;352(6285):539–44.

114. Honda K, Littman DR. The microbiome in infectious disease and inflammation. Annu Rev Immunol. 2012 Jan;30:759–95.

115. Garrett WS, Gordon JI, Glimcher LH. Homeostasis and inflammation in the intestine. Cell. Elsevier Inc.; 2010 Mar 19;140(6):859–70.

116. Cani PD, Everard A, Duparc T. Gut microbiota, enteroendocrine functions and

metabolism. Curr Opin Pharmacol. 2013 Dec;13(6):935–40.

117. Sommer F, Bäckhed F. The gut microbiota--masters of host development and physiology. Nat Rev Microbiol. Nature Publishing Group; 2013;11(4):227–38.

118. Zhang K, Hornef MW, Dupont A. The intestinal epithelium as guardian of gut barrier integrity. Cell Microbiol. 2015;n/a – n/a.

119. Li J-Y, Chassaing B, Tyagi AM, Vaccaro C, Luo T, Adams J, et al. Sex steroid deficiency-associated bone loss is microbiota dependent and prevented by probiotics. J Clin Invest. 2016 Apr 25;(36):1–15.

120. Sjögren K, Engdahl C, Henning P, Lerner UH, Tremaroli V, Lagerquist MK, et al. The gut microbiota regulates bone mass in mice. J Bone Miner Res. 2012 Jun 17;27(6):1357–67.

121. Cho I, Yamanishi S, Cox L, Methé BA, Zavadil J, Li K, et al. Antibiotics in early life alter the murine colonic microbiome and adiposity. Nature. 2012 Aug 30;488(7413):621–6.

122. Roberfroid M, Gibson GR, Hoyles L, McCartney AL, Rastall R, Rowland I, et al. Prebiotic effects: metabolic and health benefits. Br J Nutr. 2010 Aug;104 Suppl :S1–63.

123. Macfarlane S, Macfarlane GT, Cummings JH. Review article: prebiotics in the gastrointestinal tract. Aliment Pharmacol Ther. 2006 Sep 1;24(5):701–14.

124. Scholz-Ahrens KE, Ade P, Marten B, Weber P, Timm W, Açil Y, et al. Prebiotics, probiotics, and synbiotics affect mineral absorption, bone mineral content, and bone structure. J Nutr. 2007;137(3 Suppl 2):838S – 46S.

125. García-Vieyra MI, Del Real A, López MG. Agave fructans: their effect on mineral absorption and bone mineral content. J Med Food. 2014 Nov;17(11):1247–55.

126. Takahara S, Morohashi T, Sano T, Ohta A, Yamada S, Sasa R. Fructooligosaccharide consumption enhances femoral bone volume and mineral concentrations in rats. J Nutr. 2000 Jul;130(7):1792–5.

127. Chonan O, Matsumoto K, Watanuki M. Effect of galactooligosaccharides on calcium absorption and preventing bone loss in ovariectomized rats. Biosci Biotechnol Biochem. 1995 Feb;59(2):236–9.

128. Ohta A, Uehara M, Sakai K, Takasaki M, Adlercreutz H, Morohashi T, et al. A combination of dietary fructooligosaccharides and isoflavone conjugates increases femoral bone mineral density and equol production in ovariectomized mice. J Nutr. 2002 Jul;132(7):2048–54.

129. Ghishan FK, Kiela PR. Advances in the understanding of mineral and bone metabolism in inflammatory bowel diseases. Am J Physiol Gastrointest Liver Physiol. 2010 Nov 18;300(November 2010):G191–201.

130. Bianchi ML. Inflammatory bowel diseases, celiac disease, and bone. Arch Biochem Biophys. Elsevier Inc.; 2010 Nov 1;503(1):54–65.

131. Groschwitz KR, Hogan SP. Intestinal barrier function: molecular regulation and disease pathogenesis. J Allergy Clin Immunol. Elsevier Ltd; 2009 Jul;124(1):3–20; quiz 21–2.

132. Clayburgh DR, Shen L, Turner JR. A porous defense: the leaky epithelial barrier in intestinal disease. Lab Invest. 2004 Mar;84(3):282–91.

133. Navabi N, McGuckin MA, Lindén SK. Gastrointestinal Cell Lines Form Polarized Epithelia with an Adherent Mucus Layer when Cultured in Semi-Wet Interfaces with Mechanical Stimulation. PLoS One. 2013;8(7).

134. Wada-Hiraike O, Imamov O, Hiraike H, Hultenby K, Schwend T, Omoto Y, et al. Role of estrogen receptor beta in colonic epithelium. Proc Natl Acad Sci U S A. 2006 Feb 21;103(5):1605–8.

135. Wada-Hiraike O, Warner M, Gustafsson J-A. New developments in oestrogen signalling in colonic epithelium. Biochem Soc Trans. 2006 Dec;34(Pt 6):1114–6.

136. Braniste V, Leveque M, Buisson-Brenac C, Bueno L, Fioramonti J, Houdeau E. Oestradiol decreases colonic permeability through oestrogen receptor beta-mediated up-regulation of occludin and junctional adhesion molecule-A in epithelial cells. J Physiol. 2009;587(Pt 13):3317–28.

137. Trunova G V., Makarova O V., Diatroptov ME, Bogdanova IM, Mikchailova LP, Abdulaeva SO. Morphofunctional characteristic of the immune system in BALB/c and C57Bl/6 mice. Bull Exp Biol Med. 2011;151(1):99–102.

138. Kawano N, Koji T, Hishikawa Y, Murase K, Murata I, Kohno S. Identification and localization of estrogen receptor alpha- and beta-positive cells in adult male and female mouse intestine at various estrogen levels. Histochem Cell Biol. 2004;121(5):399–405.

139. Dey P, Barros RPA, Warner M, Str??m A, Gustafsson J ??ke. Insight into the mechanisms of action of estrogen receptor ?? in the breast, prostate, colon, and CNS. J Mol Endocrinol. 2013;51(3).

140. Prossnitz ER, Arterburn JB, Smith HO, Oprea TI, Sklar L a, Hathaway HJ. Estrogen signaling through the transmembrane G protein-coupled receptor GPR30. Annu Rev Physiol. 2008;70:165–90.

141. Javid SH, Moran AE, Carothers AM, Redston M, Bertagnolli MM. Modulation of tumor formation and intestinal cell migration by estrogens in the ApcMin/+ mouse model of colorectal cancer. Carcinogenesis. 2005;26(3):587–95.

142. Dong XL, Zhang Y, Wong MS. Estrogen deficiency-induced Ca balance impairment is associated with decrease in expression of epithelial Ca transport proteins in aged female rats. Life Sci. Elsevier B.V.; 2014;96(1-2):26–32.

143. Hoenderop JGJ, Nilius B, Bindels RJM. Calcium absorption across epithelia. Physiol Rev. 2005;85(1):373–422.

144. Prince RL, Smith M, Dick IM, Price RI, Webb PG, Henderson NK, et al. Prevention of postmenopausal osteoporosis. A comparative study of exercise, calcium supplementation, and hormone-replacement therapy. N Engl J Med. Massachusetts Medical Society; 1991 Oct 24;325(17):1189–95.

145. Heshmati HM, Khosla S, Burritt MF, O'Fallon WM, Riggs BL. A defect in renal calcium conservation may contribute to the pathogenesis of postmenopausal osteoporosis. J Clin Endocrinol Metab. 1998 Jun;83(6):1916–20.

146. O'Loughlin PD, Morris HA. Oestrogen deficiency impairs intestinal calcium absorption in the rat. J Physiol. 1998;511 (Pt 1:313–22.

147. O'Loughlin PD, Morris HA. Oestrogen deficiency impairs intestinal calcium absorption in the rat. J Physiol. 1998 Aug 22;511(1):313–22.

148. Schwartz B, Smirnoff P, Shany S, Liel Y. Estrogen controls expression and bioresponse of 1,25-dihydroxyvitamin D receptors in the rat colon. Mol Cell Biochem. 2000;203(1-2):87–93.

149. Gilad LA, Bresler T, Gnainsky J, Smirnoff P, Schwartz B. Regulation of vitamin D receptor expression via estrogen-induced activation of the ERK 1/2 signaling pathway in colon and breast cancer cells. J Endocrinol. 2005;185(3):577–92.

150. Alexander RT, Rievaj J, Dimke H. Paracellular calcium transport across renal and intestinal epithelia. Biochem Cell Biol. 2014;92(6):467–80.

151. Bronner F. Mechanisms of intestinal calcium absorption. J Cell Biochem. 2003 Feb 1;88(2):387–93.

152. Frenkel B, Hong A, Baniwal SK, Coetzee G a, Ohlsson C, Khalid O, et al. Regulation of adult bone turnover by sex steroids. J Cell Physiol. 2010 Aug;224(2):305–10.

153. Khosla S, Oursler MJ, Monroe DG. Estrogen and the skeleton. Trends Endocrinol Metab. Elsevier Ltd; 2012 Nov;23(11):576–81.

154. Henderson P, van Limbergen JE, Schwarze J, Wilson DC. Function of the intestinal epithelium and its dysregulation in inflammatory bowel disease. Inflamm Bowel Dis. 2011 Jan;17(1):382–95.

155. Diebel ME, Diebel LN, Manke CW, Liberati DM. Estrogen modulates intestinal mucus physiochemical properties and protects against oxidant injury. J Trauma Acute Care Surg. 2015;78(1):94–9.

156. Kampa M, Saint-Criq V, Rapetti-Mauss R, Yusef YR, Harvey BJ. Estrogen regulation of epithelial ion transport: Implications in health and disease. Steroids. 2012;77(10):918–23.

157. Hogan AM, Collins D, Baird AW, Winter DC. Estrogen and its role in gastrointestinal health and disease. Int J Colorectal Dis. 2009 Dec;24(12):1367–75.

158. Kim YS, Ho SB. Intestinal goblet cells and mucins in health and disease: Recent insights and progress. Curr Gastroenterol Rep. 2010;12(5):319–30.

159. Deuring JJ, de Haar C, Kuipers EJ, Peppelenbosch MP, van der Woude CJ. The cell biology of the intestinal epithelium and its relation to inflammatory bowel disease. Int J Biochem Cell Biol. Elsevier Ltd; 2013 Apr;45(4):798–806.

160. Müller C a, Autenrieth IB, Peschel a. Innate defenses of the intestinal epithelial barrier. Cell Mol Life Sci. 2005 Jun;62(12):1297–307.

161. Cornick S, Tawiah A, Chadee K. Roles and regulation of the mucus barrier in the gut. Tissue Barriers. 2015;3(1-2):e982426.

162. Guttmacher AF, Shettles LB. Cyclic changes in cervical mucus, and its practical importance. Hum Fertil. 1940 Mar;5(1):4–9.

163. Valuckaite V, Zaborina O, Long J, Hauer-jensen M, Wang J, Holbrook C, et al. Oral PEG 15 – 20 protects the intestine against radiation : role of lipid rafts. 2009;60637:1041–52.

164. Henry-Stanley MJ, Wells CL. Polyethylene glycol influences microbial interactions with intestinal epithelium. Shock. 2009;31(4):390–6.

165. Wu L, Zaborina O, Zaborin A, Chang EB, Musch M, Holbrook C, et al. High-Molecular-Weight Polyethylene Glycol Prevents Lethal Sepsis Due to Intestinal. 2004;488–98.

166. Oltean M, Joshi M, Björkman E, Oltean S, Casselbrant a, Herlenius G, et al. Intraluminal polyethylene glycol stabilizes tight junctions and improves intestinal preservation in the rat. Am J Transplant. 2012 Aug;12(8):2044–51.

167. Valuckaite V, Seal J, Zaborina O, Tretiakova M, Testa G, Alverdy JC. High molecular weight polyethylene glycol (PEG 15-20) maintains mucosal microbial barrier function during intestinal graft preservation. J Surg Res. 2013 Aug;183(2):869–75.

168. Oltean M, Hellstr??m M, Ciuce C, Zhu C, Casselbrant A. Luminal solutions protect mucosal barrier during extended preservation. J Surg Res. 2015;194(1):289–96.

169. Pelaseyed T, Bergstr??m JH, Gustafsson JK, Ermund A, Birchenough GMH, Sch??tte A, et al. The mucus and mucins of the goblet cells and enterocytes provide the first defense line of the gastrointestinal tract and interact with the immune system. Immunol Rev. 2014;260(1):8–20.

170. Taupin D, Podolsky DK. Trefoil factors: initiators of mucosal healing. Nat Rev Mol Cell Biol. 2003;4(9):721–32.

171. van der Flier LG, Clevers HC. Stem cells, self-renewal, and differentiation in the intestinal epithelium. Annu Rev Physiol. 2009;71:241–60.

172. Al-sadi R, Khatib K, Guo S, Ye D, Youssef M, Ma T. Occludin regulates macromolecule flux across the intestinal epithelial tight junction barrier. 2011;1054–64.

173. Tam A, Wadsworth S, Dorscheid D, Man S-FP, Sin DD. Estradiol increases mucus synthesis in bronchial epithelial cells. PLoS One. 2014 Jan;9(6):e100633.

174. Check JH. Diagnosis and treatment of cervical mucus abnormalities. Clin Exp Obstet Gynecol. 2006 Jan;33(3):140–2.

175. Andersson A, Windahl SH, Farman HH, Ohlsson C, Engdahl C, Fa F, et al. Probiotics Protect Mice from Ovariectomy-Induced Cortical Bone Loss. 2014;9(3).

176. David M Maahs, Nancy A West, Jean M. Lawrence, And Mayer-Davis EJ. Epidemiology of Type 1 Diabetes. Endocrinol Metab Clin North Am. 2010;39:481–97.

177. Botolin S, McCabe LR. Chronic hyperglycemia modulates osteoblast gene expression through osmotic and non-osmotic pathways. J Cell Biochem. 2006 Oct 1;99(2):411–24.

178. Coe LM, Irwin R, Lippner D, McCabe LR. The bone marrow microenvironment contributes to type I diabetes induced osteoblast death. J Cell Physiol. 2011 Feb;226(2):477–83.

179. Vaarala O, Atkinson M a, Neu J. The “perfect storm” for type 1 diabetes: the complex interplay between intestinal microbiota, gut permeability, and mucosal immunity. Diabetes. 2008 Oct;57(10):2555–62.

180. Vaarala O. Is the origin of type 1 diabetes in the gut? Immunol Cell Biol. 2012;90(3):271–6.

181. Graham S, Courtois P, Malaisse WJ, Rozing J, Scott FW, Mowat AMI. Enteropathy precedes type 1 diabetes in the BB rat. Gut. 2004 Oct;53(10):1437–44.

182. Bosi E, Molteni L, Radaelli MG, Folini L, Fermo I, Bazzigaluppi E, et al. Increased intestinal permeability precedes clinical onset of type 1 diabetes. Diabetologia. 2006;49(12):2824–7.

183. Sapone A, de Magistris L, Pietzak M, Clemente MG, Tripathi A, Cucca F, et al. Zonulin upregulation is associated with increased gut permeability in subjects with type 1 diabetes and their relatives. Diabetes. 2006 May;55(5):1443–9.

184. Secondulfo M, Iafusco D, Carratù R, deMagistris L, Sapone A, Generoso M, et al. Ultrastructural mucosal alterations and increased intestinal permeability in non-celiac, type I diabetic patients. Dig Liver Dis. 2004 Jan;36(1):35–45.

185. Hara N, Alkanani AK, Ir D, Robertson CE, Wagner BD, Frank DN, et al. The role of the intestinal microbiota in type 1 diabetes. Clin Immunol. Elsevier Inc.; 2013;146(2):112–9.

186. Wirth R, Bódi N, Maróti G, Bagyánszki M, Talapka P, Fekete É, et al. Regionally distinct alterations in the composition of the gut microbiota in rats with streptozotocin-induced diabetes. PLoS One. 2014;9(12):e110440.

187. Li Y, Liu Y, Chu C. Th17 Cells in Type 1 Diabetes : Role in the Pathogenesis and Regulation by Gut Microbiome. 2015;2015.

188. Dunne JL, Triplett EW, Gevers D, Xavier R, Insel R, Danska J, et al. The intestinal microbiome in type 1 diabetes. Clin Exp Immunol. 2014;177(1):30–7.

189. Davis-Richardson AG, Triplett EW. A model for the role of gut bacteria in the development of autoimmunity for type 1 diabetes. Diabetologia. 2015;1386–93.

190. Tlaskalová-Hogenová H, Stěpánková R, Kozáková H, Hudcovic T, Vannucci L, Tučková L, et al. The role of gut microbiota (commensal bacteria) and the mucosal barrier in the pathogenesis of inflammatory and autoimmune diseases

and cancer: contribution of germ-free and gnotobiotic animal models of human diseases. Cell Mol Immunol. 2011;8(2):110–20.

191. Cani PD, Possemiers S, Van de Wiele T, Guiot Y, Everard a, Rottier O, et al. Changes in gut microbiota control inflammation in obese mice through a mechanism involving GLP-2-driven improvement of gut permeability. Gut. 2009;58(8):1091–103.

192. Hara N, Alkanani AK, Ir D, Robertson CE, Wagner BD, Frank DN, et al. The role of the intestinal microbiota in type 1 diabetes. Clin Immunol. Nature Publishing Group; 2013;146(2):112–9.

193. Horvath VJ, Putz Z, Izbeki F, Korei AE, Gero L, Lengyel C, et al. Diabetes-Related Dysfunction of the Small Intestine and the Colon: Focus on Motility. Curr Diab Rep. 2015;15(11).

194. Pacifici R. The immune system and bone. Arch Biochem Biophys. 2010;503(1):41–53.

195. Mangialardi G, Oikawa A, Reni C, Madeddu P. Bone marrow microenvironment: a newly recognized target for diabetes-induced cellular damage. Endocr Metab Immune Disord Drug Targets. 2012 Jun;12(2):159–67.

196. Mori G, D'Amelio P, Faccio R, Brunetti G. Bone-immune cell crosstalk: Bone diseases. J Immunol Res. Hindawi Publishing Corporation; 2015;2015.

197. Demedts I, Masaoka T, Kindt S, Hertogh G De, Geboes K, Farr?? R, et al. Gastrointestinal motility changes and myenteric plexus alterations in spontaneously diabetic biobreeding rats. J Neurogastroenterol Motil. 2013;19(2):161–70.

198. de Kort S, Keszthelyi D, Masclee a a M. Leaky gut and diabetes mellitus: what is the link? Obes Rev. 2011 Jun;12(6):449–58.

199. Valuckaite V, Seal J, Zaborina O, Tretiakova M, Testa G, Alver. High molecular weight polyethylene glycol (PEG 15-20) maintains mucosal microbial barrier function during intestinal graft preservation. August. 2013;183(2):869–75.

200. Polymeris A, Michalakis K, Sarantopoulou V. Secondary osteoporosis - an

endocrinological approach focusing on underlying mechanisms. Endocr Regul. 2013 Jul;47(3):137–48.

201. Atkinson MA, Eisenbarth GS, Michels AW. Type 1 diabetes. Lancet. 2014;383(9911):69–82.

202. Huang ES, Brown SES, Ewigman BG, Foley EC, Meltzer DO. Patient perceptions of quality of life with diabetes-related complications and treatments. Diabetes Care. 2007 Oct;30(10):2478–83.

203. The effect of intensive treatment of diabetes on the development and progression of long-term complications in insulin-dependent diabetes mellitus. The Diabetes Control and Complications Trial Research Group. N Engl J Med. 1993 Sep 30;329(14):977–86.

204. Hothersall EJ, Livingstone SJ, Looker HC, Ahmed SF, Cleland S, Leese GP, et al. Contemporary risk of hip fracture in type 1 and type 2 diabetes: a national registry study from Scotland. J Bone Miner Res. 2014 Jan;29(5):1054–60.

205. Hofbauer LC, Brueck CC, Singh SK, Dobnig H. Osteoporosis in patients with diabetes mellitus. J Bone Miner Res. 2007 Sep;22(9):1317–28.

206. McCabe LR. Understanding the pathology and mechanisms of type I diabetic bone loss. J Cell Biochem. 2007 Dec 15;102(6):1343–57.

207. Maddaloni E, D'Onofrio L, Lauria A, Maurizi AR, Strollo R, Palermo A, et al. Osteocalcin levels are inversely associated with Hba1c and BMI in adult subjects with long-standing type 1 diabetes. J Endocrinol Invest. 2014 Jul;37(7):661–6.

208. Loureiro MB, Ururahy MAG, Freire-Neto FP, Oliveira GHM, Duarte VMG, Luchessi AD, et al. Low bone mineral density is associated to poor glycemic control and increased OPG expression in children and adolescents with type 1 diabetes. Diabetes Res Clin Pract. 2014 Mar;103(3):452–7.

209. Slade JM, Coe LM, Meyer R a, McCabe LR. Human bone marrow adiposity is linked with serum lipid levels not T1-diabetes. J Diabetes Complications. Elsevier Inc.; 2012;26(1):1–9.

210. Motyl KJ, McCabe LR, Schwartz A V. Bone and glucose metabolism: a two-way

street. Arch Biochem Biophys. Elsevier Inc.; 2010 Nov 1;503(1):2–10.

211. Lumachi F, Camozzi V, Tombolan V, Luisetto G. Bone mineral density, osteocalcin, and bone-specific alkaline phosphatase in patients with insulin-dependent diabetes mellitus. Ann N Y Acad Sci. 2009 Sep;1173 Suppl:E64–7.

212. Motyl KJ, McCauley LK, McCabe LR. Amelioration of type I diabetes-induced osteoporosis by parathyroid hormone is associated with improved osteoblast survival. J Cell Physiol. 2012 Apr;227(4):1326–34.

213. Pater A, Sypniewska G, Pilecki O. Biochemical markers of bone cell activity in children with type 1 diabetes mellitus. J Pediatr Endocrinol Metab. Jan;23(1-2):81–6.

214. Peters AL, Davidson MB, Schriger DL, Hasselblad V. A clinical approach for the diagnosis of diabetes mellitus: an analysis using glycosylated hemoglobin levels. Meta-analysis Research Group on the Diagnosis of Diabetes Using Glycated Hemoglobin Levels. JAMA. 1996 Oct 16;276(15):1246–52.

215. Kaneko H, Sasaki T, Ramamurthy NS, Golub LM. Tetracycline administration normalizes the structure and acid phosphatase activity of osteoclasts in streptozotocin-induced diabetic rats. Anat Rec. 1990 Aug;227(4):427–36.

216. Miller RG, Secrest AM, Sharma RK, Songer TJ, Orchard TJ. Improvements in the life expectancy of type 1 diabetes: The Pittsburgh Epidemiology of Diabetes Complications Study cohort. Diabetes. 2012;61(11):2987–92.

217. Drever A. Bone health and osteoporosis. Pract Nurse. Elsevier Inc; 2009;38(6):13–22.

218. Riggs BL. The mechanisms of estrogen regulation of bone resorption. J Clin Invest. 2000;106(10):1203–4.

219. Syed F, Khosla S. Mechanisms of sex steroid effects on bone. Biochem Biophys Res Commun. ACADEMIC PRESS INC ELSEVIER SCIENCE, 525 B ST, STE 1900, SAN DIEGO, CA 92101-4495 USA; 2005 Mar 18;328(3):688–96.

220. Gilbert L, He X, Farmer P, Boden S, Kozlowski M, Rubin J, et al. Inhibition of Osteoblast Differentiation by Tumor Necrosis Factor-α. Endocrinology.

2000;141(11):3956–64.

221. Manolagas SC. Birth and death of bone cells: basic regulatory mechanisms and implications for the pathogenesis and treatment of osteoporosis. Endocr Rev. 2000;21(2):115–37.

222. Pacifici R. Editorial : Cytokines , Estrogen , and Postmenopausal Osteoporosis — The Second Decade. Endocrinology. 1996;139(6):2659–61.

223. Fowlkes JL, Bunn RC, Liu L, Wahl EC, Coleman HN, Cockrell GE, et al. Runt-related transcription factor 2 (RUNX2) and RUNX2-related osteogenic genes are down-regulated throughout osteogenesis in type 1 diabetes mellitus. Endocrinology. 2008 Apr;149(4):1697–704.

224. Lu H, Kraut D, Gerstenfeld LC, Graves DT. Diabetes interferes with the bone formation by affecting the expression of transcription factors that regulate osteoblast differentiation. Endocrinology. 2003;144(1):346–52.

225. Weinberg E, Maymon T, Moses O, Weinreb M. Streptozotocin-induced diabetes in rats diminishes the size of the osteoprogenitor pool in bone marrow. Diabetes Res Clin Pract. 2014 Jan;103(1):35–41.

226. Martin RB, Zissimos SL. Relationships between marrow fat and bone turnover in ovariectomized and intact rats. Bone. 1991 Jan;12(2):123–31.

227. Fukuharu M, Sato J, Ohsawa I, Oshida Y, Nagasaki M, Nakai N, et al. Additive effects of estrogen deficiency and diabetes on bone mineral density in rats. Diabetes Res Clin Pract. 2000 Apr;48(1):1–8.

228. Gopalakrishnan V, Arunakaran J, Aruldhas MM, Srinivasan N. Effects of streptozotocin-induced diabetes mellitus on some bone turnover markers in the vertebrae of ovary-intact and ovariectomized adult rats. Biochem Cell Biol. 2006 Oct;84(5):728–36.

229. Motyl KJ, Botolin S, Irwin R, Appledorn DM, Kadakia T, Amalfitano A, et al. Bone inflammation and altered gene expression with type I diabetes early onset. J Cell Physiol. 2009 Mar;218(3):575–83.

230. Pino AM, Ríos S, Astudillo P, Fernández M, Figueroa P, Seitz G, et al.

Concentration of adipogenic and proinflammatory cytokines in the bone marrow supernatant fluid of osteoporotic women. J Bone Miner Res. 2010 Mar;25(3):492–8.

231. Duque G. Bone and fat connection in aging bone. Curr Opin Rheumatol. 2008;20(4):429–34.

232. Iwaniec UT, Turner RT. Failure to generate bone marrow adipocytes does not protect mice from ovariectomy-induced osteopenia. Bone. Elsevier Inc.; 2013;53(1):145–53.